NOAA Technical Memorandum NOS CS 61

REGIONAL VDATUM UPGRADE FOR THE U.S. WEST COAST: TIDAL DATUMS, TIDES ASSIMULATION, SPATIALLY VARYING UNCERTAINTY, AND TOPOGRAPHY OF THE SEA SURFACE

Silver Spring, Maryland

July 2025

noaa National Oceanic and Atmospheric Administration

U.S. DEPARTMENT OF COMMERCE
National Ocean Service
Coast Survey Development Laboratory

Office of Coast Survey
National Ocean Service
National Oceanic and Atmospheric Administration
U.S. Department of Commerce

The Office of Coast Survey (OCS) is the Nation's only official chartmaker. As the oldest United States scientific organization, dating from 1807, this office has a long history. Today it promotes safe navigation by managing the National Oceanic and Atmospheric Administration's (NOAA) nautical chart and oceanographic data collection and information programs.

There are four components of OCS:

The Coast Survey Development Laboratory develops new and efficient techniques to accomplish Coast Survey missions and to produce new and improved products and services for the maritime community and other coastal users.

The Marine Chart Division acquires marine navigational data to construct and maintain nautical charts, Coast Pilots, and related marine products for the United States.

The Hydrographic Surveys Division directs programs for ship and shore-based hydrographic survey units and conducts general hydrographic survey operations.

The Navigational Services Division is the focal point for Coast Survey customer service activities, concentrating predominately on charting issues, fast-response hydrographic surveys, and Coast Pilot updates.

NOAA Technical Memorandum NOS CS 61

REGIONAL VDATUM UPGRADE FOR THE U.S. WEST COAST: TIDAL DATUMS, TIDES ASSIMULATION, SPATIALLY VARYING UNCERTAINTY, AND TOPOGRAPHY OF THE SEA SURFACE

Liujuan Tang[1], Lei Shi[1], Edward Myers[1], Inseong Jeong[2], Stephen White[2], Jack Riley[1], Shachak Peeri[1], Nathan Murry[3], Lijuan Huang[3], Michael Michalski[3], Colleen Fanelli[3], Cuong Hoang[1], and Doug Graham[2]

[1] NOAA/Office of Coast Survey, Coast Survey Development Laboratory
[2] NOAA/National Geodetic Survey
[3] NOAA/Center for Operational Oceanographic Products and Services

July 2025

noaa National Oceanic and Atmospheric Administration

U. S. DEPARTMENT OF COMMERCE
Howard Lutnick, Secretary

National Oceanic and Atmospheric Administration
Laura Grimm, Under Secretary of Commerce for Oceans and Atmosphere (Performing the duty)

National Ocean Service
Nicole LeBoeuf, Assistant Administrator

Office of Coast Survey
Rear Admiral Benjamin K. Evans
Director

Coast Survey Development Lab
Corey Allen
Chief

NOTICE

Mention of a commercial company or product does not constitute an endorsement by NOAA. Use for publicity or advertising purposes of information from this publication concerning proprietary products or the tests of such products is not authorized.

TABLE OF CONTENTS

LIST OF FIGURES

LIST OF TABLES

ABSTRACT

A new regional VDatum tide model has been developed to replace several first-generation VDatum coastal models along the U.S. West Coast, incorporating the latest available data from various courses.

The unstructured triangular regional model grid for the West Coast contains 821,766 nodes and 1,465,125 cells. Tidal datums were derived from tidal simulations using the finite element hydrodynamic model, ADvanced CIRCulation (ADCIRC) v55, forced by a reconstructed tide at the ocean boundary using eight major tidal constituents, K_1, O_1, P_1, Q_1, M_2, S_2, N_2, and K_2, from the global tidal database TPXO9. Model-derived tidal datums were compared with observations from 253 NOAA tide gauges, with an average error of 4.6 cm (5.2%) and a root mean square error of 6.5 cm for the four tidal datums, Mean Higher High Water (MHHW), Mean High Water (MHW), Mean Low Water (MLW), and Mean Lower Low Water (MLLW).

To reduce this error, a Spatially Varying Uncertainty (SVU) method was applied to produce the corrected tidal datums products and estimate associated uncertainty. These corrected tidal datums and uncertainty were further interpolated from the unstructured triangular grid onto 13 structured marine grids to be used by the VDatum software.

The Topography of the Sea Surface (TSS), which is defined as the elevation of xGEOID20B relative to local mean sea level (LMSL), was derived by interpolating orthometric-to-LMSL relationships at 123 NOAA tide gauges and satellite altimetry datasets from eight missions. The final TSS fields on the marine grids were created using Surfer© software's minimum curvature algorithm. The TSS spatially varying uncertainty was estimated through a rigorous error propagation approach and a simple objective analysis based on the given tide gauge observation and altimetry data uncertainties

For this upgrade, we have developed a tides assimilation method based on the representor approach using finite element method for VDatum tide modeling. Data from the deep ocean DART stations and open coast tide stations were assimilated to optimize the open boundary conditions for the ADCIRC model. This report also documents the global and high-resolution San Francisco test cases for the representor assimilation method. In addition, we have conducted a preliminary test on the next version of tides assimilation method, which is based on incremental variation approach, on the west Coast model. By optimizing both open boundary conditions and tidal potential forcing, model accuracy can be further improved.

Key Words: tides, tidal datums, data assimilation, spatially varying uncertainty, ADCIRC, bathymetry, West Coast, coastline

1. INTRODUCTION

The U.S. West Coast was covered by several first-generation VDatum coastal tide models as shown in Figure 1, which were developed from 2004 to 2016. Since then, new observations on tidal datums and bathymetry survey data have become available. In addition, we have received users' requests to extend the VDatum coverage further offshore as well as into rivers to support a broad range of applications, including bathymetry survey, Digital Elevation Models (DEMs) developments, etc. Here we have developed a regional tide model for the U.S. West Coast to replace the several first-generation coastal models, and to reflect the new information and coverage as best possible. This upgrade also provides spatially varying uncertainty estimates associated with tidal datums products and tests on tides assimilation on unstructured grids.

The VDatum vertical datum transformation software is an outcome of the national VDatum project in U.S., a joint effort of the tri-office VDatum team of NOAA's Office of Coast Survey (OCS), National Geodetic Survey (NGS), and Center for Operational Oceanographic Products and Services (CO-OPS) (https://vdatum.noaa.gov/). It is designed to vertically transform geospatial data among a variety of tidal, orthometric, and ellipsoid-based vertical datums. The goal is to have complete coverage of U.S. coastal waters from the landward (i.e., navigable) reaches of estuaries and embayments out to at least 220 nautical mile (nmi) offshore. At present, VDatum includes 36 different vertical datums. It allows users to convert their data from different horizontal/vertical references into a common system and to enable the fusion of diverse geospatial data in desired reference levels.

In this study, we focus on tidal datums from astronomical tides for VDatum software. VDatum includes a class of seven tidal datums: mean higher high water (MHHW), mean high water (MHW), mean low water (MLW), mean lower low water (MLLW), mean tide level (MTL), diurnal tide level (DTL), and mean sea level (MSL). CO-OPS' coastal water level stations have been providing these tidal datums data, which are derived from time series of the observed water level data at 6 minute intervals except the MSL, which is the hourly average. Figure 2 illustrates examples of time series of water level data and tidal datums at several tide stations. A full 19-year epoch period is used for the computation of the datums at CO-OPS' long term control stations (CO-OPS, 2003). For example, MSL is computed as the arithmetic mean of hourly water observations over the National Tidal Datum Epoch (NTDE), which presently is the 1983–2001 NTDE. All other shorter period subordinate gauges rely on simultaneous comparisons between their data and the epoch control station (CO-OPS, 2003). The differences between these two stations are applied to the control station datum to acquire a 19-year's equivalent at the subordinate stations. This helps to mute out the short period meteorological and oceanographic effects which are expected to be experienced by both the control and the subordinate stations.

For the applications developed prior to 2016, the model-data corrections were made using the Tidal Constituent and Residual Interpolation (TCARI) tool developed by Hess et al. (1999; 2002). TCARI is a first-order deterministic spatial interpolation tool based on the solution of Laplace's equation. The errors between the model results and the CO-OPS station data are interpolated throughout the domain to create an error field for each tidal datum. The error field is then used to correct the model results to create a datum field that matches the station data at those locations

(Hess et al., 2005). The approach produces a single-value uncertainty estimate of the tidal datums for each model region (https://vdatum.noaa.gov/docs/est_uncertainties.html).

To provide a more accurate representation of the uncertainty in each model region, Shi and Myers (2016) developed a new statistical interpolation method, namely the spatially varying uncertainty (SVU) method, for VDatum applications. It was derived from the variational principle to calculate the corrected tidal datums by blending the model results, observations, and measurement errors together. They show that the new interpolation approach not only reduces the bias and errors, but also produces a spatially varying uncertainty. The uncertainty results can also provide important guidance for decision-making on placement of new tide gauges to further reduce the uncertainty in the VDatum products. This spatially varying uncertainty method has become the new standard for use for developing VDatum applications since then.

Here we apply Shi and Myers' method to study spatially varying uncertainty on the U.S. West Coast. This may induce uncertainty in the tidal datums in the area. The SVU helps to identify locations where new gauges would be beneficial in reducing uncertainty in VDatum. Once new data are collected, they will then be merged with the model to update the VDatum for this region. The same process will be used as we update other VDatum regions as well.

The rest of this technical report is organized as follows: Section 2 briefly describes the method; Section 3 presents the data, grid development, and model setup of the tide model; Section 4 discusses the modeling results, including datum validation, associated spatially varying uncertainty, tides assimilation test cases, and lessons learned; summary and conclusion are provided in Section 5.

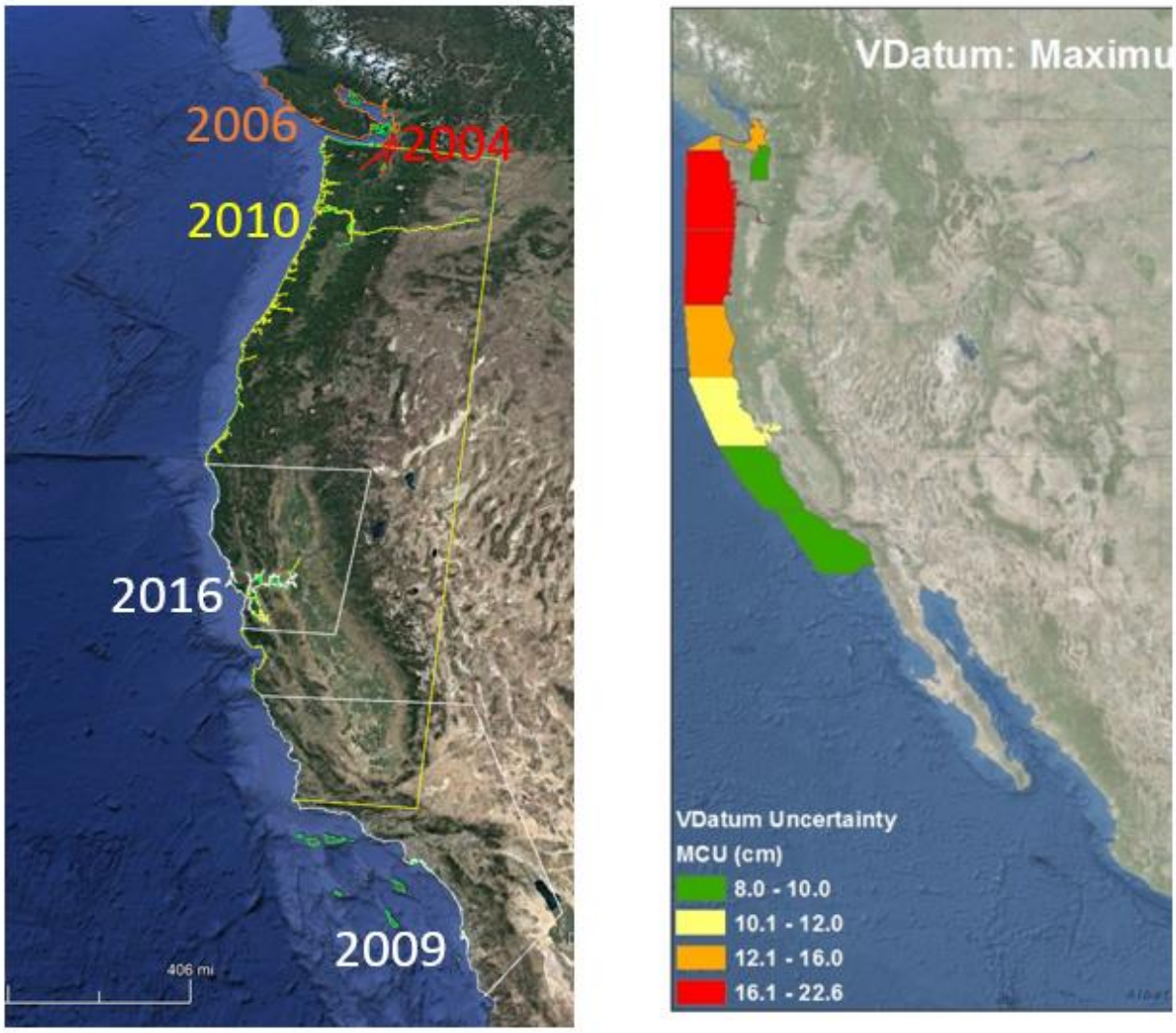

(a) **(b)**

Figure 1 **(a) The U.S. West Coast was covered by several 1st generation VDatum tide models developed from 2004-2016. (b) A single number was then used to represent the uncertainty for an area covered by a marine grid. Red indicates large uncertainty in the area.**

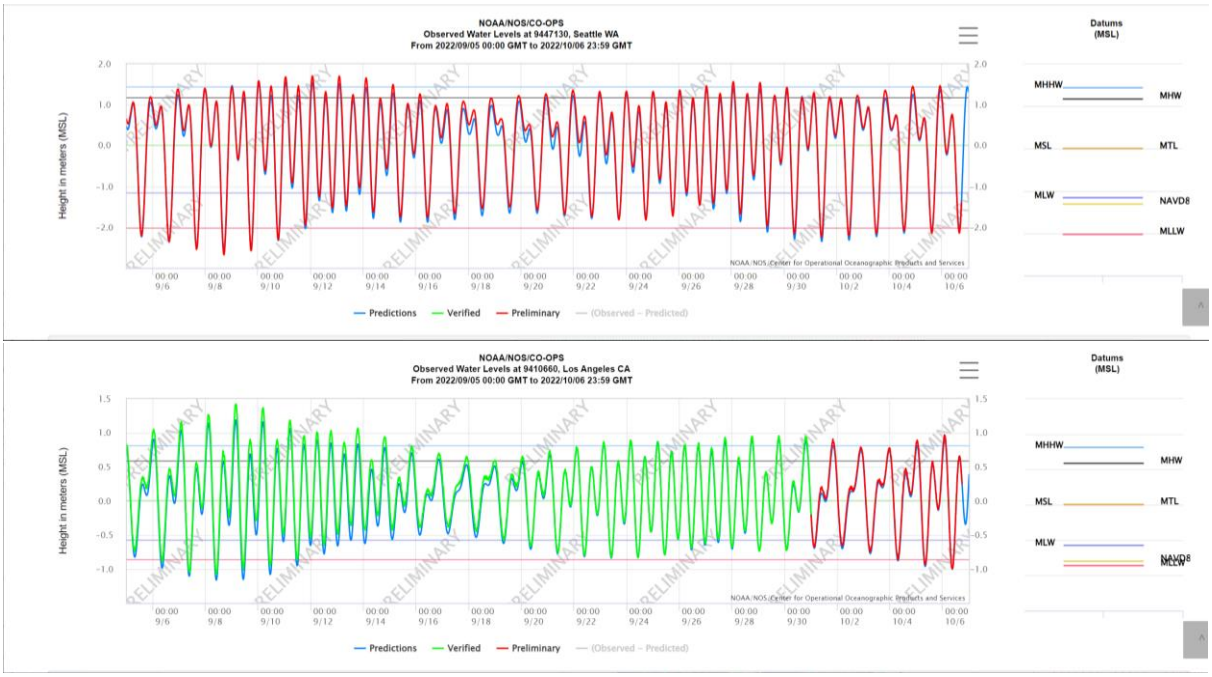

Figure 2 **Examples of water level time series data and tidal datums at (a) Seattle and (Los Angeles tide stations.**

2. Method

In general, tidal datum fields may vary over geographical locations. Tidal datums at stations are referenced to measured local water levels and should not be extended into areas of differing oceanographic characteristics. To resolve the spatially varying nature of the tidal datums in between observation locations, hydrodynamic models and spatial interpolation, techniques have been employed for each VDatum application that simulate the tidal propagation characteristics in the region of interest. In order to merge all of the individual VDatum applications together to form a continuous national VDatum product, a consistent methodology for computing the tidal datums has been adopted for all region-specific VDatum applications (NOS, 2010). The approach consists of the following four major steps (Myers et al., 2005; NOS, 2010):

(1) First use the bathymetric and coastline data to develop a grid to be used by the hydrodynamic model.
(2) Next calibrate a hydrodynamic model to best simulate the observed tidal datum characteristics for the region, e.g. tides assimilation when available.
(3) Then correct the model-data errors using a spatial interpolation technique.
(4) Finally provide the corrected modeled datums (i.e., datum products) on several structured grids of points to be used by the VDatum software.

2.1 Hydrodynamic Modeling

The hydrodynamic model used for this study is the two-dimensional, depth-integrated version of the ADvanced CIRCulation (ADCIRC) model version 55 (Luettich et al., 1992; Luettich and Westerink, 2004; Pringle, 2021). The ADCIRC model has been used in the previous VDatum areas (Hess et al., 2005; Spargo and Woolard, 2005), taking advantage of highly flexible, irregularly spaced grids. Numerous studies have shown this model to be robust throughout the Eastern North Atlantic and Gulf of Mexico regions (Luettich et al., 1995; Mukai et al., 2002), and the West Coast (Spargo, 2004).

ADCIRC utilizes the fully nonlinear shallow water equations with hydrostatic pressure and Boussinesq approximations. It solves the continuity (in the form of the Generalized Wave Continuity Equation) and the non-conservative momentum equations for free surface elevation and the depth-averaged velocity components. The equations are discretized: horizontally in space using the finite element method with three-node linear triangles; and in time using the finite difference method. The ADCIRC code allows a variety of user(?) specified input parameters. Here we used the fully nonlinear form of the equations, which includes non-linear bottom friction, finite amplitude, and convection terms.

ADCIRC version 55 has several numerical improvements. It reformatted the governing equations using a rectilinear mapping projection and utilized coordinate rotation to remove pole singularity. It removed the gravity-wave-based (Courant–Friedrichs–Lewy, CFL) constraint through the choice of numerical parameters, allowing for larger computational time steps to achieve computational efficiency. Pringle (2021) shows that the computational performance of

the new numerical treatment is 1 to 2 orders of magnitude faster than studies using previous ADCIRC versions.

The ADCIRC model has been parallelized using domain decomposition, a conjugate gradient solver, and Message Passing Interface (MPI) based message passing. This parallel version of the code was compiled and run on the NOAA's Jet high performance computing system in Boulder, Colorado.

2.2 Tides Assimilation

Through the integration of observations and modeling, tides assimilation can further improve model accuracy. In the past VDatum modeling, the offshore boundary inputs to the ADCIRC model were taken directly from tidal databases without assimilation of tides. In this study, two versions of data assimilations schemes, representor and incremental variational approaches, have been developed and tested.

Version 1 is a conceptually simple tides assimilation scheme based on linearized shallow water equations to assimilate the observed tidal harmonic constants. It optimizes/improves offshore tidal boundary conditions for the ADCIRC tidal model (Tang et al., 2019).

We denote the dynamic and observations systems for tidal water level and velocity field u as Eqs. (1) and (2), respectively:

$$Su = f_o \quad (1)$$
$$d = Lu \quad (2)$$

where S is the shallow water equation operator. f_o is a forcing term. d is the observed state variable fields. L is the projection operator projecting the state variables into the observation location. The combination of Eqs. (1) and (2) is an over-deterministic system of equations.

To solve the problem, the cost function $J(u)$ to compromise Eqs. (1) and (2) is defined as

$$J(u) = (Lu-d)' \ R^{-1} (Lu-d) + (Su-f_o)' B^{-1} (Su-f_o)^{-1} \quad (3)$$

where R and B are the observation and model error covariance matrixes, respectively.

In the deep ocean we assume the dynamic equation (1) is linear. Then the representor approach (Egbert et al., 1994) can be used to minimize the cost function $J(u)$. The system is solved using the finite element method. The original version of the code was in Cartesian coordinates (Shi, Personal communications). We made several implementations, including adding in Geographic and natural coordinates, tidal potential forcing terms, internal tides dissipation scheme, and triplet approach to improve the speed.

This version of tides assimilations scheme has been tested on a global scale as well as on a high resolution San Francisco Bay model. Good model accuracy was achieved for both test cases. It was then applied to the West Coast VDatum tide model. This is also the first VDatum modeling application with data assimilation.

Version 2 is an incremental variational method that can optimize both tidal boundary conditions and tidal forcing (Shi et al., 2020). A cost function was constructed with tidal boundary conditions and tidal forcing as its control (independent) variables. To minimize the cost function, optimal boundary conditions and tidal forcing were derived using a conventional dual 4-Dimensional Variational (4D-Var) Physical-space Statistical Analysis System. The tangent linear and adjoint model were solved by using a finite element method. By adapting the incremental form, the variational method streamlines the workflow to provide the incremental correction to the boundary conditions and tidal forcing. This scheme is still in testing mode.

2.3 Datum Products and Spatially Varying Uncertainty

The VDatum's vertical datum transformations require that the values returned by the VDatum software need to be equivalent to the values determined through observations at tide gauge locations. Therefore, the modeled tidal datum fields need to be corrected with tide station data. Here we refer to the corrected model datum fields as the datum products.

In the past, this was achieved by a deterministic interpolation method (Hess and Gill, 2003; NOS, 2010). It spatially interpolated the error between the model and the station data to allow the final datum fields to match the station data at those locations. This was through a prediction and correction procedure, the latter of which uses a deterministic spatial interpolation method. A solver based on Laplace's equation was used for the spatial interpolation of modeled tidal datum and observed tidal datum discrepancies over the water.

As VDatum currently provides single-value uncertainty estimates in the tidal datums for each regional application, the next goal is to provide a spatially varying uncertainty field for each tidal datum to improve the uncertainty estimates. Therefore in this upgrade, we apply Shi and Myers' (2016) statistical method to blend the modeled and the observed tidal datums, as well as to compute the associated spatially varying uncertainty for the entire domain.

Here we give a brief introduction to the method. The method is derived from the variational principle in data assimilation to obtain an analysis solution by minimizing a cost function. The construction of the cost function is such that the discrepancy between the analysis solution and observations satisfies the constraint prescribed by the user. The constraint that the VDatum technical team adopted for statistical interpolation is that the discrepancy between the analysis field and the observations at all tide stations should be equal to or less than 1 cm or the CO-OPS' error value, whichever is less. This is achieved by introducing a diagonal weight matrix that regulates not only the weight of the model error for a particular station in the cost function but also the analysis results. More details can be found in Shi and Myers (2016).

2.4 VDatum Marine Grids, Bounding Polygons, and Quality Analyses

The VDatum software requires regularly spaced grids called "marine grids" that contain the datum information at the water nodes and null information at the land nodes (NOS, 2010). The datum product and associated spatially varying uncertainty from section 2.3 are based on the unstructured grid. Therefore, they need to be populated to the marine grids to be used by the software.

We use the grid generating software (vgridder21.f) to generate the VDatum marine grid for a specific area, which consists of points with uniform spacing in the longitude and latitude directions. Digitized coastline data are used to determine which points in this marine grid are water and which are land. Points located within water, or within a distance of approximately one-half a marine grid element size of water, are set to water. The water points of the VDatum marine grid are then populated with the tidal datum and uncertainty information, which are interpolated from the corrected model datums using the program vpop28.f. The output will then be saved in GTX format for use by the VDatum software.

The final tidal datum products as represented on the VDatum marine grid in the GTX format must be checked in several ways, including (1) validation test at station locations, (2) continuity test at common boundaries, (3) overlapping test, and (4) polygon test (NOS, 2010). For the validation test, the GTX files are checked against observations to confirm that the datums approximately match at the tide stations. The error at each station should be no greater than 1 or 2 cm. When there are adjacent tidal datum grids, there must be a check for continuity of values across the common boundaries (e.g., continuity test). This is done with program test_cont15.f. In some regions, the tidal marine grids can actually overlap, resulting in ambiguity in the selection of the correct grid (NOS, 2010). Therefore, the use of a bounding polygon is necessary. Given a latitude-longitude point in the overlapped region, a check is made of whether the point falls within a specific bounding polygon; if so, the marine grid for that region can be used. If not, additional polygons are checked. The overlapping test is to ensure that the bounding polygons do not overlap with each other. We use test_ovlp8.f to check and ensure that there is no overlapping between the adjacent bounding polygons. The polygon test is to check the bounding polygon to ensure it is completely inside the marine grid (NOS, 2010). The test_poly4.f is used to check and ensure the bounding polygon is completely inside the marine grid.

3.DATA AND MODEL DEVELOPMENT

3.1 Tidal Datum Data

The West Coast VDatum region extends from San Diego, California, in the south to Boundary Bay, Washington, in the North. There are 259 NOAA CO-OPS coastal tide stations and five deep-ocean DART stations on the U.S. West Coast. Figure 3 shows the station locations, and color indicates tidal datums. Table 1 summarizes the ranges of the tidal datums referred to MSL for the stations. In general, tidal amplitudes on the open coast water increases from south to north. For example, MHW increases from about half meter to a meter along the open coast from California to Washington. Tidal range decreases from the open coast to rivers in the upstream direction, with the smallest range at station 9416174, Sacramento River, California (Table 1). Amplification of tides can be seen in San Francisco Bay, Puget Sound, and Willapa Bay, especially in the southern portion of the bays/sound, which result in larger tidal ranges than those in the open coast. The stations at the southern end of Puget Sound show the largest tidal ranges among the West Coast stations (Table 1).

Table 1 Ranges of four tidal datums at stations along the West Coast.

Range	MHHW (m)	MHW (m)	MLW (m)	MLLW (m)
From	[1]0.220	[1]0.129	[1]-0.140	[1]-0.186
To	[2]1.899	[3]1.603	[2]-1.611	[2]-2.546

[1]: Station 9416174, Sacramento River, California.
[2]: Station 9446969, Olympia, Bud Inlet, Puget Sound, Washington.
[3]: Station 9446742, Barron Point, Little Skookum Inlet, Washington.

Figure 4 shows the measurement root mean square error (RMS) at the tide stations. The maximum error is 3.8 cm at station 9440079, Beacon Rock State Park, Columbia river. For details on how the RMS for tidal datums were computed for CO-OPS tide stations, please see Bondar (1981).

Figure 5 shows the topographic sea surface (TSS) at tide stations. TSS is the xGEOID20B above MSL, ranging from -2.29 to 0.438 m. Negative value indicates xGEOID20B below MSL. The majority of stations have negative TSS. In the Columbia River, the TSS magnitude increases in the upstream direction and reaches -2.29 m at station 9440079, Beacon Rock State Park. Six stations have positive TSS. Four are located in two bays with narrow entrances that well protected the bays from open ocean, and two are in Puget Sound.

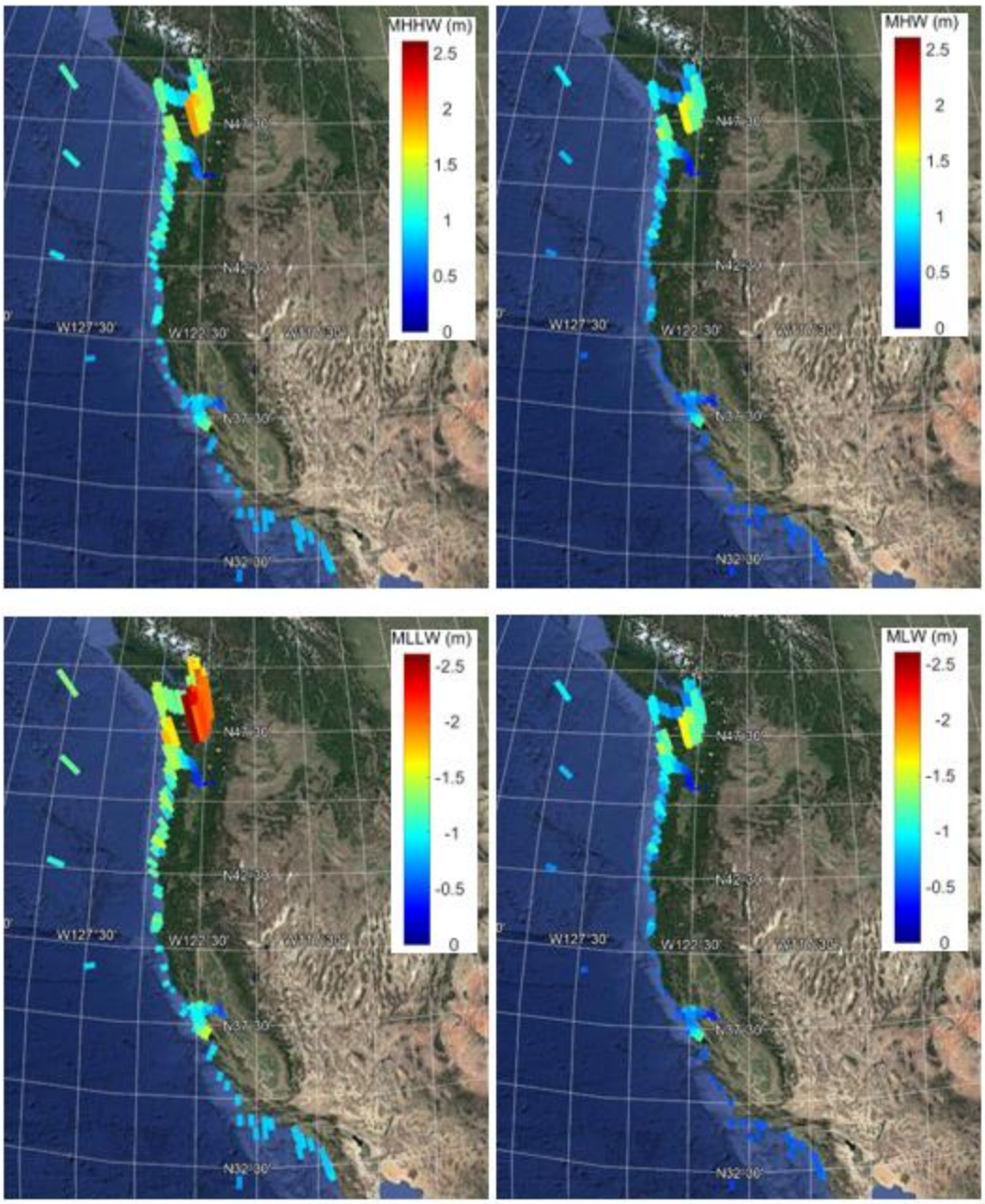

Figure 3 **Observed tidal datums, MHHW, MHW, MLLW, and MLW, at 259 CO-OPS' tide stations and 5 Deep-Ocean DART stations. Datums are referenced to MSL.**

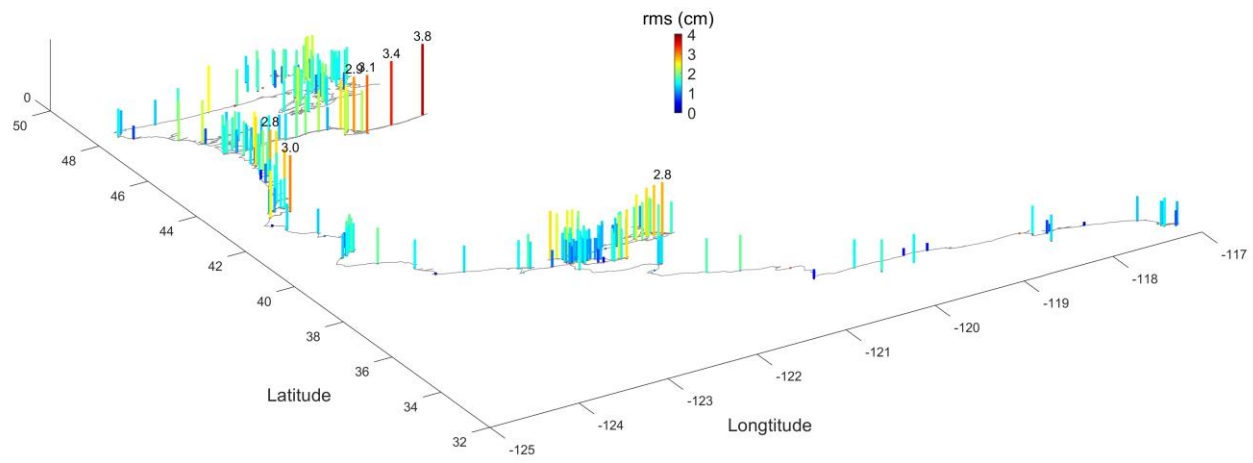

Figure 4 **Error (root mean square errors) in centimeter (cm) for observed datums at CO-OPS' tide stations.**

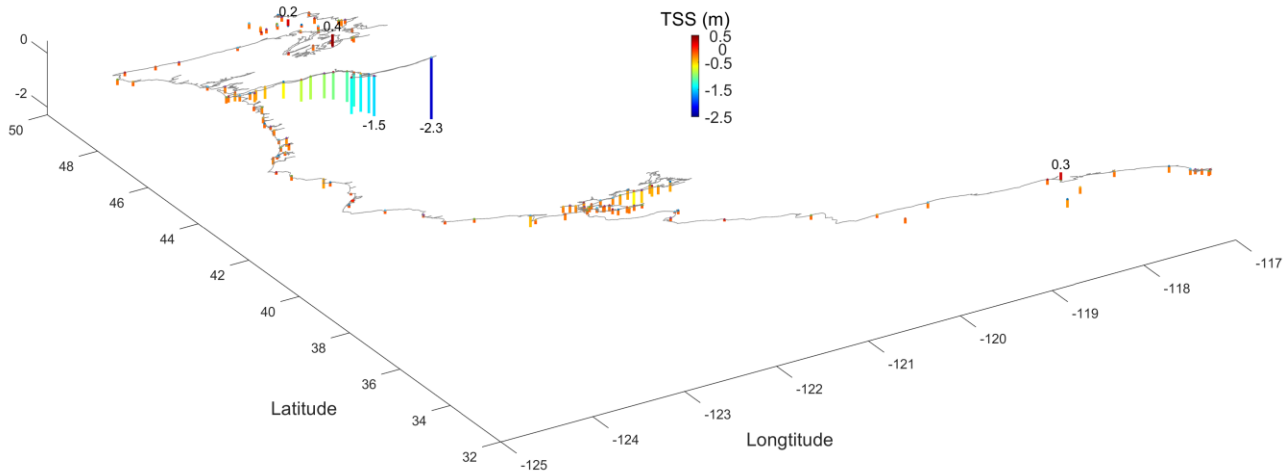

Figure 5 **Topographic Sea Surface (TSS) in meters at CO-OPS' tide stations.**

3.2 Shoreline Data

The MHW shoreline is used as the land boundary for creating the unstructured grid for the tide model. It also defines the extent of the VDatum marine grid. Table 2 summarizes the shoreline data sources.

The MHW shoreline from NOAA's Continually Updated Shoreline Product (CUSP) data are considered the most recent and accurate shoreline data available (https://www.ngs.noaa.gov/CUSP/). The Horizontal Datum is the North American Datum of 1983 (NAD83). The data have scales between 1:1,000 – 1:24,000. Individual national shoreline projects and high-resolution LiDAR-derived shoreline were merged to form the framework of the CUSP data.

The CUSP shoreline data have covered most of the U.S. West Coast except in some rivers and bays as listed in Table 3. For example, Figure 6 shows that in Washington, the Camano Island area has no CUSP data coverage. For locations without CUSP data, the MHW shoreline from the NGS Vector Shoreline Data are used. All data were compared with Google Earth Satellite images. Corrections were made to certain areas where shoreline appears to be incomplete or inaccurate. The final compiled coastline is illustrated in Figure 7, with a total of 7 million points: 1 M for mainland boundary points and 6 M for island boundary points.

Table 2 Shoreline data source overview.

Data Sources	Year	Vertical Datum	Horizontal Datum
NOAA Continually updated shoreline product (CUSP) data	2019	MHW	NAD 83
NGS Vector shoreline		MHW	NAD 83
Global Self-consistent, Hierarchical, High resolution Geography shoreline (GSHHG)	2017		WGS 84
Google Earth Satellite Image	2015-2018		WGS 84

Table 3 Locations with only partial CUSP data coverage and alternative shoreline sources.

Locations	Alternative shoreline sources	Year
Umpqua River, Winchester Bay, OR	PH22	1951
Florence, OR	Google Earth	2016
Waldport, OR	OR43B01	1925
New Port, OR	PH113	1953
Depoe Bay, OR	OR1952A	1952
Siletz Bay, Kernville, OR	OR43C04	1926
Netarts Bay, OR	PH157	1957
Tillamook Bay, OR	PH132B	1955
Nehalem Bay , Brighton, OR	Google Earth	2016
Bandon, OR	Google Earth	201505
Wedderburn, OR	Google Earth	201607
Camano Island, WA	Google Earth	201807
Elkhorn, (Monterey Bay), CA	Google Earth	201811

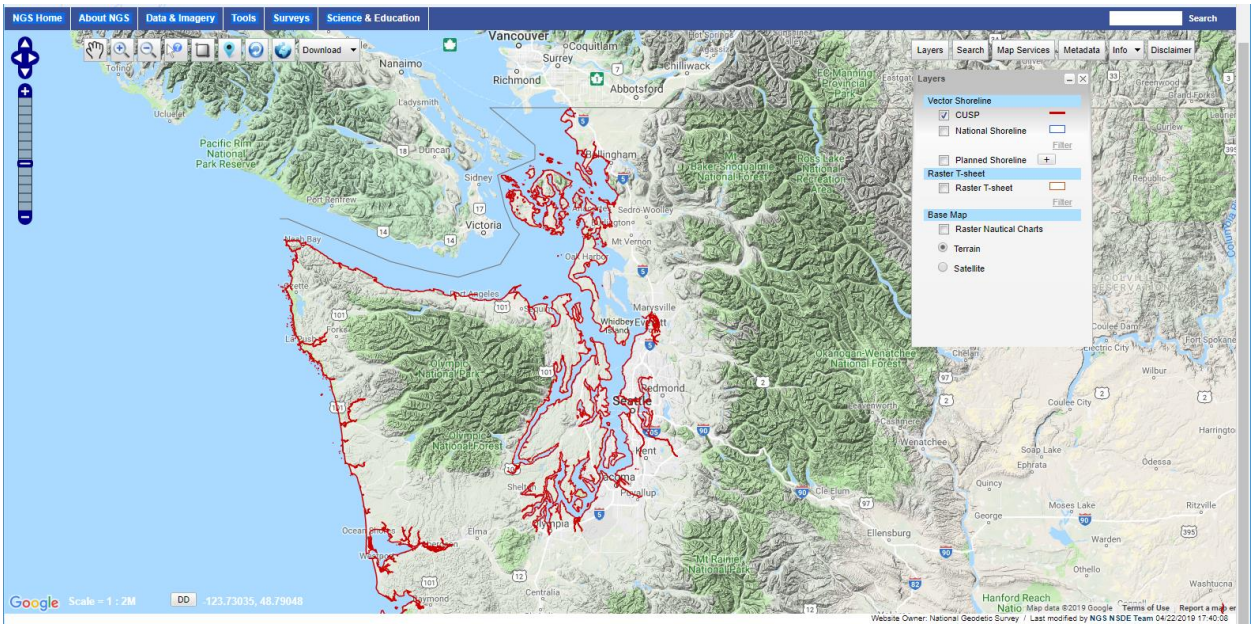

Figure 6 **CUSP shoreline data coverage in Washington. Data are downloaded from https://www.ngs.noaa.gov/CUSP/.**

Figure 7 **Compiled shoreline in white for the U.S. West Coast.**

3.3 Bathymetry Data

Table 4 summarizes the bathymetry data used to compile the model grid. In general, the new data sources superseded the old sources where they overlapped.

Data are from several primary sources/agencies: NOAA's NOS bathymetry survey and ENC data, National Centers for Environmental Information's (NCEI) Digital Elevation Models (DEMs).

The NOS sounding data possess the most coastal coverage in the domain (Fig. 8). It includes surveys conducted between 1851 and 2016. The datums are referenced to either MLW or MLLW, depending on the years of data collection.

Twenty high resolution DEMs (1/3 arc-sec, or approximately10 m) from NCEI are available for the region as shown in Figure 9 (Carignan et al., 2008, 2009a,b, 2011a,b, 2012, 2014, 2015a,b, 2016; Friday et al., 2010, 2011; Caldwell et al., 2011; Grothe et al., 2010, 2012; Lim et al., 2012; Love et al., 2012). These DEMs contain some LiDAR bathymetry and USACE survey data for some of the rivers or intracoastal waterways that are not included in the NOS data. The NCEI 3 arc-sec British Columbia DEM based on MSL developed in 2013 was also used in the study (Carignan et al., 2013).

The more recent data have the higher priority. Data values were converted, when necessary, to the NAD83 horizontal datum. Since MLLW/MLW to Mean Sea Level was already computed by previous VDatum models on the West Coast, data were converted to MSL. We have checked the difference between MSL and Model Zero, which is very small, within 5cm for the majority of computational domain.

Table 4 Bathymetry data source overview.

Data Sources	Year	Datum Vertical	Horizontal
NOS Bathymetry Survey	1851–2016	MLLW/MLW	NAD83
NCEI 1/3" DEMs	2008-2015	MHW/NAVD88	WGS 84
ENC/RNC	2005	MLLW	NAD 83
NCEI 3" British Columbia DEM	2013	MSL	WGS 84
SRTM 15 sec V2	2019	MSL	WGS 84

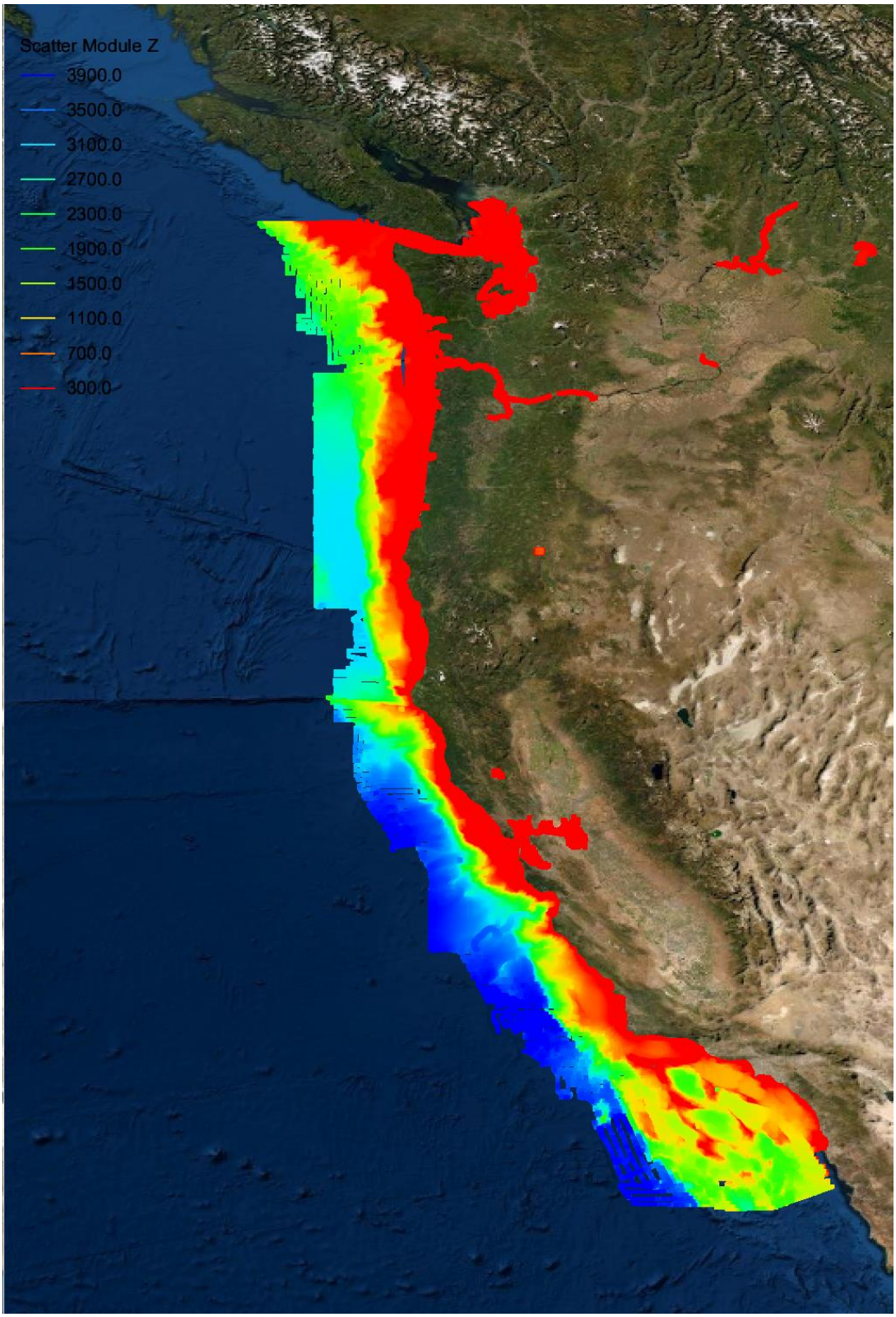

Figure 8 **NOS bathymetry survey data on West Coast. Color indicates depth in meters.**

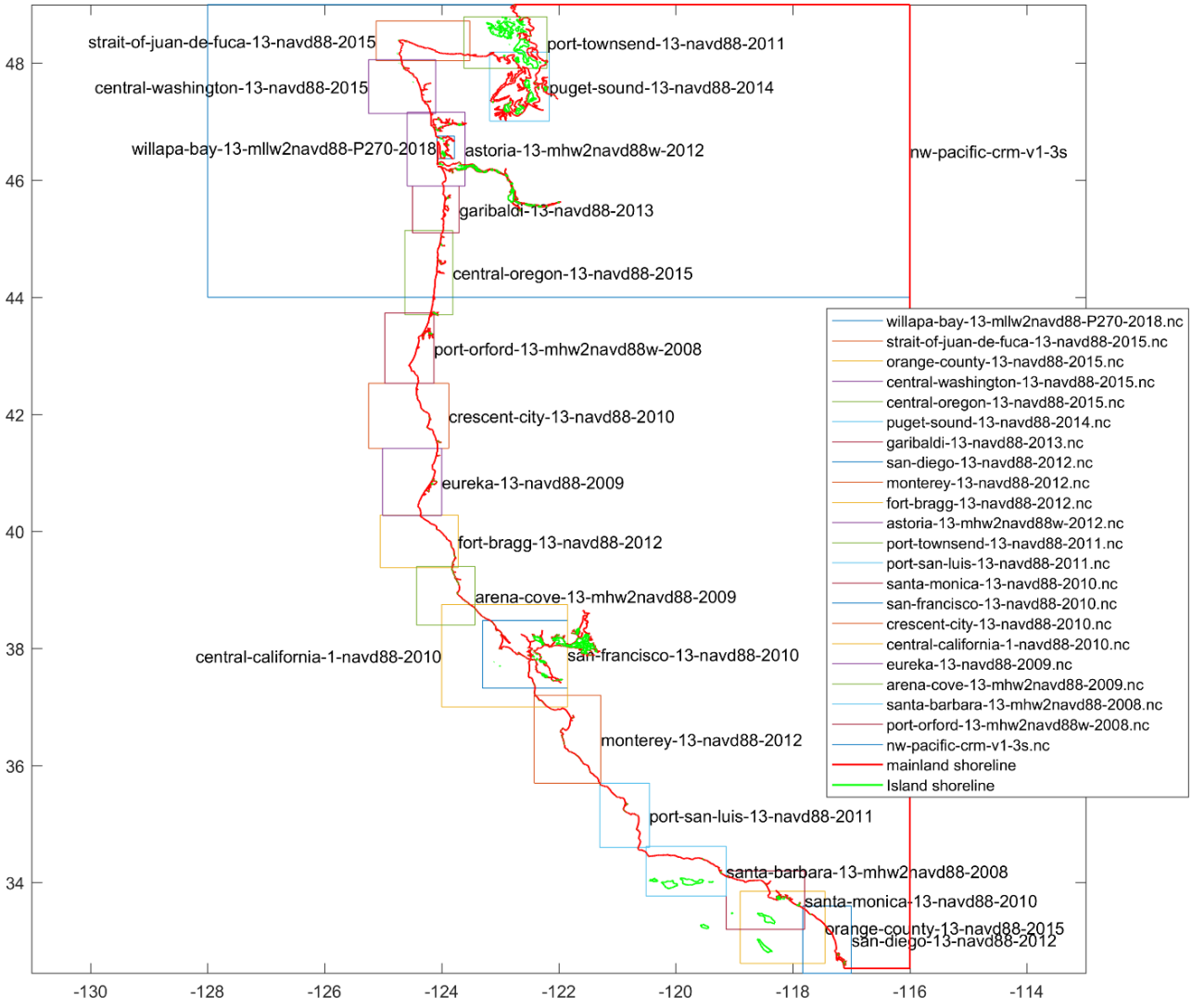

Figure 9 NCEI 1/3 arc sec DEMs for size function.

3.4 Grid Development

The grid development includes two main processes, (1) mesh generation and (2) water depth interpolation. The mesh generation process uses two softwares, the OceanMesh 2D and the Surface-water Modeling System (SMS) software (https://www.aquaveo.com/). We used OceanMesh 2D to generate majority parts of the mesh while manual edits were done in SMS.

The precise distanced-based OceanMesh2D toolbox takes into consideration a variety of geometric and bathymetric mesh size functions driven by features such as wavelength, distance, slopes, feature size, shoreline curvature, etc. (Roberts and Pringle, 2018; Roberts et al., 2019). It is an effective approach since it can assign high resolution only to areas that are in need, such as shoreline with high curvatures, coastal area of shallow depth, bathymetry with steep slope, etc. In this way, it can give an accurate representation of local geometry and bathymetry.

We used a four-layer setup approach with increasing resolutions in OceanMesh2D (Table 5). For the offshore layer, which is also the base layer, the minimum resolution is set to 500 m. Minimum resolution of 30-100 m was then applied to the coastal layers within the U.S. For some important coastal features such as harbors, bays, and rivers, the minimum resolution was set to 15-30 m. For the finest features such as breakwaters and jetties, minimum resolution of 5-10 m was used.

Figure 10 shows the offshore (base) and coastal layers, which used STRM V2 15" DEM and 20 NCEI 1/3" DEMs, respectively, to determine the mesh size functions. The mesh domain was defined by the coastline (i.e., as the land boundary) and offshore open boundary. The U.S. West Coast coastal region was centered in the domain. Figure 11 illustrates the harbor and breakwaters layers in Los Angeles Harbor.

In the open ocean, the grid resolution is primarily controlled by the wavelength/depth (60 nodes per M_2 wavelength) and bathymetry slope to achieve efficiency. The dt for Courant-Friedrichs-Lewy (CFL) conditions was set to 4 sec.

Once the preliminary mesh was generated using OceanMesh 2D as shown in Figure 10, two mesh pieces were merged onto it: one is the Columbia River from Columbia River Estuary Operational Forecast System (CREOFS, Karna and Baptista, 2016) and the other is the San Francisco Bay SCHISM grid from California Department of Water Resources and Virginia Institute of Marine Sciences (Figures 12 and 13). Both were converted to NAD83 and MSL datums before merging.

The merged mesh was then examined and edited in SMS. Figure 14 illustrates several typical edits made to the mesh, which include extension to rivers to cover the CO-OPS tide stations, adding in missing jetties and breakwaters, and replacing portions of the mesh with higher resolution to better represent the shoreline to meet VDatum standards and requirements. All the breakwaters and jetties in the mesh were examined; and edits were made as necessary.

The coastal water depth at the nodes were interpolated from the NOS bathymetry survey data while available. The offshore depth was from the STRM15 DEM. For several rivers with no NOS survey data, the depth was estimated either from the 1/3" NCEI DEMs or ENC maps. Figure 15 shows the final regional tide model mesh for the U.S West Coast, while Figure 16 a-j shows the close-up of the mesh. The mesh has 821,766 nodes and 1,465,125 elements.

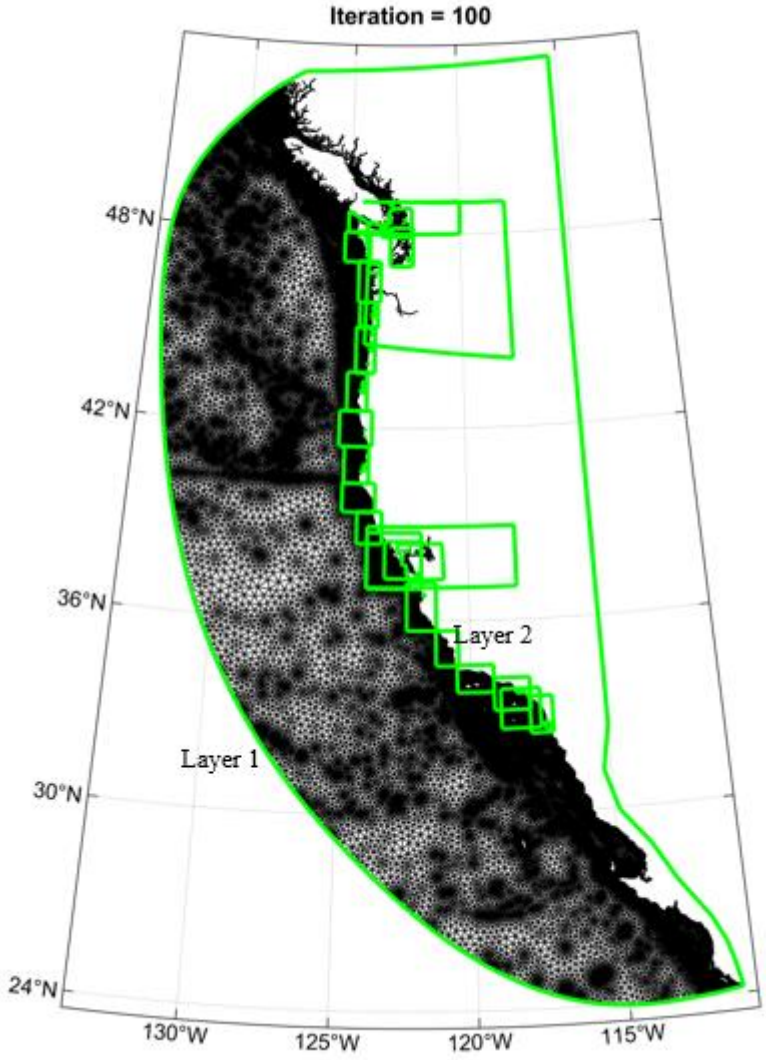

Figure 10 OceanMesh2D polygons setup for Layer 1, offshore layer, and Layer 2, coastal layers (small boxes).

Figure 11 Examples of OceanMesh 2D Layers 3 and 4 in Los Angeles. White, the one Layer 3 polygon for the Harbor and 9 Layer 4 polygons for breakwaters and jetties. Green, island shoreline; Orange, mainland shoreline.

Table 5 Minimum resolution for 4 layers.

Layer	**Min resolution (m)**
Offshore	500
Coastal	30-100
Harbors, Bays, Rivers	15-30
Breakwaters, Jetties	5-10

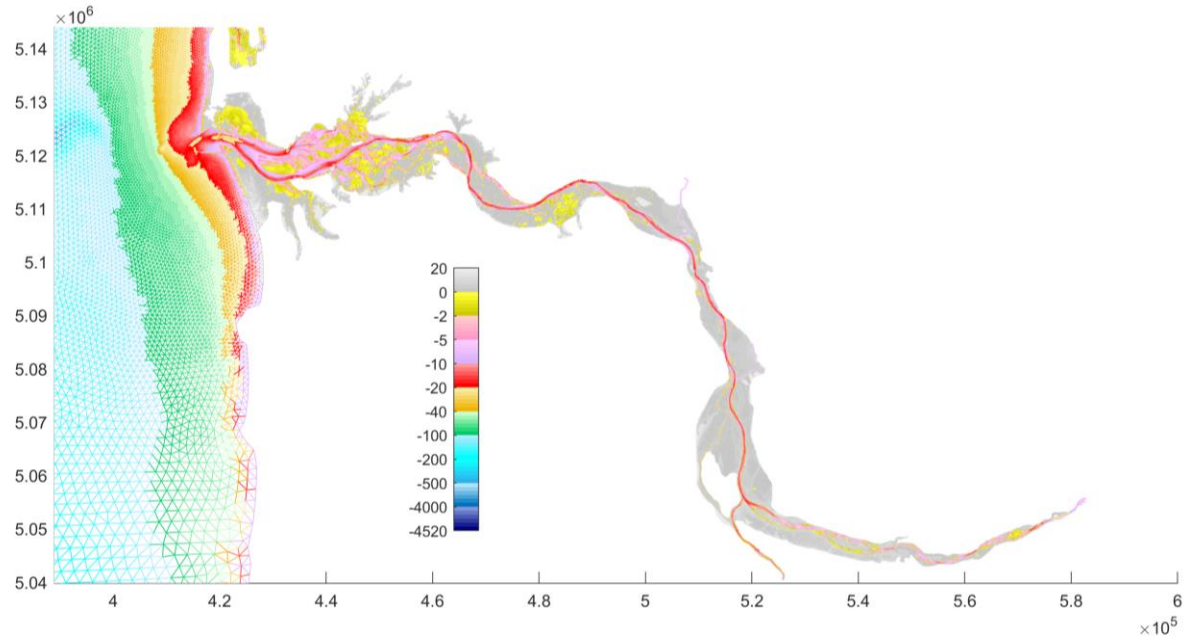

Figure 12 Columbia River portion of the Columbia River Estuary Operational Forecast System (CREOFS), has been merged onto the West Coast Regional VDatum model (Mesh was provided by Charles Seaton in 2019). The mesh is in UTM zone 10.

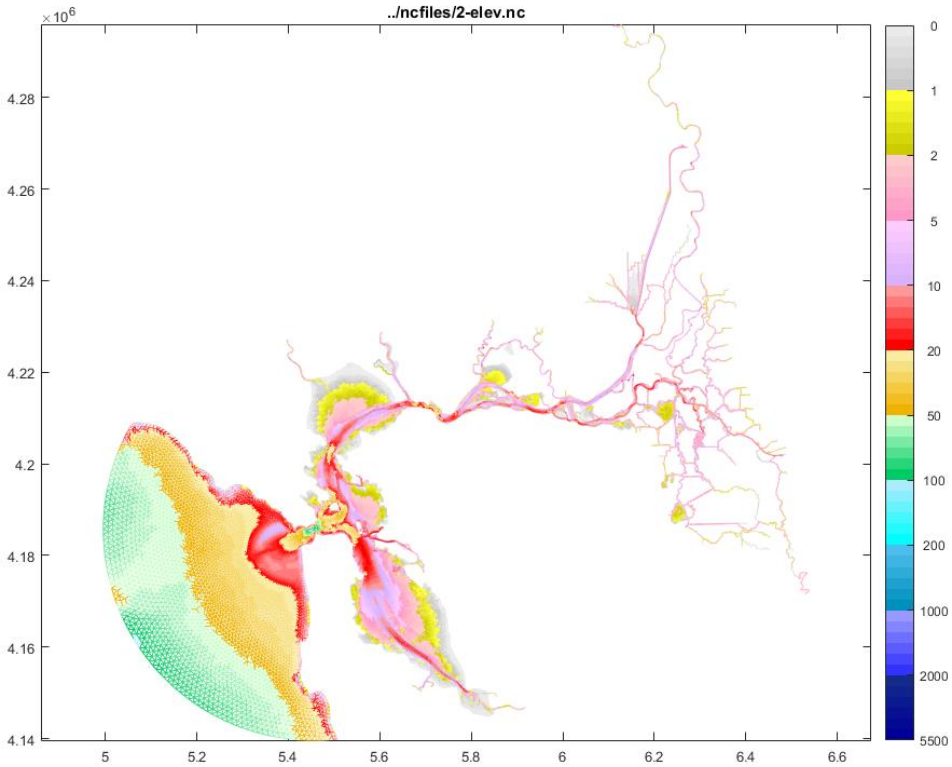

Figure 13 San Francisco Bay SCHISM mesh developed by Virginia Institute of Marine Sciences and California Department of Water Resources. Vertical datum is NAVD88.

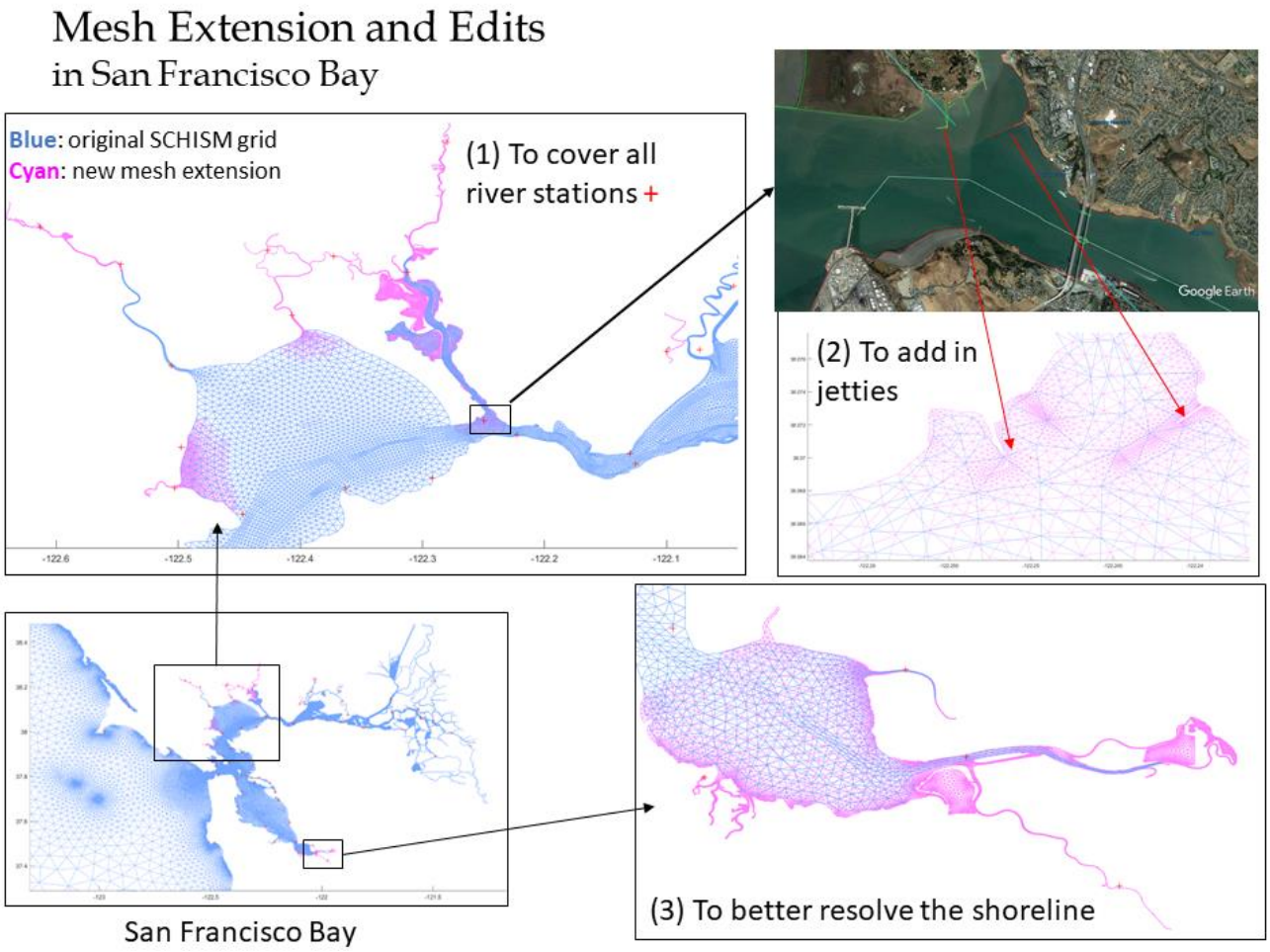

Figure 14 Examples of additional mesh edits were made to the merged San Francisco Bay SCHISM mesh, to include (1) all CO-OPS tide stations, (2) jetties and breakwaters, and (3) to better represent the shoreline in high resolution. Edits are shown in cyan.

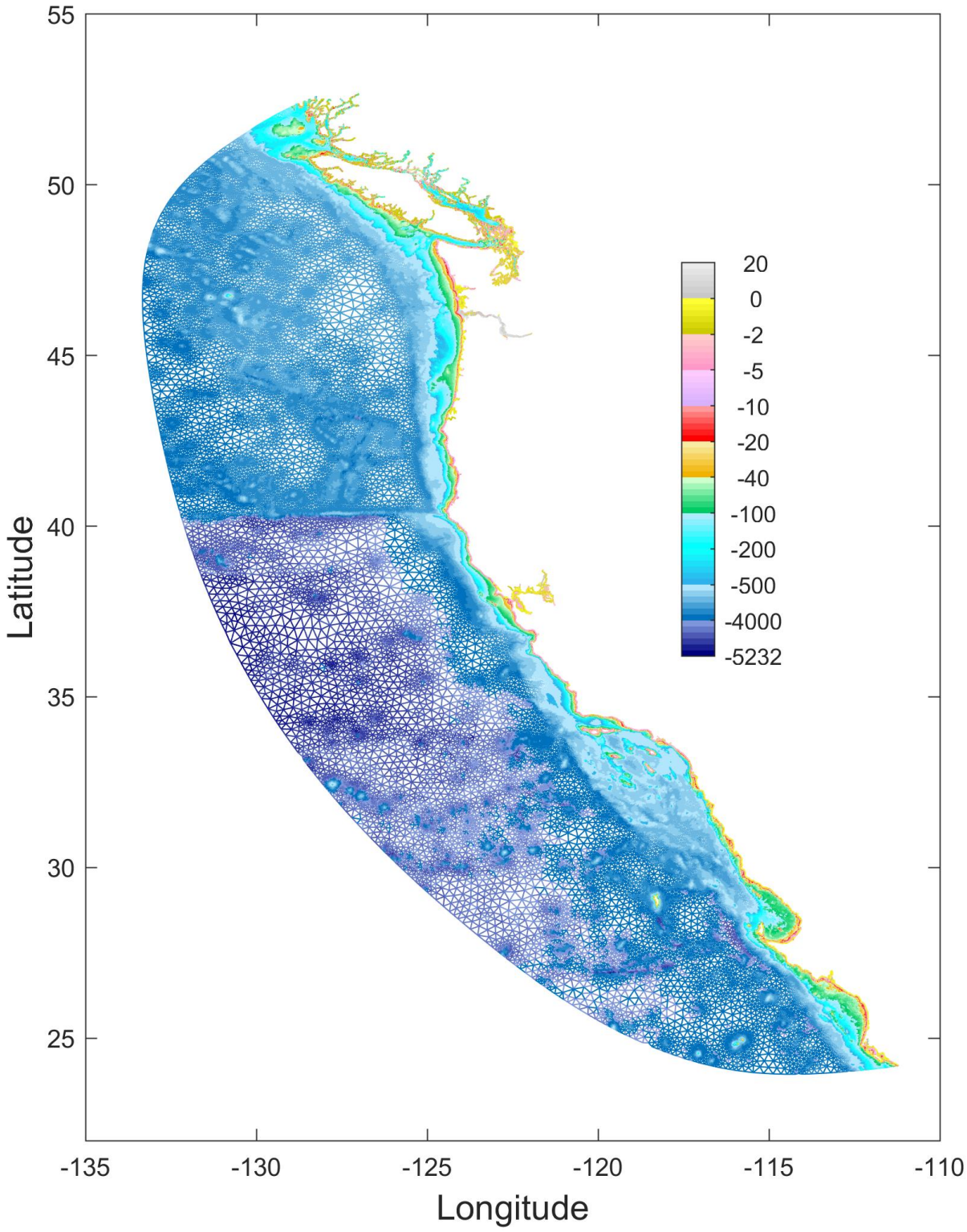

Figure 15 West Coast regional VDatum model mesh. Depth is in meters.

(a) San Juan Islands

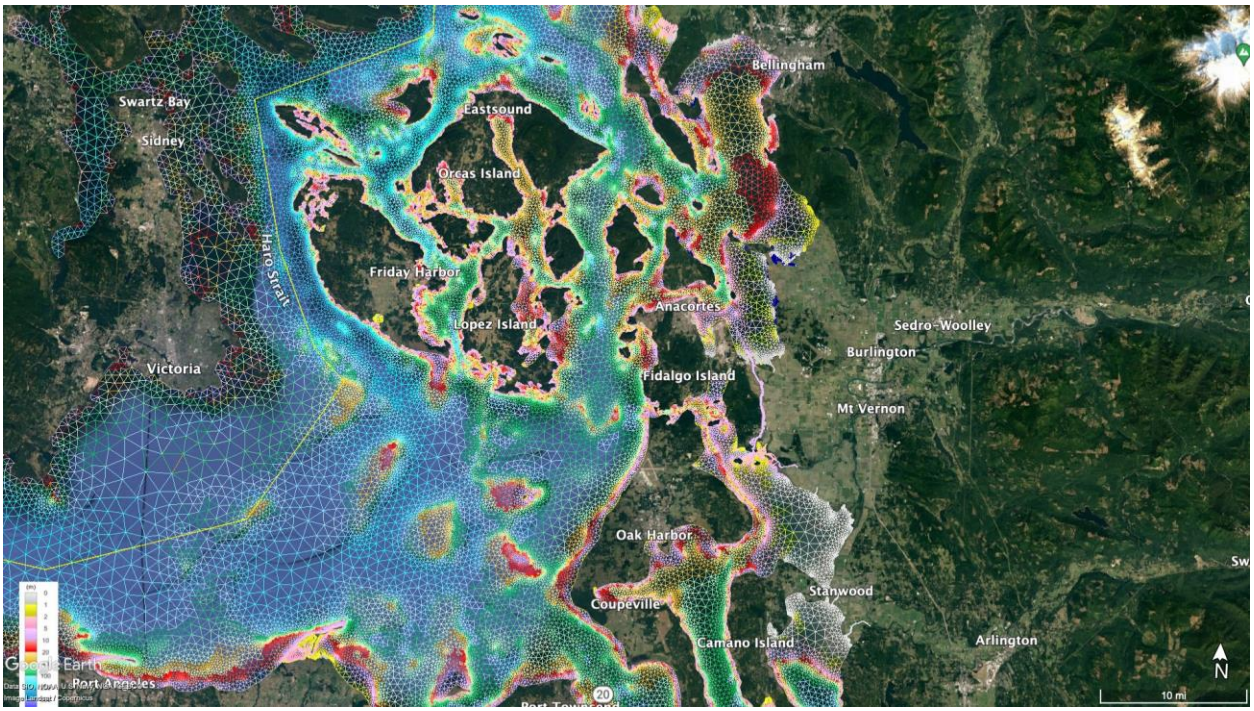

(b) Puget Sound

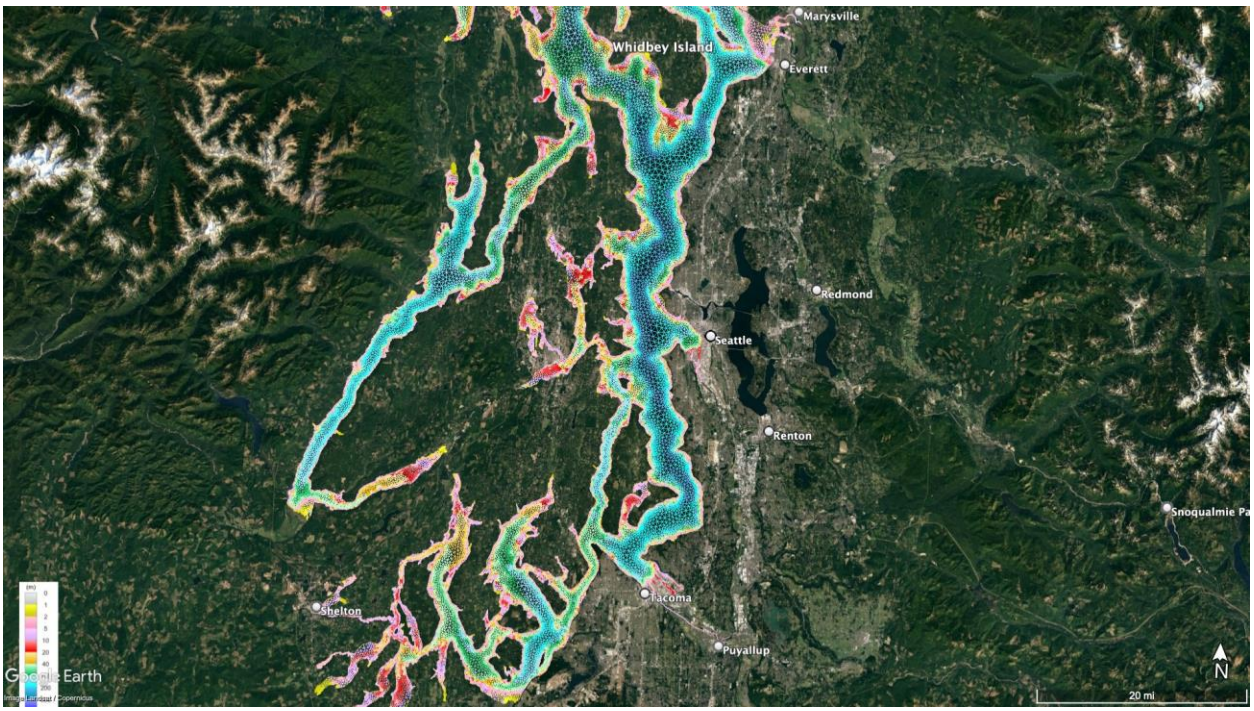

(c) Strait of Juan de Fuca

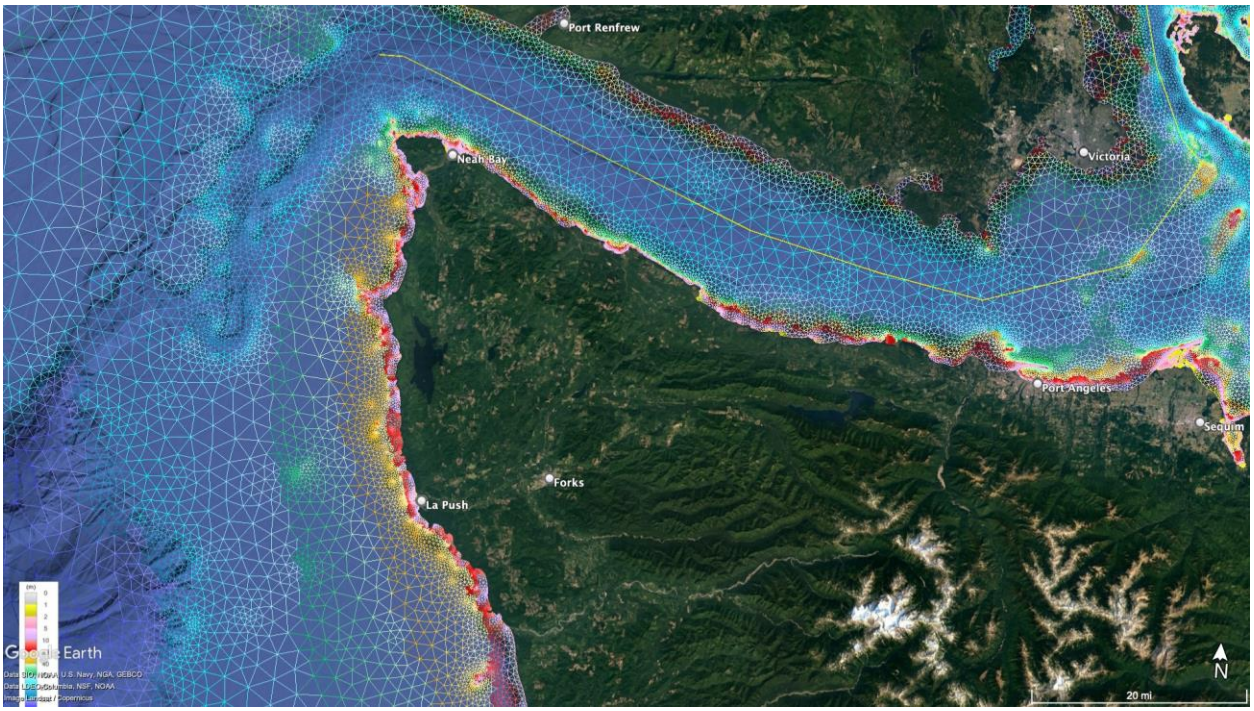

(d) Grays Harbor and Willapa Bay

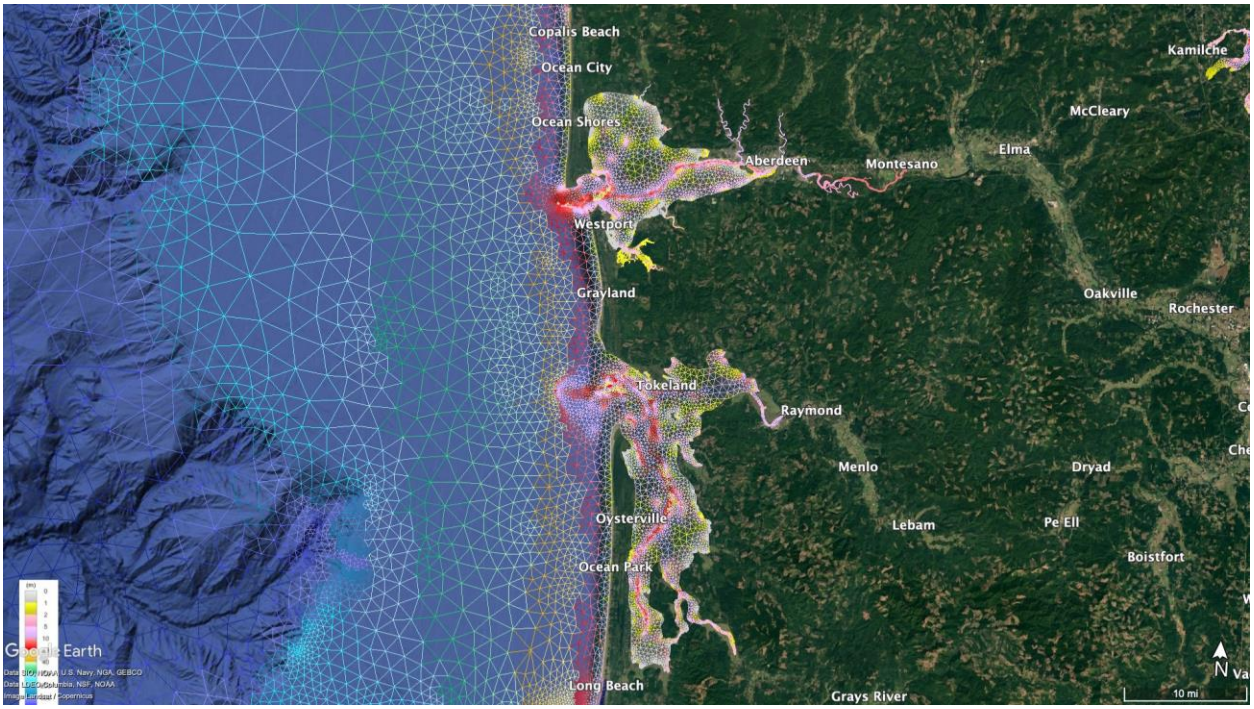

(e) Columbia River

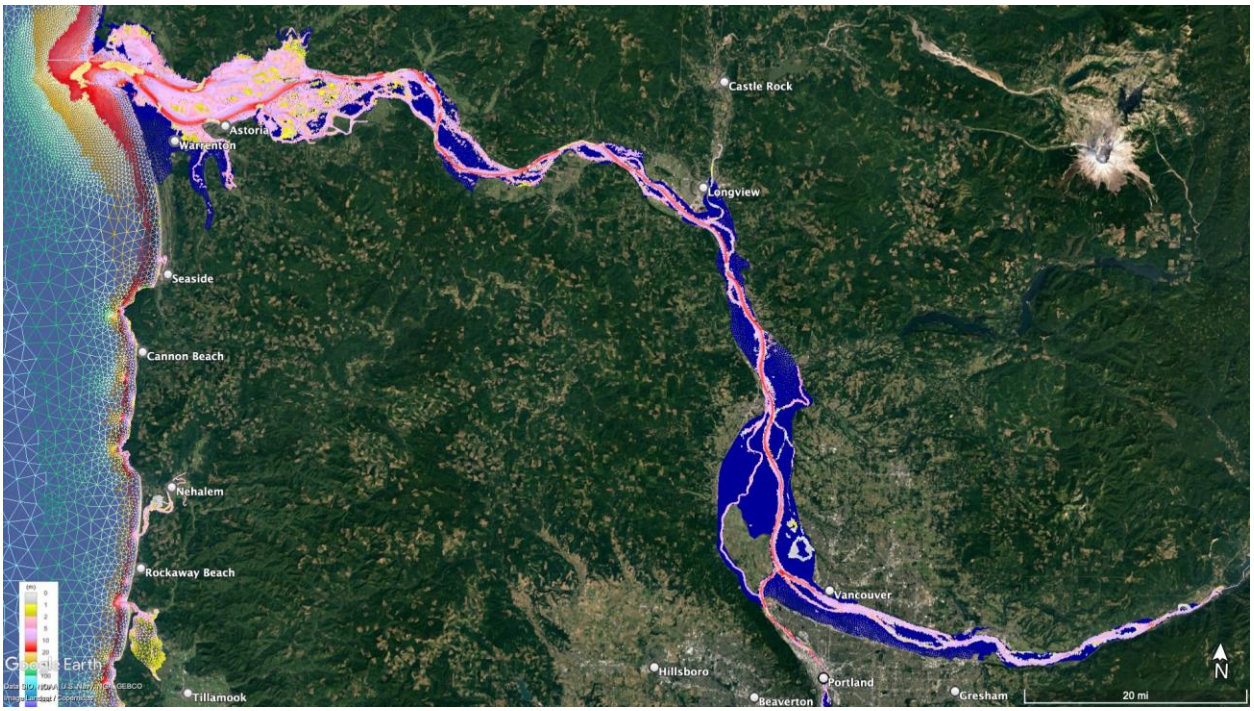

(f) Oregon Coast (northern)

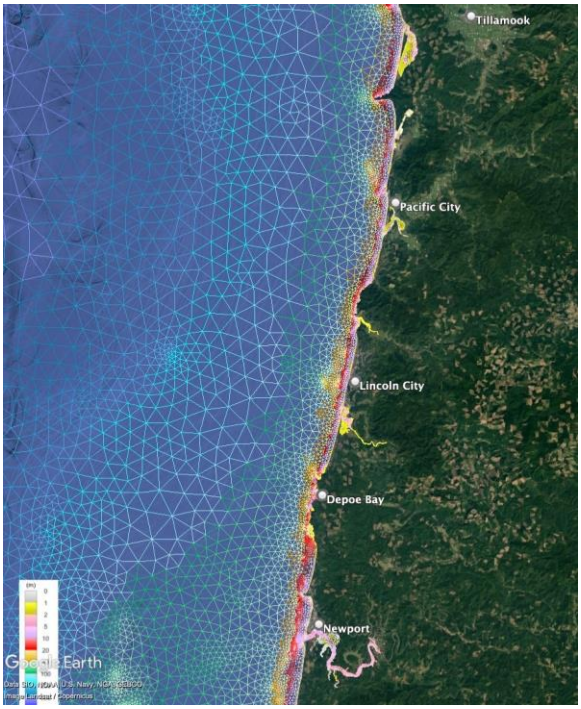

(g) Oregon Coast (south)

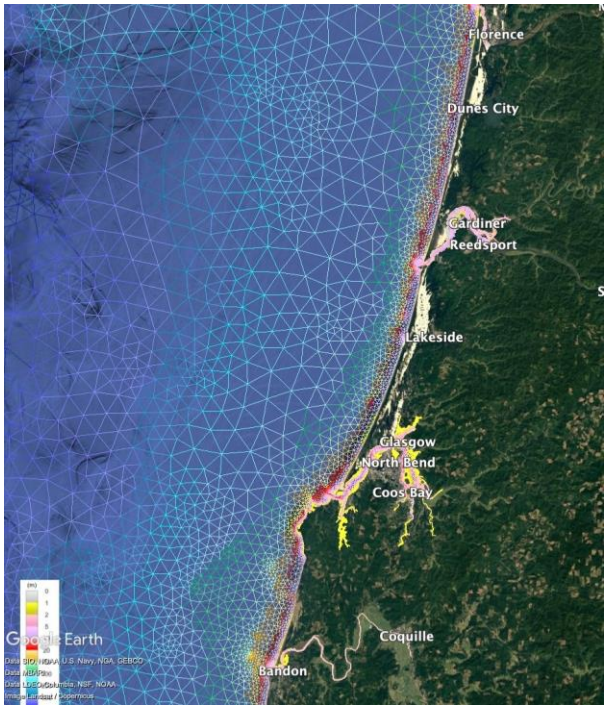

(h)San Francisco Bay entrance

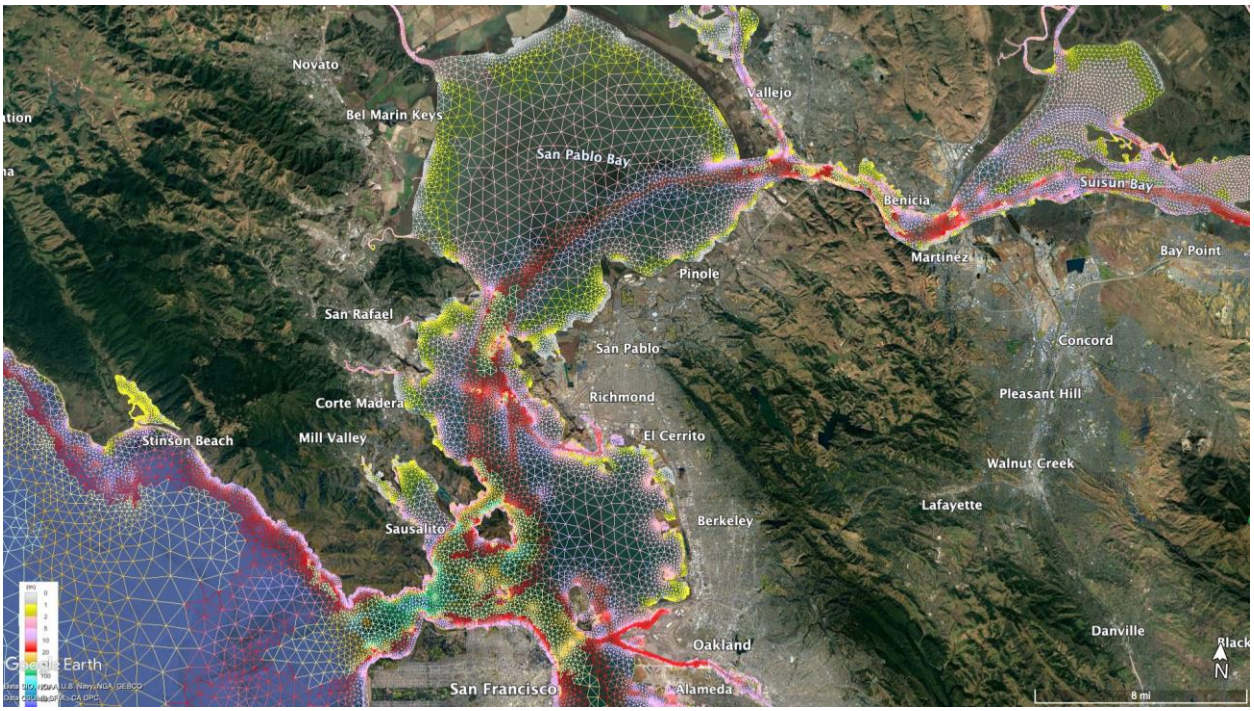

(i) San Francisco Bay

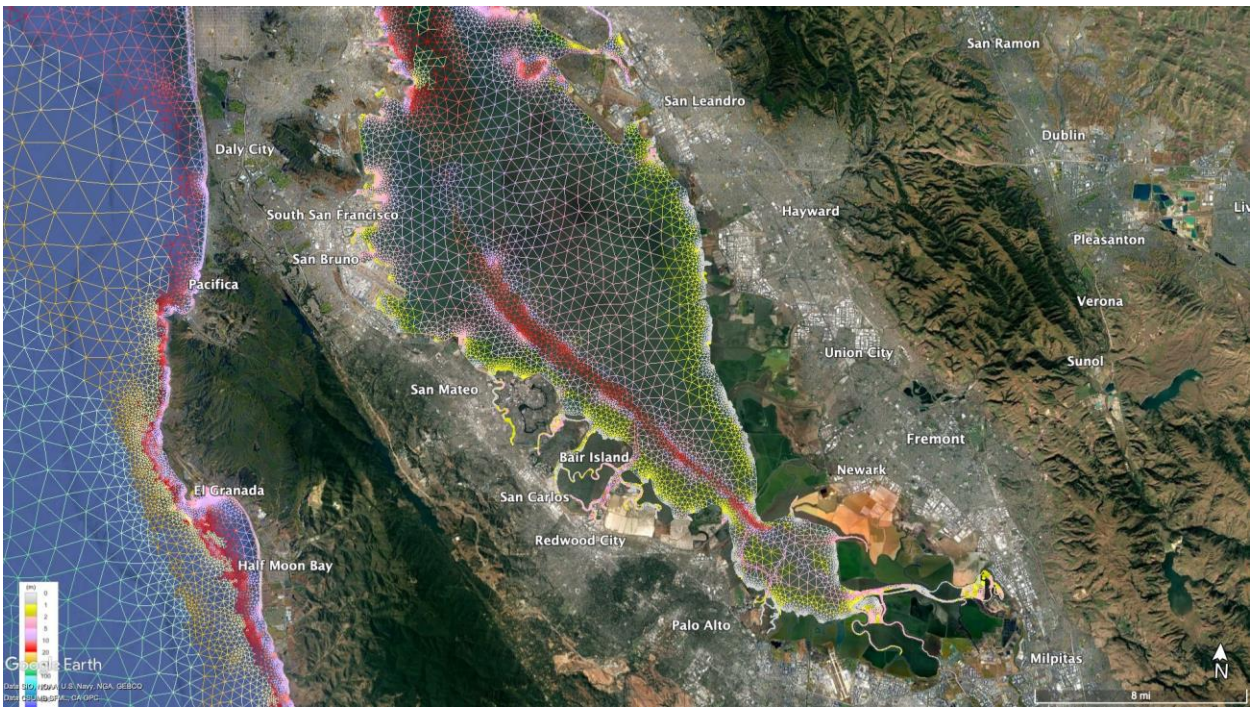

(j)San Francisco Delta

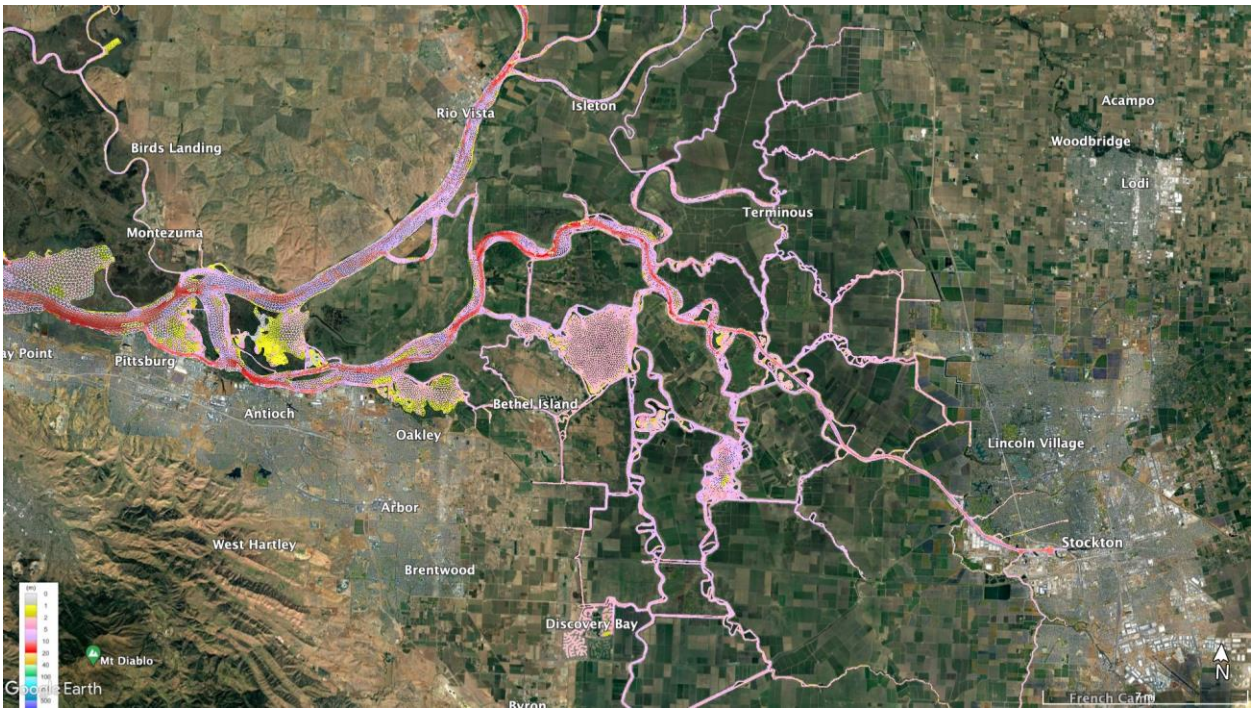

(k) Los Angeles

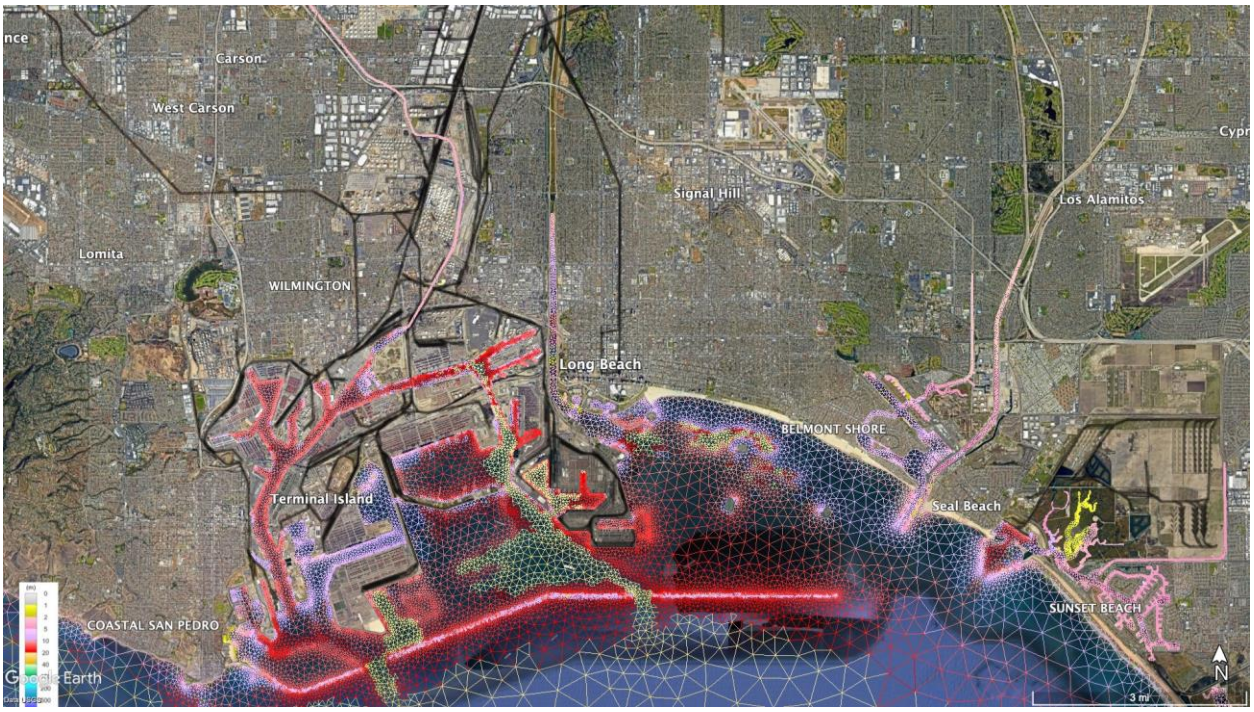

(l) San Diego Bay

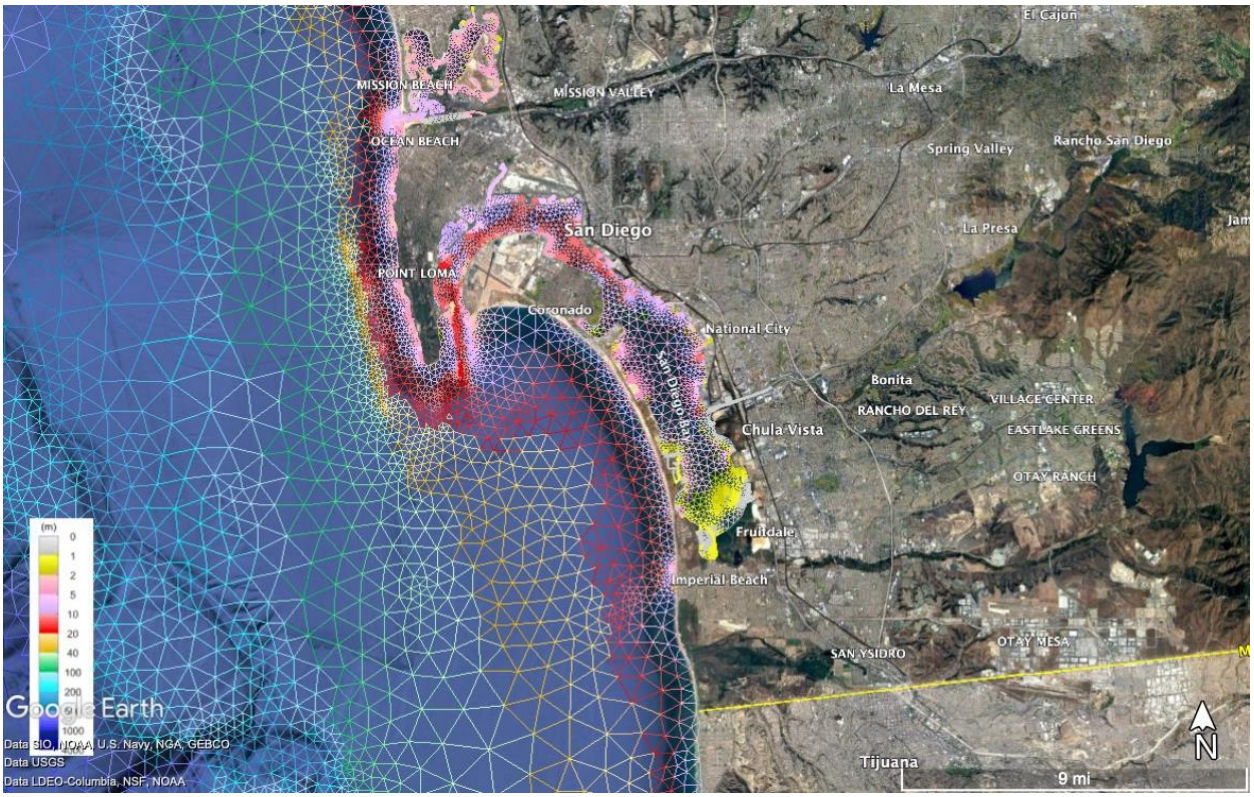

Figure 16 Close-up view of the West Coast mesh. Depth is in meter.

3.5 Model Setup

The open boundary of the model grid offshore West Coast, which consists of 393 nodes, was forced with a synthetic tide that was generated using the amplitude and phase of eight tidal constituents (K_1, O_1, P_1, Q_1, M_2, S_2, N_2, and K_2), which were extracted from the TPXO9 tidal constituent database (Egbert et al, 2002). Similar to Xu et al. (2010), the model runs began with a smooth, hyperbolic tangent, time ramp function, which was applied to the boundary forcing tide for the first 7 days. After comparing the model accuracy among the several VDatum reports for the U.S. West Coast in the past, the nodal factors and equilibrium arguments were taken from Yang et al. (2009), since it gave the best model accuracy. The values correspond to the middle of 1992 (which is in the middle of the 1983-2001 NTDE). A no flow boundary was set for all land segments. In addition,17 nodes were set to river boundary type 22, with non-zero normal flow, for four rivers, including Columbia River.

The model was run for 67 days with a 4-second time step. The clock time is 2 hours 5 minutes using 512 CPUs on Jet. The water surface elevation was output at every node in the grid at every 6 minutes for the last 60 days of the 67-day model run. The output file size is 12.8 GB for fort.63.nc.

During the early stage of model testing, we encountered model instability issues similar to Xu et al. (2010). One such unstable location is also on the northeast open boundary near Queen Charlotte Sound, Canada, where the steep offshore slope might contribute to the unrealistic large modeled speed and elevation. Among the several tests we did, increasing friction, which acts as a sponge layer, appears to be the more effective way to stabilize the model, compared with changing mesh resolutions or numerical parameters/schemes.

In the past, increasing friction was a manually iterative process and it's time consuming. To improve efficiency, we developed a script to automate the friction setting process and therefore to stabilize the ADCIRC model automatically. The initial friction coefficient was set to a constant value of 0.0025 in fort.13. Once the script detects a model run has stopped, it reads in the velocity warning points from the ADCIRC job output file. Then it increases the friction coefficient on the warning points as well as adjacent two layers of points and resubmit the run. The process is iterated until no more warning messages are detected in the job output file. It took approximately 12 hours for 28 iterations to get a stable run for the West Coast model.

For the Columbia River, the current model encountered difficulty in simulating the difference between MSL and xGEOID20B, which increase to 2.3 m at the end of river mesh at the Bonneville Dam. To reduce the model overestimates, the river discharge was tuned to account for part of the sloping river surface based on observations.

4. RESULTS AND DISCUSSION

The model results discussed in sections 4.1 and 4.2 are the results to produce the tidal datums products for the VDatum software updates, in which the representor tides assimilation approach was applied to optimize the boundary conditions. Section 4.3 also includes results from additional testing on incremental variation tides assimilation which will be used for future applications.

4.1 Validation

Figure 17 compares the modeled tidal datums to observations at the 253 tide stations in the U.S. West Coast. Detailed model results and observations at each station are listed in Appendix A. Table 6 summarizes the model error. The CO-OPS' value of the datum at a station is obs_i and the modeled datum is $model_i$. The model error (err_i), percentage error, average error (err_{avg}), and root mean square error (rmse) are calculated as follows:

$$err_i = model_i - obs_i$$

$$\text{percentage } err_i = (model_i - obs_i)/obs_i \times 100$$

$$err_{avg} = \frac{1}{N}\sum_{i=1}^{N}|err_i|$$

$$\text{percentage } err_{avg} = \frac{1}{N}\sum_{i=1}^{N}|\text{percentage } err_i|$$

$$rmse = \sqrt{\frac{1}{N}\sum_{i=1}^{N} {err_i}^2}$$

where i is the i^{th} station, and N is the number of stations used.

The average error is 4.6 (5.2%) and RMSE is 6.5 m for all four datums for the 253 tide stations. For MHHW, MHW, MLW, and MLLW, the average error is 4.7, 3.5, 4.2, and 6.0 cm respectively (Table 6). This is an improvement over the average error of 7.3, 4.5, 6.1, and 8.1 cm for the 105 tide stations reported in Xu et al (2009). The MLLW shows the greatest error among the four datums. We have noticed that the lv8j Fortran code for model datums computation, which was an adoption of CO-OPS' C code of the 25-hour algorithm in the 1980s, had cut off some tips from steep troughs in the model time series. This could result in some errors, especially in MLLW. We are in the process of adapting and revising CO-OPS tidal datum calculator and the 25-hour algorithm to improve the model datum computation (Tolkova, 2022, personal communication).

The model results were further examined geographically in five areas from south to north:
(1) Southern California (from south up to the entrance of San Francisco Bay);
(2) San Francisco Bay and Delta;

(3) Northern California, Oregon and Washington (e.g. the area excludes areas 1,2 4, and 5);
(4) Columbia River;
(5) Puget Sounds, WA.

Figures 18 (a)-(e) compares the model with observations for the five areas and errors are also summarized in Table 6 respectively. As the tidal range increases from south to north in general, so does the model error.

The southern California area shows the best model accuracy, with only 1.1 cm average error for the four tidal datums for 32 tide stations. This is similar to what reported before, the Southern California in Yang et al. (2009) shows the least model error among the past VDatum reports on the West Coast (2.65 cm average error for 38 tide stations). In this update, the average error for Southern California was further reduced by more than half. The water depth quickly increases to 500m from the Southern California coast, which may also contribute to the small model error, due to less significant nonlinear wave dynamics effect.

The San Francisco Bay and Columbia River, where the mesh pieces are adapted from the two well-tested CREOFS and SCHISM models, produce average model error of 4.8 and 3.5 cm, respectively. This is considered to be of reasonably good model accuracy, given the fact that many of the stations are river stations at relatively shallow depth, meanwhile the model has limitations in simulating river dynamics.

Area 3, Northern California, Oregon and Washington, has a relatively large average error of 6.6 cm in MHHW. Figure 18 panel c1 shows a trend of overestimation in MHHW. As will be discussed in section 4.4.3, the incremental variational tides assimilation can reduce this error to 3.8 cm, by optimizing the tidal forcing term for the ADCIRC model.

Puget Sound (area 5) has the largest tidal range and unusual large model error for some stations. For example, station 9446804 has the largest model error among all stations, 25 and 33 cm overestimate in 1.51 m MHHW and 2.02m |MLLW|. Another station is 9449746 which has overestimated error of 27 and 28 cm in MHHW and |MLLW| respectively. Google Earth image reveals both stations are located on an island dock attached to the end of a long pier extended from shore (Figure 19).

Table 6 Model error on tidal datums at tide stations on the U.S. West Coast.

Location	Number of stations	Error	MHHW (m)	MHW (m)	MLW (m)	MLLW (m)	Four datums (m)
Southern California	32	avg. error	0.007	0.007	0.008	0.020	0.011
		%	0.9%	1.2%	1.5%	2.3%	1.5%
		RMSE	0.0095	0.0085	0.010	0.023	0.014
San Francisco Bay & Delta	67	avg. error	0.057	0.031	0.042	0.060	0.048
		%	7.4%	5.2%	6.6%	6.9%	6.5%
		RMSE	0.066	0.036	0.049	0.081	0.061
North CA, OR, WA	62	avg. error	0.066	0.053	0.034	0.079	0.058
		%	6.3%	6.3%	4.2%	6.7%	5.9%
		RMSE	0.083	0.070	0.046	0.096	0.076
Columbia River	26	avg. error	0.031	0.027	0.04	0.036	0.035
		%	3.7%	4.7%	10.2%	4.8%	5.8%
		RMSE	0.037	0.032	0.051	0.044	0.042
Puget Sounds	66	avg. error	0.045	0.039	0.064	0.071	0.055
		%	4.2%	4.4%	6.9%	4.3%	4.9%
		RMSE	0.074	0.061	0.080	0.10	0.080
All	253	avg. error	0.047	0.035	0.042	0.060	0.046
		%	5.1%	4.7%	5.8%	5.3%	5.2%
		RMSE	0.067	0.051	0.056	0.083	0.065

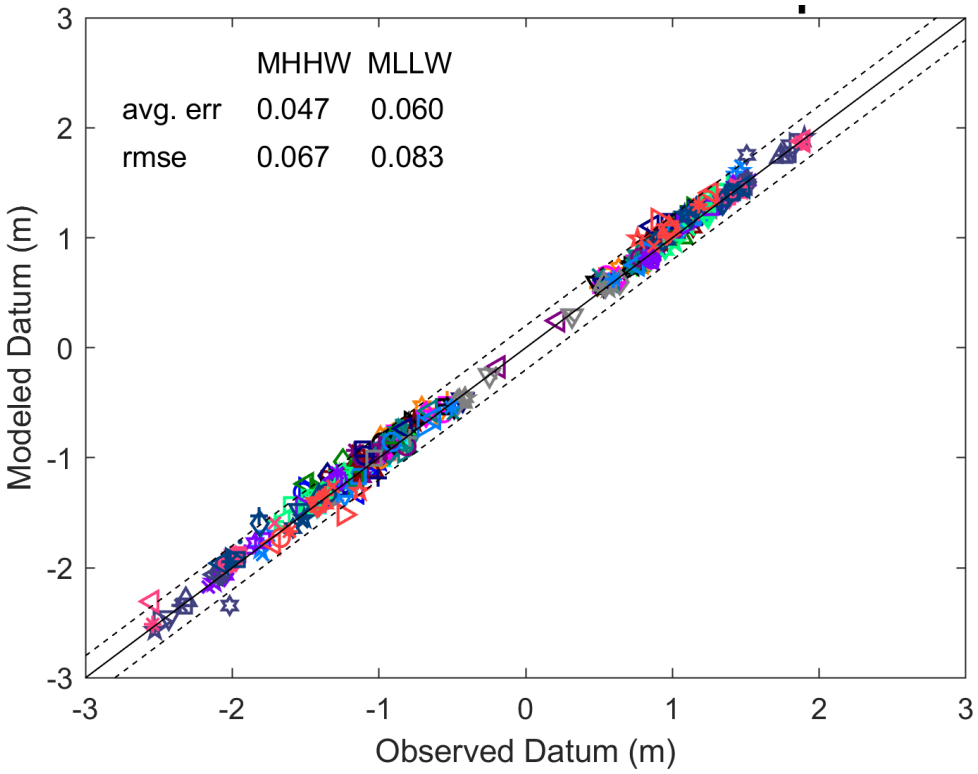
MHHW MLLW
avg. err 0.047 0.060
rmse 0.067 0.083
Modeled Datum (m)
Observed Datum (m)
3
2
1
0
-1
-2
-3

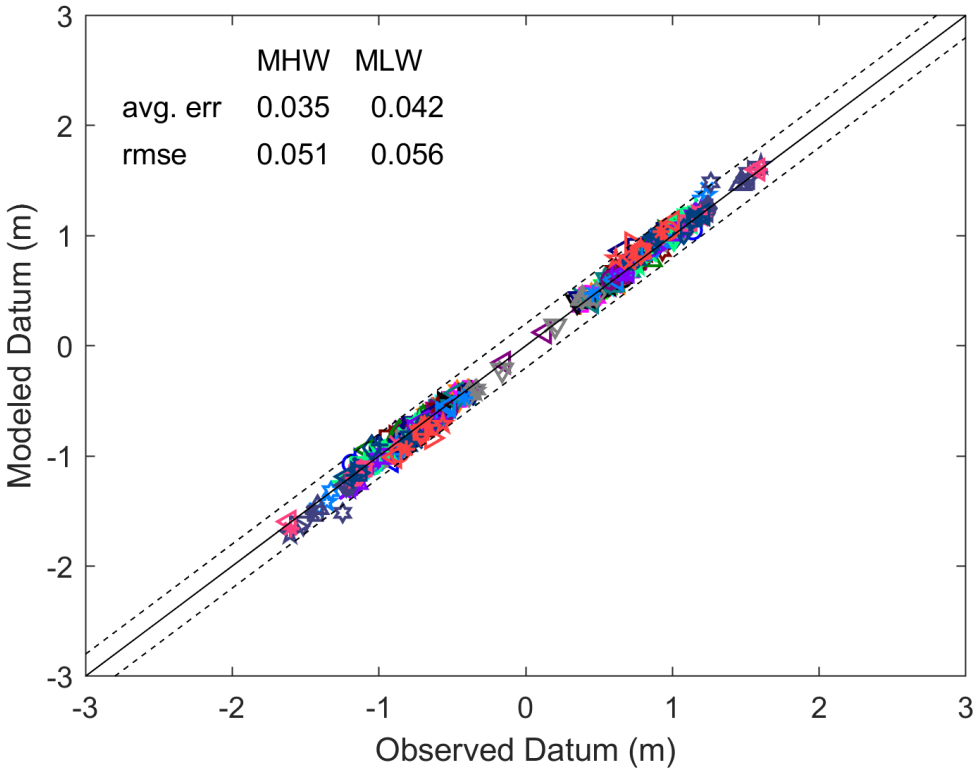
MHW MLW
avg. err 0.035 0.042
rmse 0.051 0.056
Modeled Datum (m)
Observed Datum (m)
3
2
1
0
-1
-2
-3

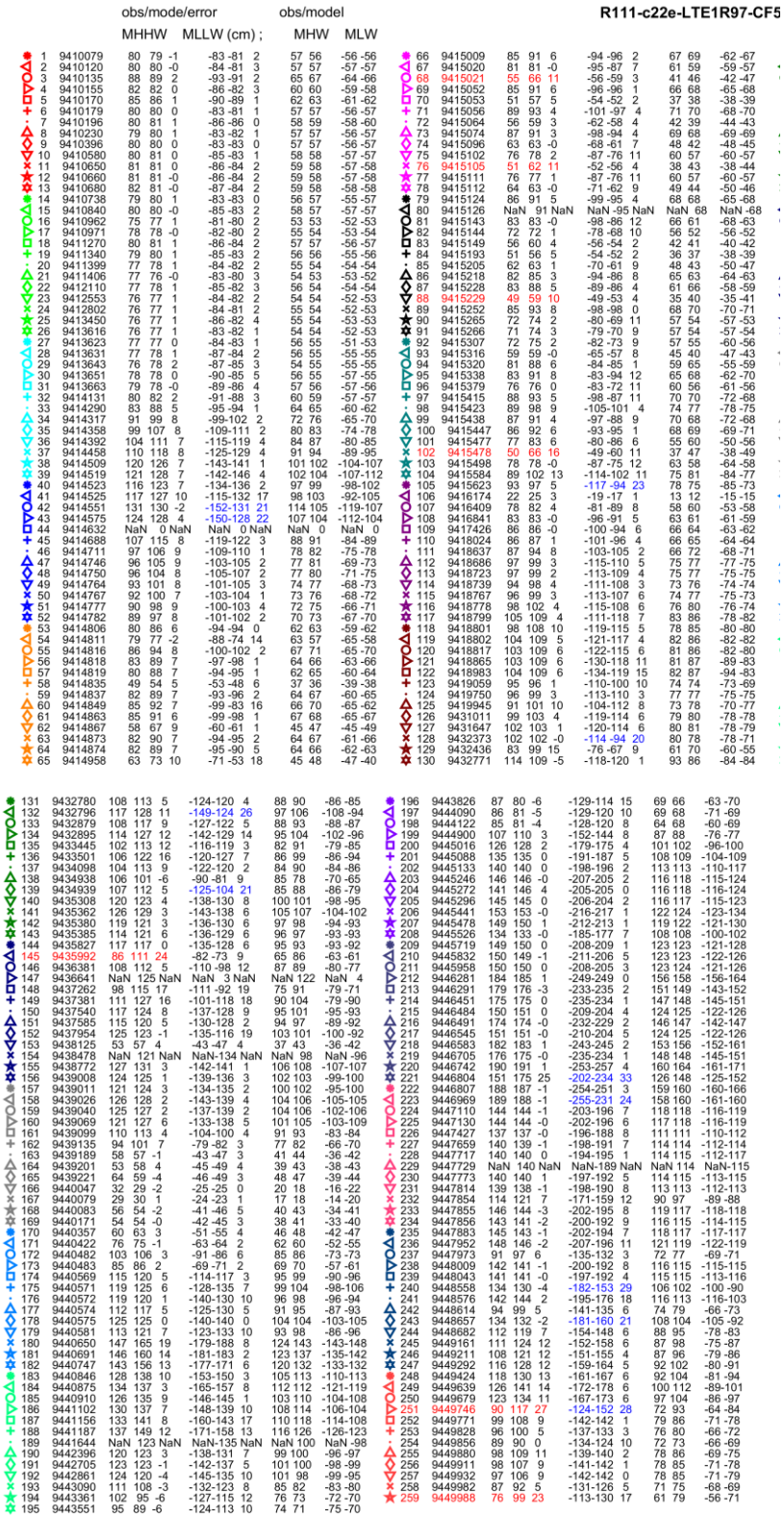

Figure 17 Comparison of the modeled tidal datum and observations for tide stations on the U.S. West Coast. The dashed lines indicate the 0.2m error band.

(a1)

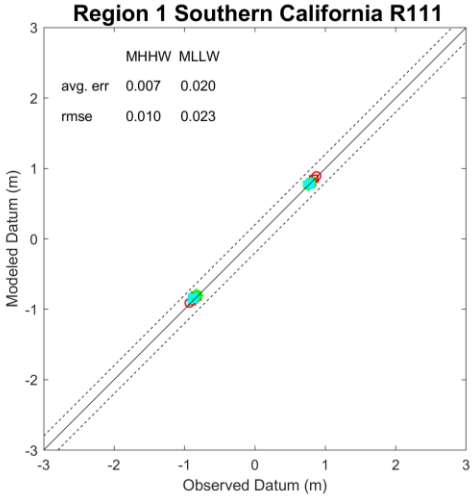
Region 1 Southern California R111
MHHW MLLW
avg. err 0.007 0.020
rmse 0.010 0.023
Modeled Datum (m)
Observed Datum (m)

(a2)

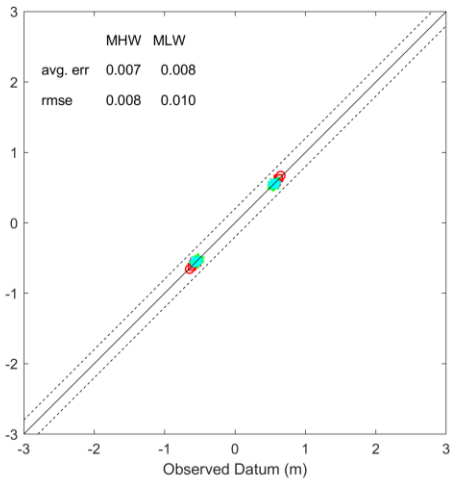
MHW MLW
avg. err 0.007 0.008
rmse 0.008 0.010
Observed Datum (m)

(b1)

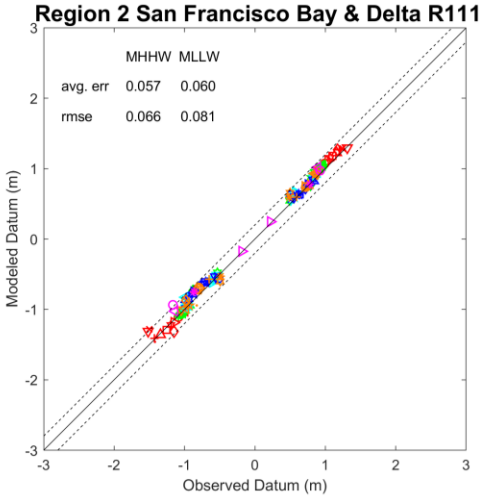
Region 2 San Francisco Bay & Delta R111
MHHW MLLW
avg. err 0.057 0.060
rmse 0.066 0.081
Modeled Datum (m)
Observed Datum (m)

(b2)

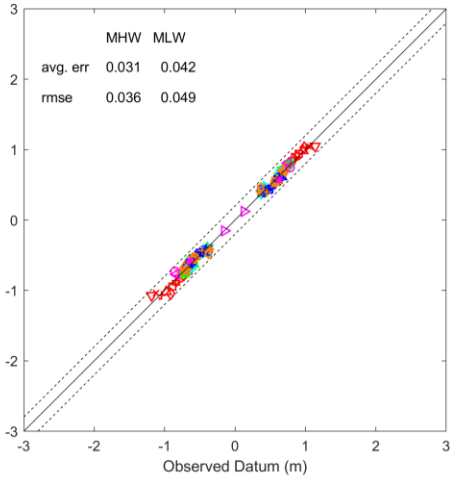
MHW MLW
avg. err 0.031 0.042
rmse 0.036 0.049
Observed Datum (m)

(c1)

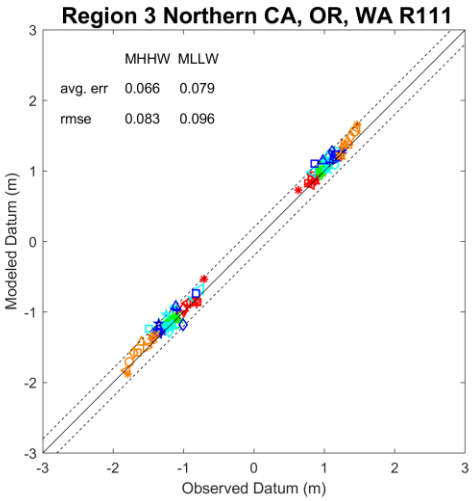
Region 3 Northern CA, OR, WA R111
MHHW MLLW
avg. err 0.066 0.079
rmse 0.083 0.096
Modeled Datum (m)
Observed Datum (m)

(c2)

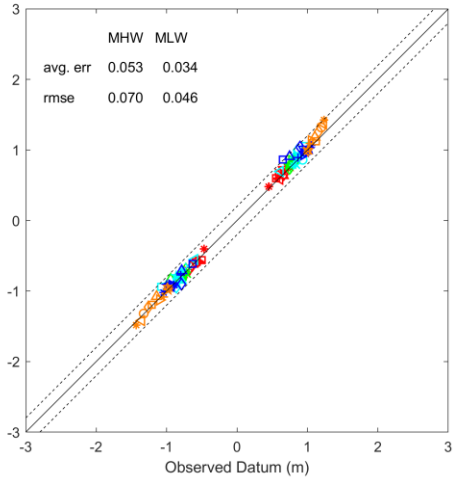
MHW MLW
avg. err 0.053 0.034
rmse 0.070 0.046
Observed Datum (m)

(d1)

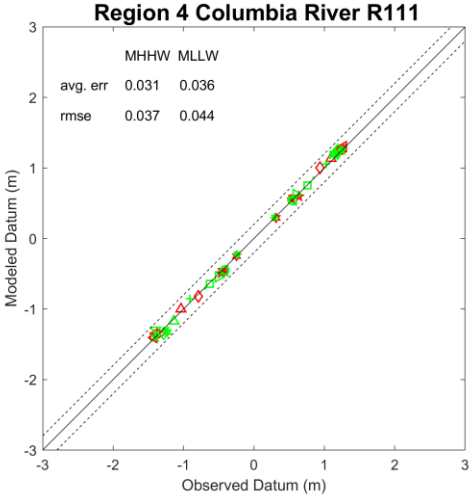
Region 4 Columbia River R111
MHHW MLLW
avg. err 0.031 0.036
rmse 0.037 0.044
Modeled Datum (m)
Observed Datum (m)

(d2)

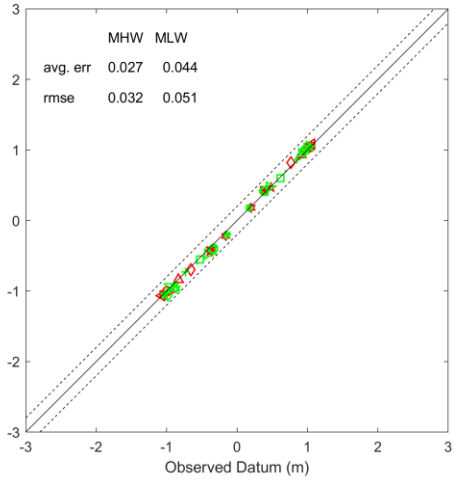
MHW MLW
avg. err 0.027 0.044
rmse 0.032 0.051
Observed Datum (m)

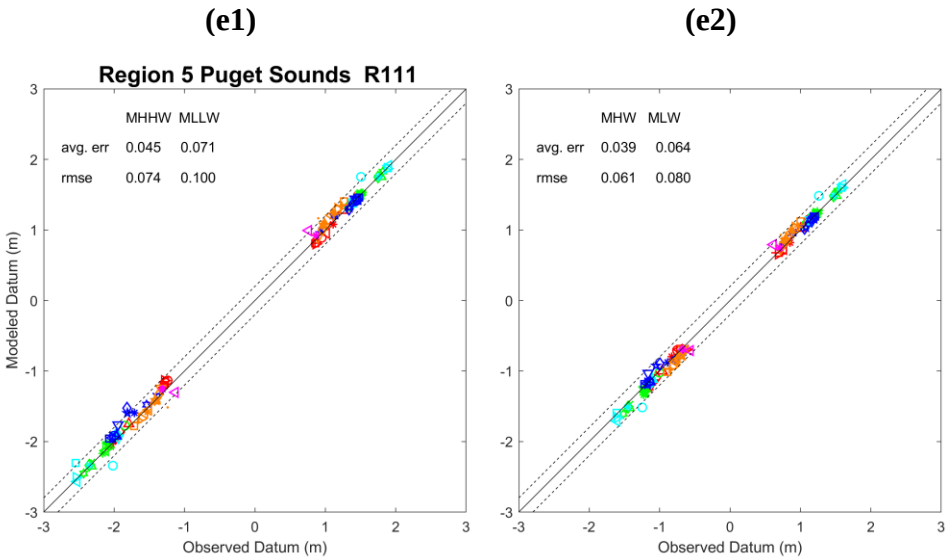

Figure 18 Comparison of the modeled tidal datum and observations for tide stations in five areas on the U.S. West Coast. The dashed lines indicate the 0.2m error band.

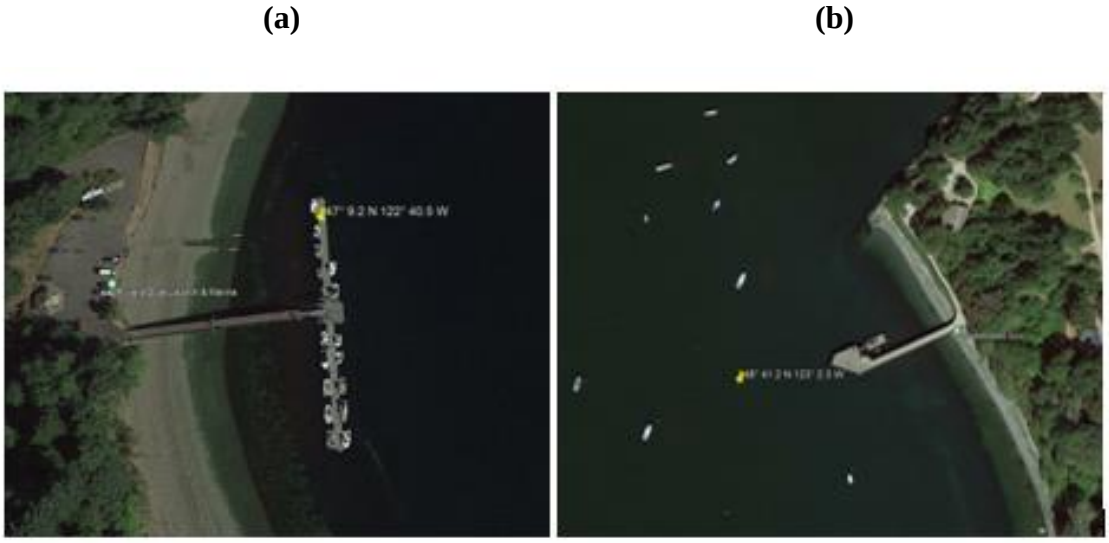

Figure 19 Two stations have large overestimate error in tidal datums: (a) Station 9446804, Sandy Point Anderson Island, Puget Sound, Washington, with 25 and 33 cm. (b) Station 9449746 Waldron Island, Washington. The overestimated error in MHHW and |MLLW| are 25 and 33 cm for (a), and 27 and 28cm for (b), respectively.

4.2 Corrected Tidal Datums and Spatially Varying Uncertainty

The model datums, observations, and errors at the tide stations were then used as inputs to the spatially varying uncertainty method to produce the corrected model datums and uncertainty.

Figure 20 columns a-d show the (a) modeled datums, (b) corrected datums, (c) the adjustment applied, and (d) associated spatially varying uncertainty for the entire model domain. Rows 1-6 are for the six datums, MHHW, MHW, MLW, MLLW, MTL, and DTL, respectively.

The corrected datums (Figure 20b) are the sum of the original model output (column a), and the adjustment (column c). The interpolation adjusts the background model values (column a) over the whole domain. It corrects discrepancies between observations (e.g., Figure 1) and model results for the datums (e.g., column a) at the observation locations by statistically blending the observations and model results. In this way, the final set of tidal datum fields match (within 1 or 2 cm limit) the observations at stations.

The statistical interpolation also produces spatially-varying uncertainty estimates (Figure 20d). The background model uncertainty had been improved at and around tide stations, and to a lesser extent in the offshore area. The maximum uncertainty is 7.6 cm for MHHW (Figure 20 column d row 4). The uncertainty for MTL and DTL are smaller due to the small magnitude for these two datums.

(a)Model **(b) Product** **(c) Correction** **(d) SVU**

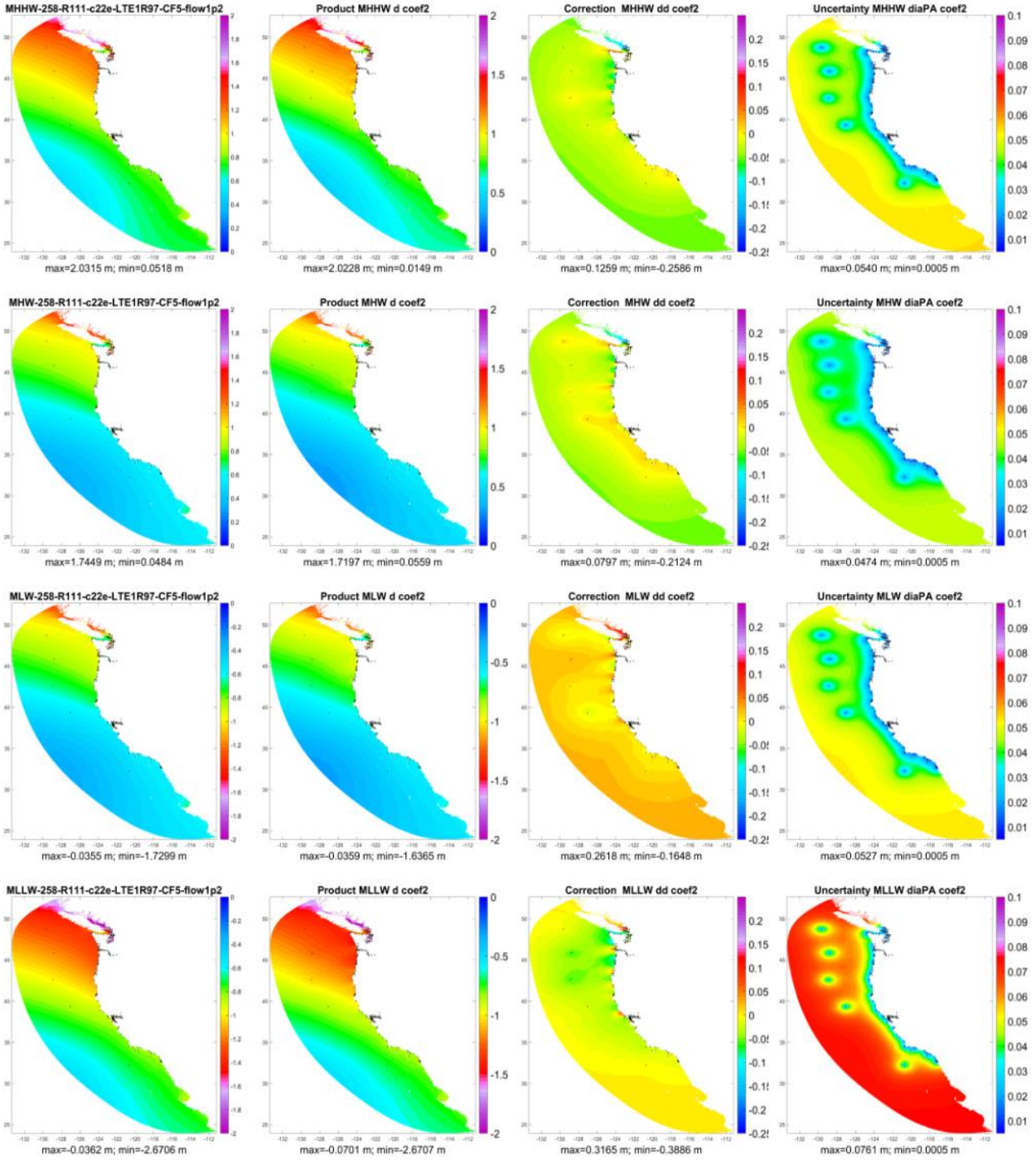

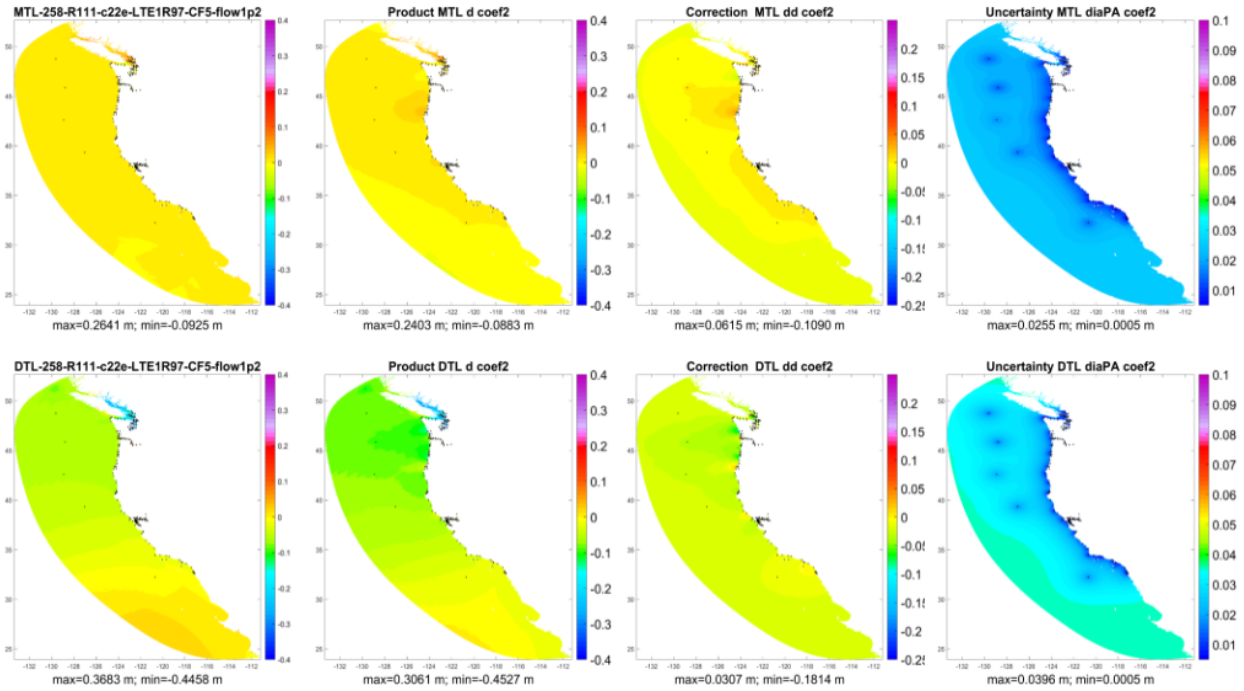

Figure 20 (a) Modeled datums, (b) datum corrected with observations, (c) the correction applied, and (d) associated spatially varying uncertainty for the domain. Rows 1-6 are the six datums, MHHW, MHW, MLW, MLLW, MTL, and DTL, respectively.

4.3 Populating the VDatum Marine Grids and Quality Check

Figure 21a shows the previous bounding polygons in VDatum region (Xu et al., 2010; Yang et al, 2009). In this update, they were reconfigured as shown in Figure 21b, to cover all the tide stations as well as the newly-added rivers. The coastal polygons cover areas similar to the previous ones while an offshore polygon was added to provide extended coverage offshore. In addition, four new inland polygons were added, to resolve the fine rivers that need higher resolution for the marine grids. The updated polygons share the common interfaces with the adjacent polygons whenever possible, e.g., no overlaps between the polygons.

For convenience, we have used the designations and abbreviations for the 13 VDatum areas as listed in Table 7. By using the new polygons, new marine grids were generated for the areas. Table 8 shows the information for the 13 marine grids. Then the datums and spatially varying uncertainty were populated into the new marine grids and saved as GTX files. Figure 22 shows an overview of the 60 GTX files.

A comparison of the VDatum values in the GTX files to the observations at the tide stations is shown in Table 9. The standard deviations range from 0.19 cm(?) to 1.64 cm.

(a)

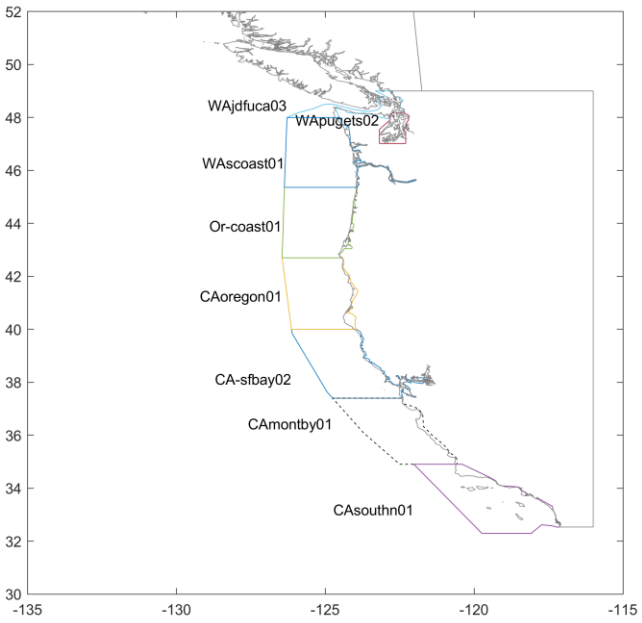

(b)

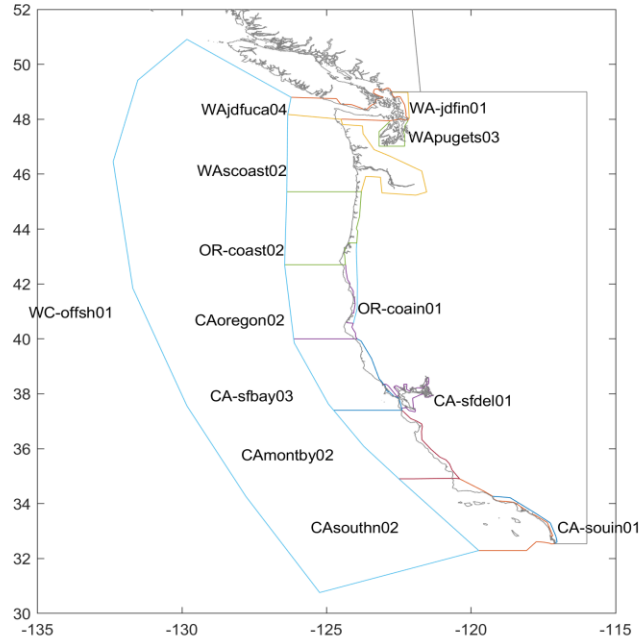

Figure 21 (a) Previous and (b) revised bounding polygons on the West Coast.

Table 7 VDatum area names, directories in the CSDL VDatum archive, and abbreviations.

AREA	ORIGINAL DIRECTORY	REVISED DIRECTORY in 2021
San Francisco Coast	CA_sfbay02	CA_sfbay03
San Francisco Bay & Delta	n/a	CA_sfdel01
San Diego Bay	n/a	CA_souin01
Monterey Bay Coast, CA	CAmontby01	CAmontby02
North CA and South OR coast	CAoregon01	CAoregon02
Southern CA Coast	CAsouthn01	CAsouthn02
Humboldt Bay, Bandon, Coos Bay, Smith River	n/a	OR_coain01
Oregon Coast	OR_coast01	OR_coast02
Drayton Harbor, Marysville,	n/a	WA_jdfin01
Strait of Juan de Fuca	WAjdfuca03	WAjdfuca04
Puget Sound, WA	WApugets02	WApugets03
WA coast	WAscoast01	WAscoast02
Offshore West Coast	n/a	WC_offsh01

Table 8 VDatum grid information for the marine grids.

VDatum Area	Southwestern Limit	Northeastern Limit	Vertical Spacing Deg	Horizontal Spacing Deg	No.of Vert. Nodes	No. of Hori. Nodes	Size of one GTX file (MB)
CA_sfbay03	37.398999 233.861374	40.001999 237.610374	0.001	0.001	2604	3750	85
CA_sfdel01	37.341100 236.934110	38.613100 238.696310	0.0006	0.0006	2121	2938	55
CA_souin01	32.562300 240.731990	34.268700 242.975390	0.0006	0.0006	2845	3740	93
CAmontby02	34.902000 235.242866	37.401000 239.601866	0.001	0.001	2500	4360	96
CAoregon02	39.999000 233.547464	42.705000 236.055464	0.001	0.001	2707	2509	60
CAsouthn02	32.290000 237.499	34.924000 242.8990	0.001	0.001	2635	5401	125
OR_coain01	40.568199 235.570900	43.502199 236.065900	0.0006	0.0006	4891	826	35
OR_coast02	42.699000 233.547462	45.368000 236.204462	0.001	0.001	2670	2658	62
WA_jdfin01	48.019100 237.207430	48.997100 237.858430	0.0006	0.0006	1631	1086	16
WAjdfuca04	47.945700 233.656000	49.146700 237.823000	0.001	0.001	1202	4168	44
WApugets03	47.015700 236.815700	48.019700 237.82270	0.001	0.001	1005	1008	9
WAscoast02	45.232000 233.622457	48.176000 238.462457	0.001	0.001	2945	4841	125
WC_offsh01	30.755000 227.615000	50.915000 240.270	0.005	0.005	4033	2532	90

Table 9 Comparison of data and GTX interpolated values (Standard deviations, cm) in the marine grids for tidal stations.

Area	No. of Tide Stations	MHHW	MHW	DTL	MTL	MLW	MLLW
CA_sfbay03	4	0.43	1.05	0.3	0.52	0.43	1.15
CA_sfdel01	71	0.61	0.66	0.55	0.46	0.65	0.65
CA_souin01	5	0.24	0.31	0.19	0.83	0.39	0.24
CAmontby02	9	0.52	0.54	0.51	0.56	0.54	0.53
CAoregon02	4	0.43	1.05	0.3	0.52	0.43	1.15
CAsouthn02	16	0.22	0.2	0.14	0.08	0.22	0.12
OR_coain01	19	0.77	0.72	0.69	0.58	0.71	0.76
OR_coast02	14	0.65	0.6	0.68	0.61	0.57	0.88
WA_jdfin01	2	0.08	0.26	0.05	0.31	0.3	0.16
WAjdfuca04	38	0.66	0.67	0.6	0.55	0.8	0.75
WApugets03	28	0.62	0.52	0.61	0.5	0.62	0.72
WAscoast02	40	1.15	1.24	0.81	0.83	0.76	1.64
WC_offsh01	5	0.24	0.31	0.19	0.83	0.39	0.24

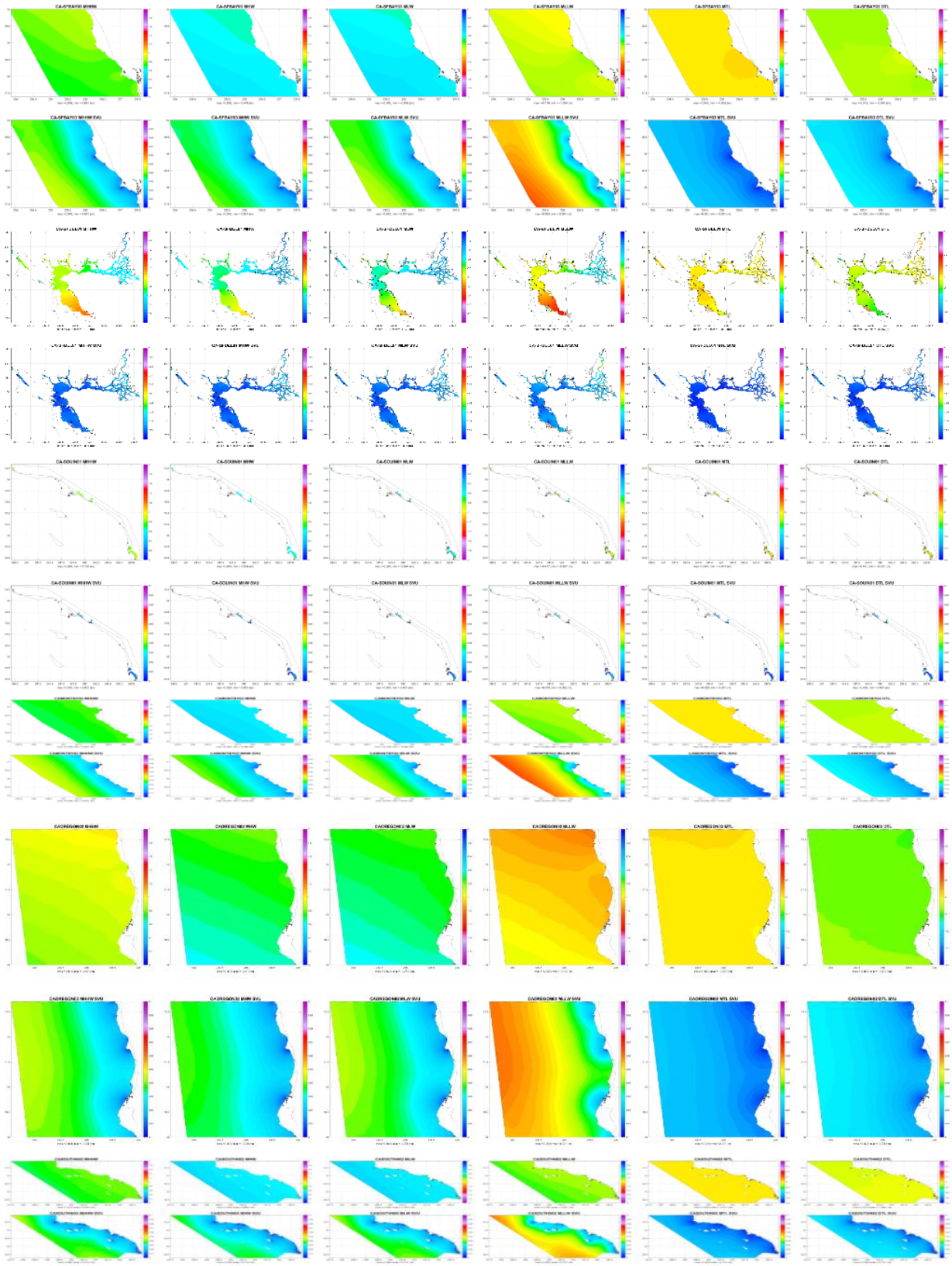

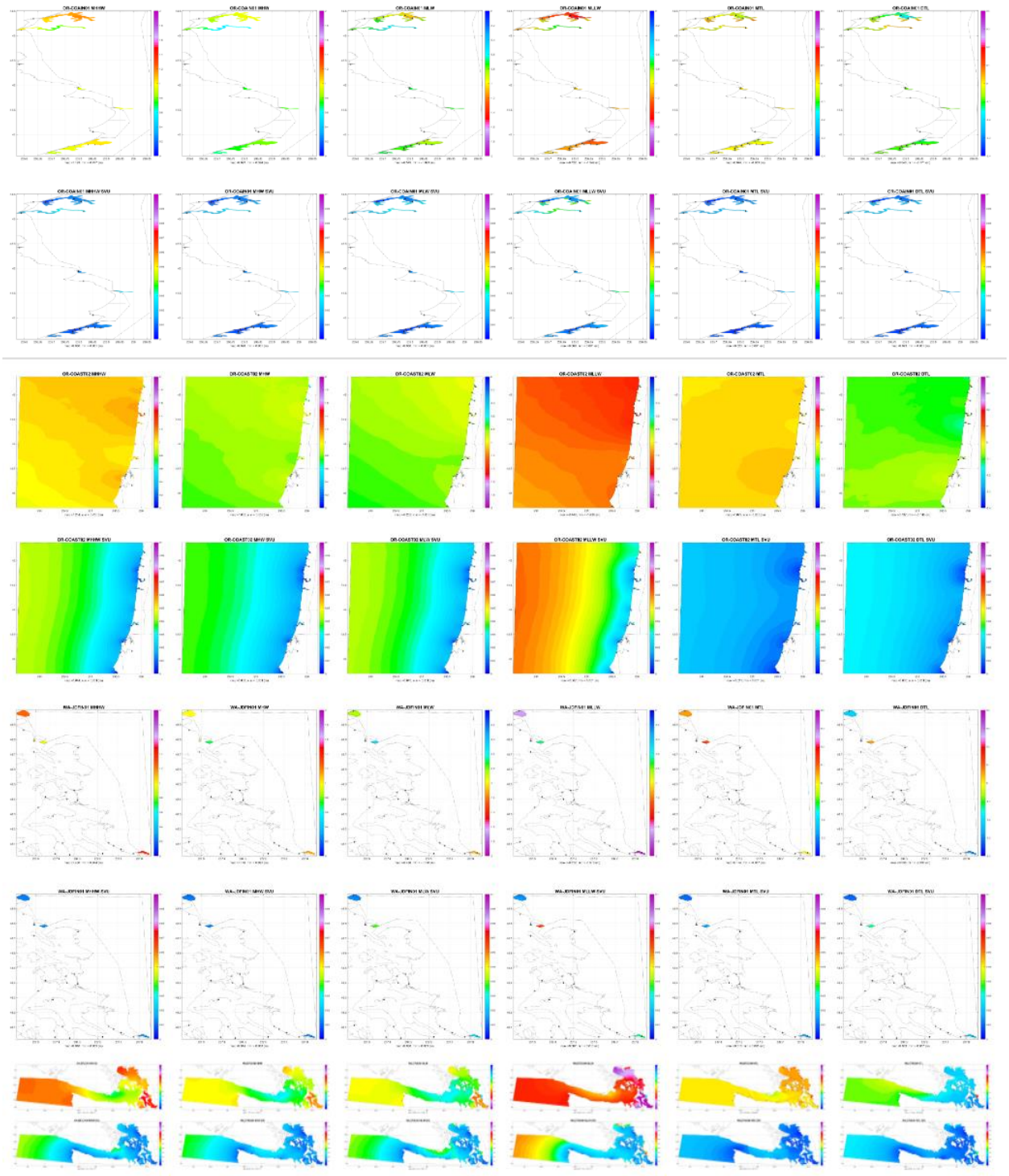

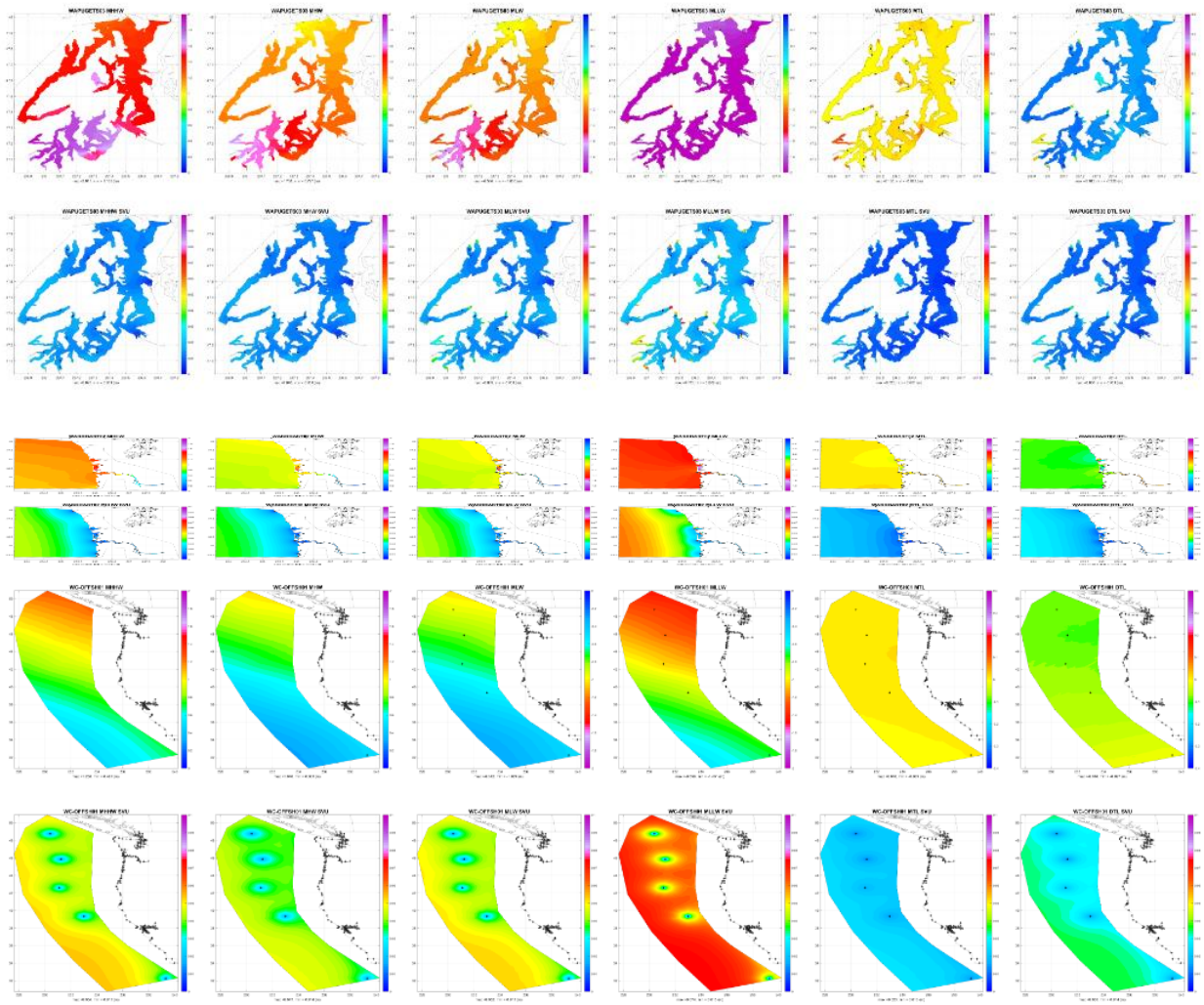

Figure 22 (1a-13a) Datum products and (1b-13b) spatially varying uncertainty for the 13 marine grids on the U.S. West Coast.

4.4 Tides Assimilation

In this section, we document the testing of the data assimilation algorithm. The representor approach was first tested for a global and then a high-resolution San Francisco case before it was applied to the West Coast VDatum regional model. In addition, we also tested the incremental variational data assimilation method using the West Coast VDatum model.

4.4.1 Assimilating Deep Ocean Data into a Global Tide Model

The data assimilation reprentator scheme described in section 2.2 was first tested on a global scale. A global mesh was developed by using OceanMesh2D, with a total number of 883,514 nodes (Figure 23). A 300 m minimum resolution was applied to the continental U.S., Puerto Rico, the

U.S. Virgin Islands, Alaska, Hawaii, and Guam while globally the minimum resolution is 2.5 km. The shoreline boundaries were from the 2017 GSHHG database (Wessel et al., 1996). The bathymetry data were taken from two DEMs, SRTM 15-sec DEM (for the majority of the grid) and ETOPO1 (for depth around Antarctic only).

In this study, we used observations from the 151 deep ocean BPR stations for data assimilation (Figure 23). In addition, we have chosen 38 CO-OPS tide stations at open coast along the U.S. West Coast as an independent dataset for model validation. Stations in bays and rivers were not used here since the global model's resolution was not enough to resolve such fine coastal features.

Eight major tidal constituents, M_2, S_2, O_1, K_1, N_2, K_2, P_1 and Q_1, were assimilated. Computational time for each is approximately 45 min on a PC using Matlab. Figure 24 (a)-(h) shows the global solutions for amplitude and phase for the eight tidal constituents. Model results at the 38 open-coast tide stations at the U.S. West Coast were plotted along with the observations as in Figure 25. Table 10 summarizes the model error in the amplitudes for both datasets.

The averaged model error at the 38 tide stations is quite small, ranging from 2.8% to 7% (0.6 – 2.7cm). Semi-diurnal tides (M_2 and S_2) show less error than the diurnal tides (O_1 and K_1). The two tide stations on the right for M_2 in Figure 25 have the largest model error. These two stations are near the entrance of Strait of Juan De Fuca. Preliminary test shows that by using the NOS bathymetry survey data in the area and Puget Sound, the model error can be reduced at the two stations.

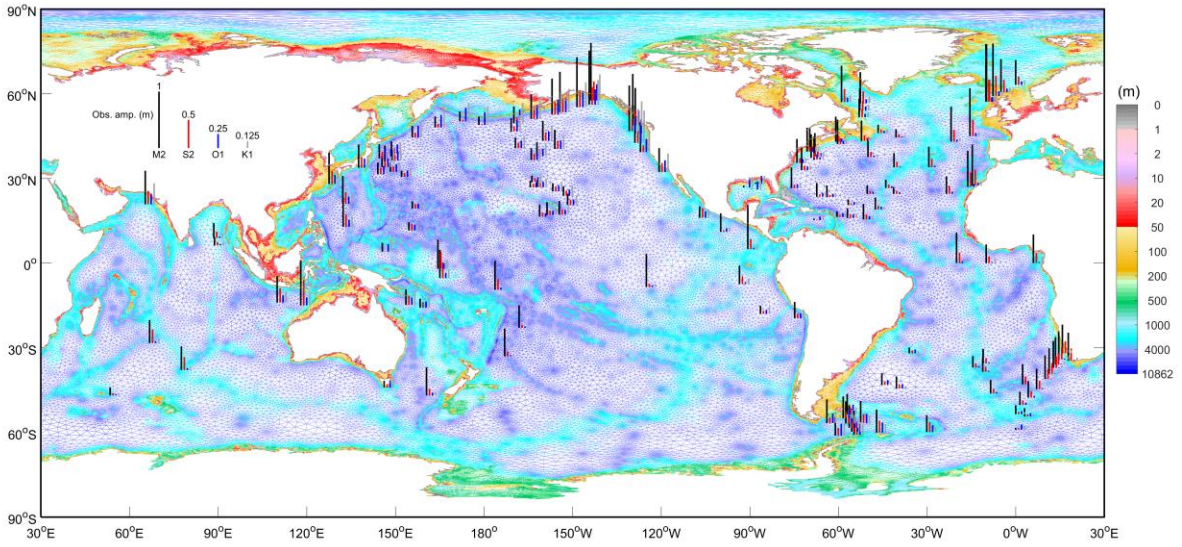

Figure 23 (a) Global tide model grid and locations of 151 Bottom Pressure Recorder (BPR) stations. Height of the bars indicate the M_2, S_2, O_1, and K_1 amplitudes at the stations. BPR data are provided by Ray (2013).

(a) M_2

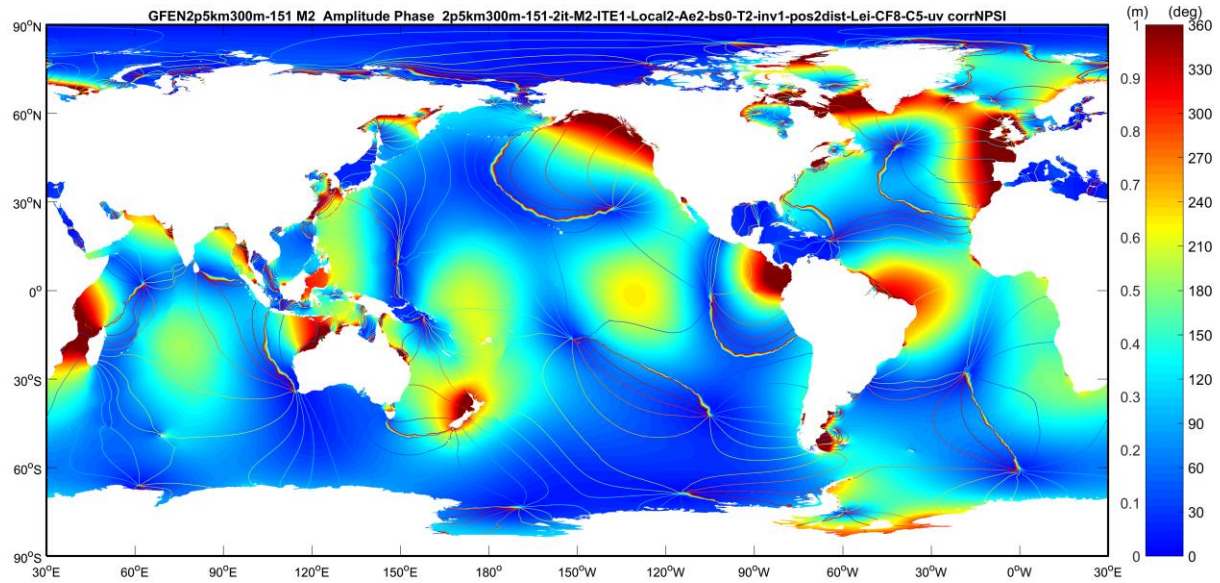
GFEN2p5km300m-151 M2 Amplitude Phase 2p5km300m-151-2it-M2-ITE1-Local2-Ae2-bs0-T2-inv1-pos2dist-Lei-CF8-C5-uv corrNPSI
(m)
(deg)
90°N
60°N
30°N
0°
30°S
60°S
90°S
30°E
60°E
90°E
120°E
150°E
180°
150°W
120°W
90°W
60°W
30°W
0°W
30°E

(b) S_2

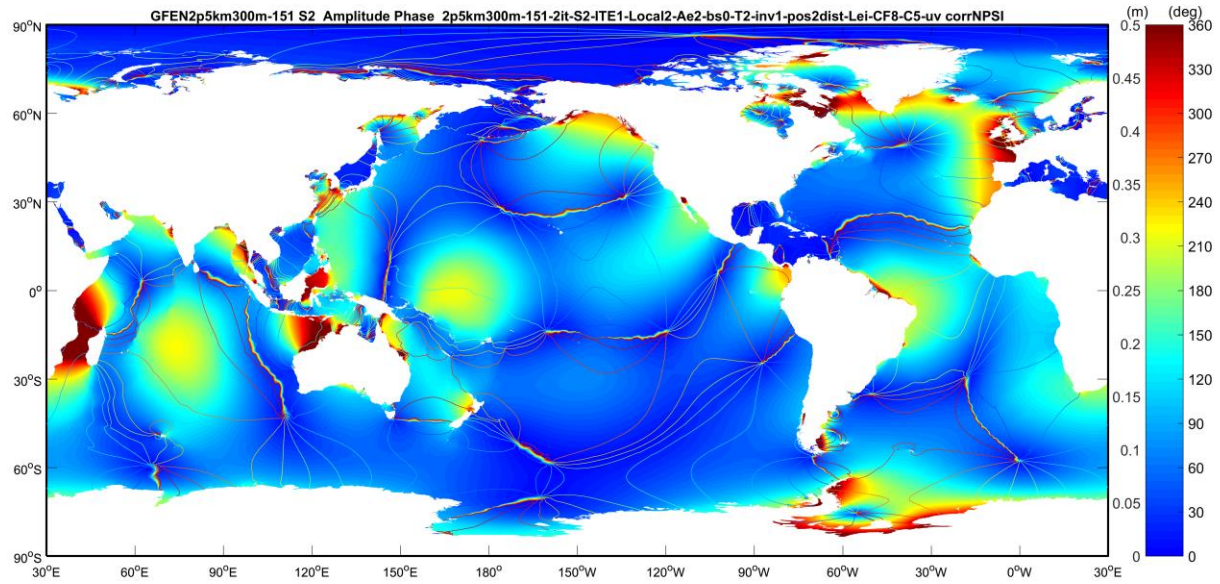
GFEN2p5km300m-151 S2 Amplitude Phase 2p5km300m-151-2it-S2-ITE1-Local2-Ae2-bs0-T2-inv1-pos2dist-Lei-CF8-C5-uv corrNPSI
(m)
(deg)
90°N
60°N
30°N
0°
30°S
60°S
90°S
30°E
60°E
90°E
120°E
150°E
180°
150°W
120°W
90°W
60°W
30°W
0°W
30°E

(c) K_1

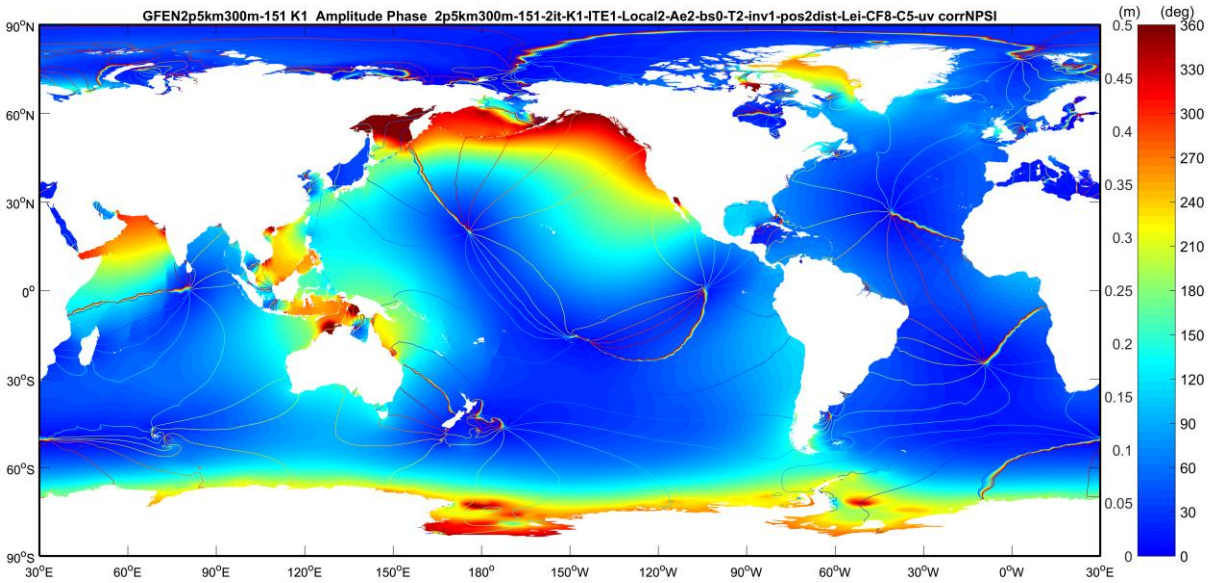
GFEN2p5km300m-151 K1 Amplitude Phase 2p5km300m-151-2it-K1-ITE1-Local2-Ae2-bs0-T2-inv1-pos2dist-Lei-CF8-C5-uv corrNPSI
(m)
(deg)
90°N
60°N
30°N
0°
30°S
60°S
90°S
30°E
60°E
90°E
120°E
150°E
180°
150°W
120°W
90°W
60°W
30°W
0°W
30°E

(d) O_1

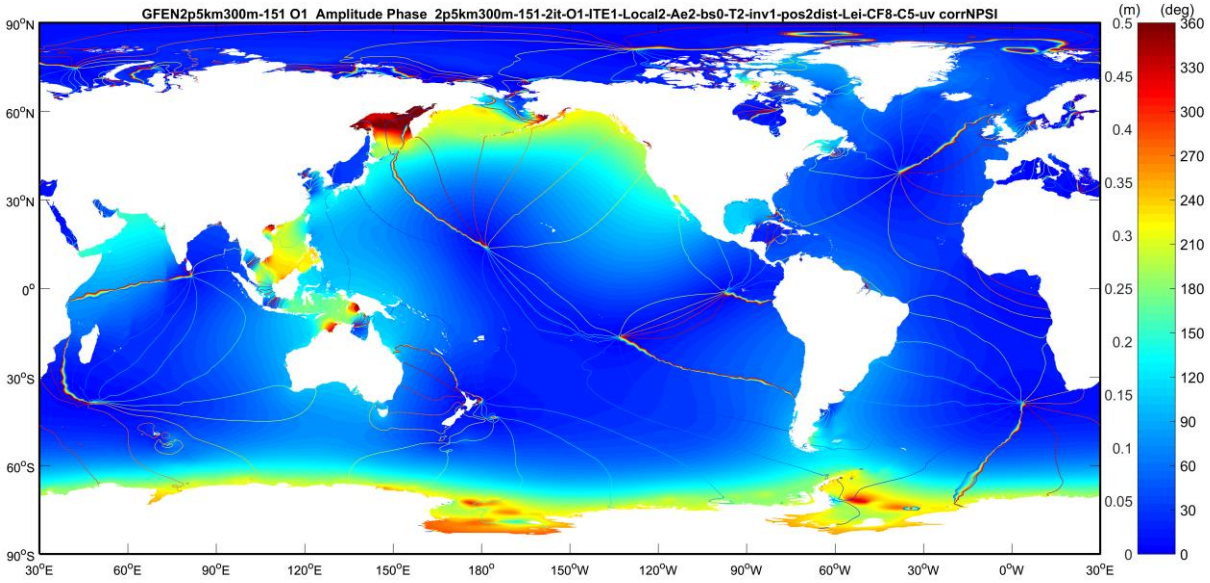
GFEN2p5km300m-151 O1 Amplitude Phase 2p5km300m-151-2it-O1-ITE1-Local2-Ae2-bs0-T2-inv1-pos2dist-Lei-CF8-C5-uv corrNPSI
(m)
(deg)
90°N
60°N
30°N
0°
30°S
60°S
90°S
30°E
60°E
90°E
120°E
150°E
180°
150°W
120°W
90°W
60°W
30°W
0°W
30°E

(e) N_2

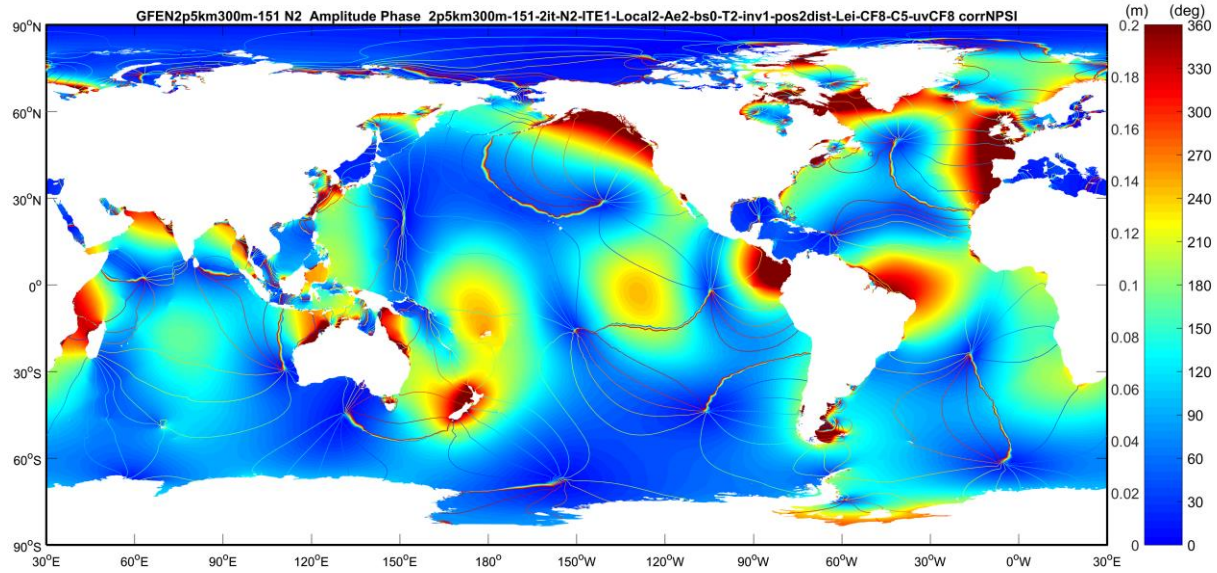
GFEN2p5km300m-151 N2 Amplitude Phase 2p5km300m-151-2it-N2-ITE1-Local2-Ae2-bs0-T2-inv1-pos2dist-Lei-CF8-C5-uvCF8 corrNPSI
(m)
(deg)
90°N
60°N
30°N
0°
30°S
60°S
90°S
30°E
60°E
90°E
120°E
150°E
180°
150°W
120°W
90°W
60°W
30°W
0°W
30°E
0.2
0.18
0.16
0.14
0.12
0.1
0.08
0.06
0.04
0.02
0
360
330
300
270
240
210
180
150
120
90
60
30
0

(f) K_2

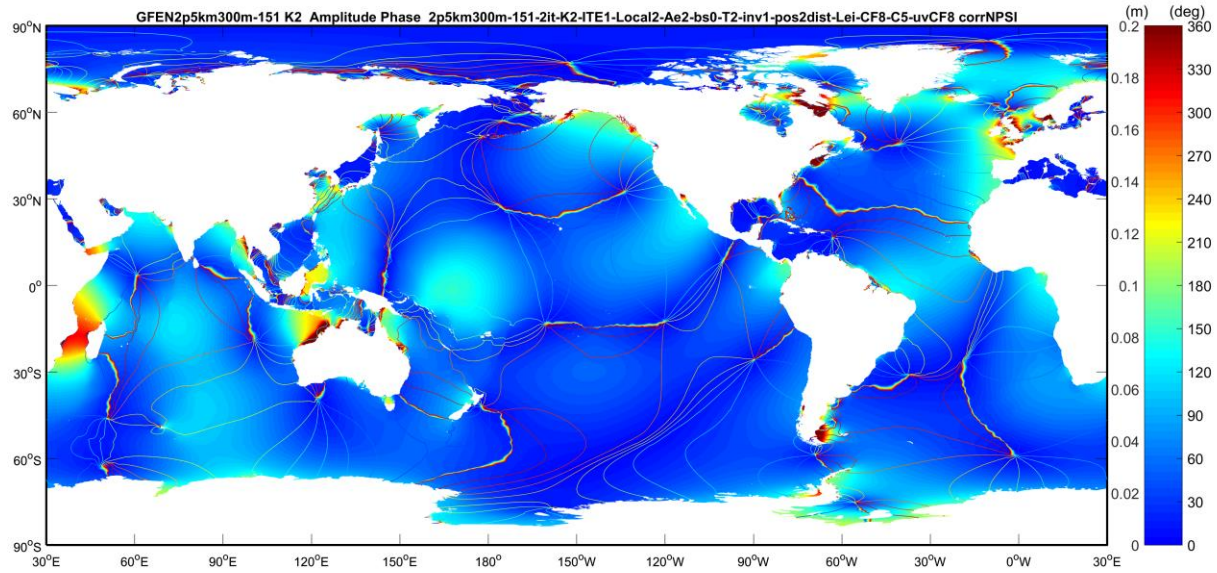
GFEN2p5km300m-151 K2 Amplitude Phase 2p5km300m-151-2it-K2-ITE1-Local2-Ae2-bs0-T2-inv1-pos2dist-Lei-CF8-C5-uvCF8 corrNPSI
(m)
(deg)
90°N
60°N
30°N
0°
30°S
60°S
90°S
30°E
60°E
90°E
120°E
150°E
180°
150°W
120°W
90°W
60°W
30°W
0°W
30°E
0.2
0.18
0.16
0.14
0.12
0.1
0.08
0.06
0.04
0.02
0
360
330
300
270
240
210
180
150
120
90
60
30
0

(g) P_1

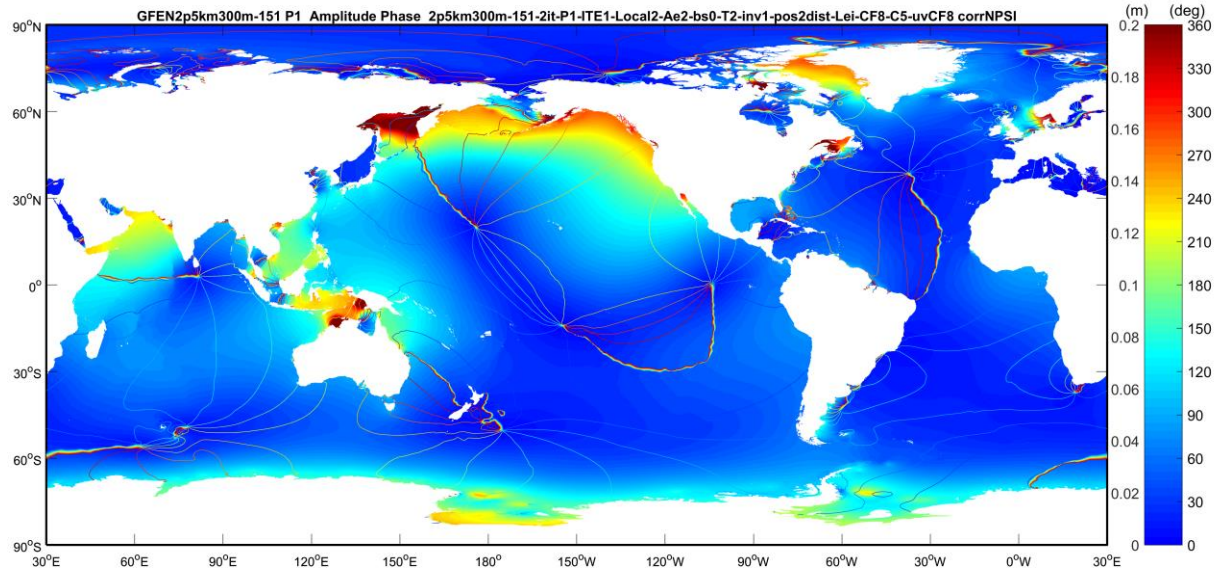

(h) Q_1

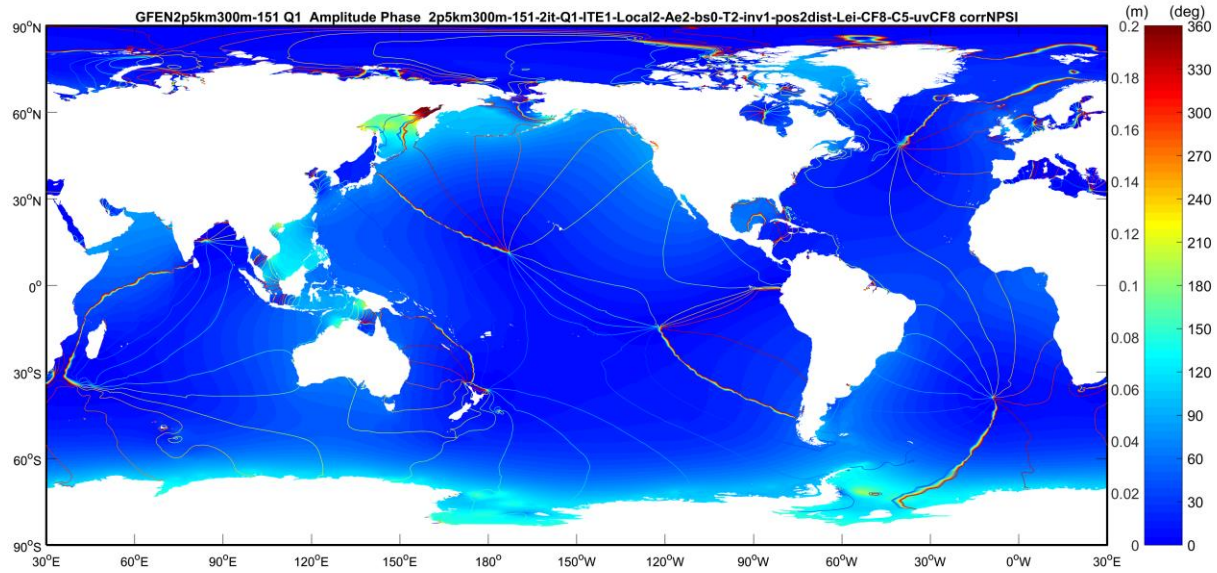

Figure 24 Amplitude and phase for eight tidal constituents by assimilating the 151 Deep Ocean BPR data. (a-h) M_2, S_2, O_1, K_1, N_2, K_2, P_1, and Q_1.

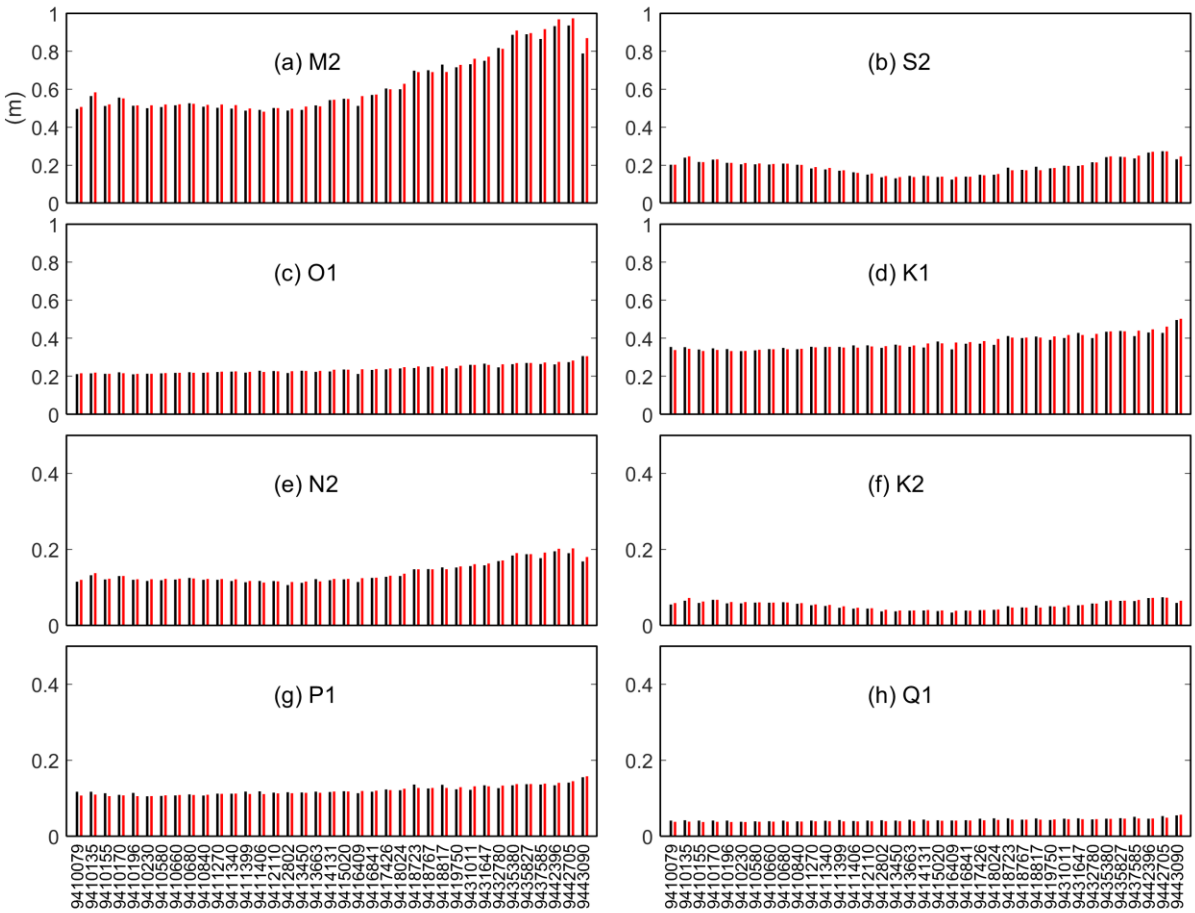
(a) M2
(b) S2
(c) O1
(d) K1
(e) N2
(f) K2
(g) P1
(h) Q1
(m)
9410079
9410135
9410155
9410170
9410196
9410230
9410580
9410660
9410680
9410840
9411270
9411340
9411399
9411406
9412110
9412802
9413450
9413663
9414131
9415020
9416409
9416841
9417426
9418024
9418723
9418767
9418817
9419750
9431011
9431647
9432780
9435380
9435827
9437585
9442396
9442705
9443090

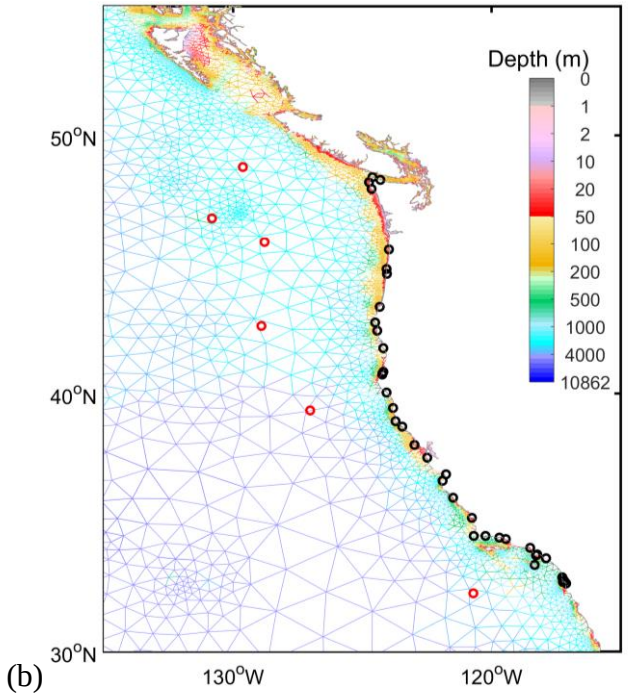
Depth (m)
0
1
2
10
20
50
100
200
500
1000
4000
10862
50°N
40°N
30°N
130°W
120°W

(b)

Figure 25 (a) Observed (black) and modeled (red) amplitudes in meters from the global model at 38 open coast tide stations along the U.S. West Coast from south to north. (b) Locations of the open coast tide stations.

Table 10 Average model error at 151 deep-ocean BPRs and 38 open coast tide stations from the global tide model.

Tidal Constituents	Stations	Error in (cm)	Error in (%)
M_2	151 BPRs 38 Tide Stations	0.6 1.9	2.5 2.9
S_2	151 BPRs 38 Tide Stations	0.3 0.5	3.9 2.9
O_1	151 BPRs 38 Tide Stations	0.2 0.5	2.4 2.3
K_1	151 BPRs 38 Tide Stations	0.3 1.1	2.8 2.9
N_2	151 BPRs 38 Tide Stations	0.2 0.4	3.0 3.1
K_2	146 BPRs 38 Tide Stations	0.8 0.2	23.9 4.5
P_1	146 BPRs 38 Tide Stations	0.6 0.4	23.1 3.2
Q_1	148 BPRs 38 Tide Stations	0.2 0.2	14.9 4.9

4.4.2 Tides assimilation on a high-resolution San Francisco model

To evaluate how the tides assimilation performs on shallow coastal features such as bays and rivers, we did the second test on a high resolution San Francisco Bay SCHISM model (http://baydeltaoffice.water.ca.gov/modeling/deltamodeling/models/bay_delta_schism/). We chose this location because the model has been well-tested, thus to eliminate uncertainty in resolution, water depth in the mesh, etc. The original SCHISM mesh has 164,016 nodes with the finest resolution of 4 meters covering the small streams in the Bay delta area. We embedded it with a preliminary West Coast base grid to extend the coverage to the deep ocean, to utilize the data from the six DART stations offshore (Figure 26). The node number increases to 222,404 for the merged grid.

For this test, data from the 6 DART stations were used as input for assimilation while 36 tide stations in the San Francisco Bay have data for validation.

For the San Francisco test case, the average error of the M_2 amplitude for the 36 tide stations is 4.4 cm or 7.8%. The largest error is 12.8 cm at station 9415338. This tide station is a river station

which was not resolved by the current grid at the time of testing. Note that the final West Coast tide model grid has already been extended to cover all CO-OPS tide stations.

The average model error for M_2 at the Bay stations is more than double the average error at the open coast tide stations. The tests also show Bay stations are more sensitive to the friction coefficient than the open coast stations. The reason is that the U.S. West Coast has a steep offshore slope to the deep ocean. Therefore, it has less significant continental effect on the open coast stations

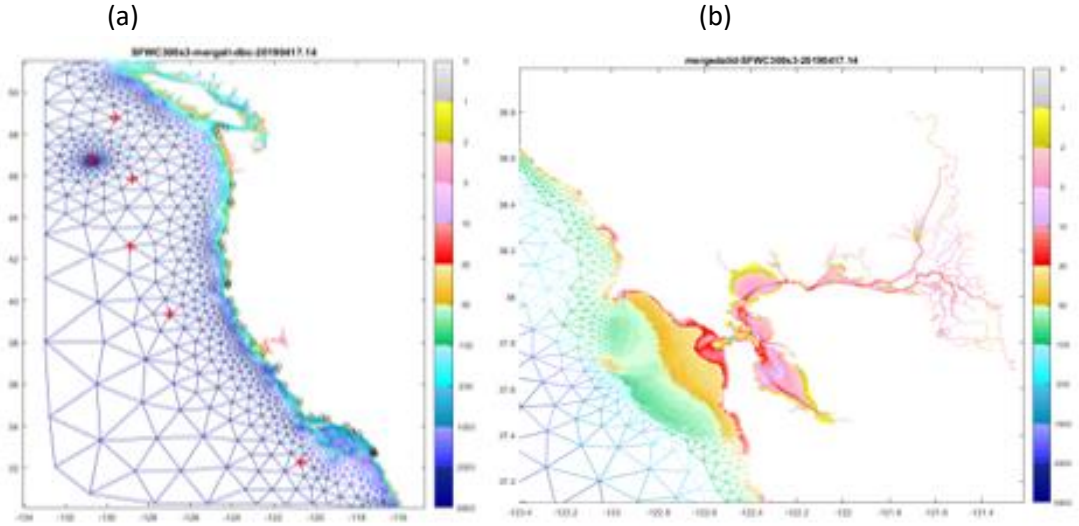

Figure 26 Preliminary model for quick testing of tides assimilation in San Francisco Bay and Delta. (a) Model grid; (2) Close-up in the high-resolution San Francisco Bay and Delta mesh. Depth in meter referred to MSL. +, DART stations; o, open coast tide stations.

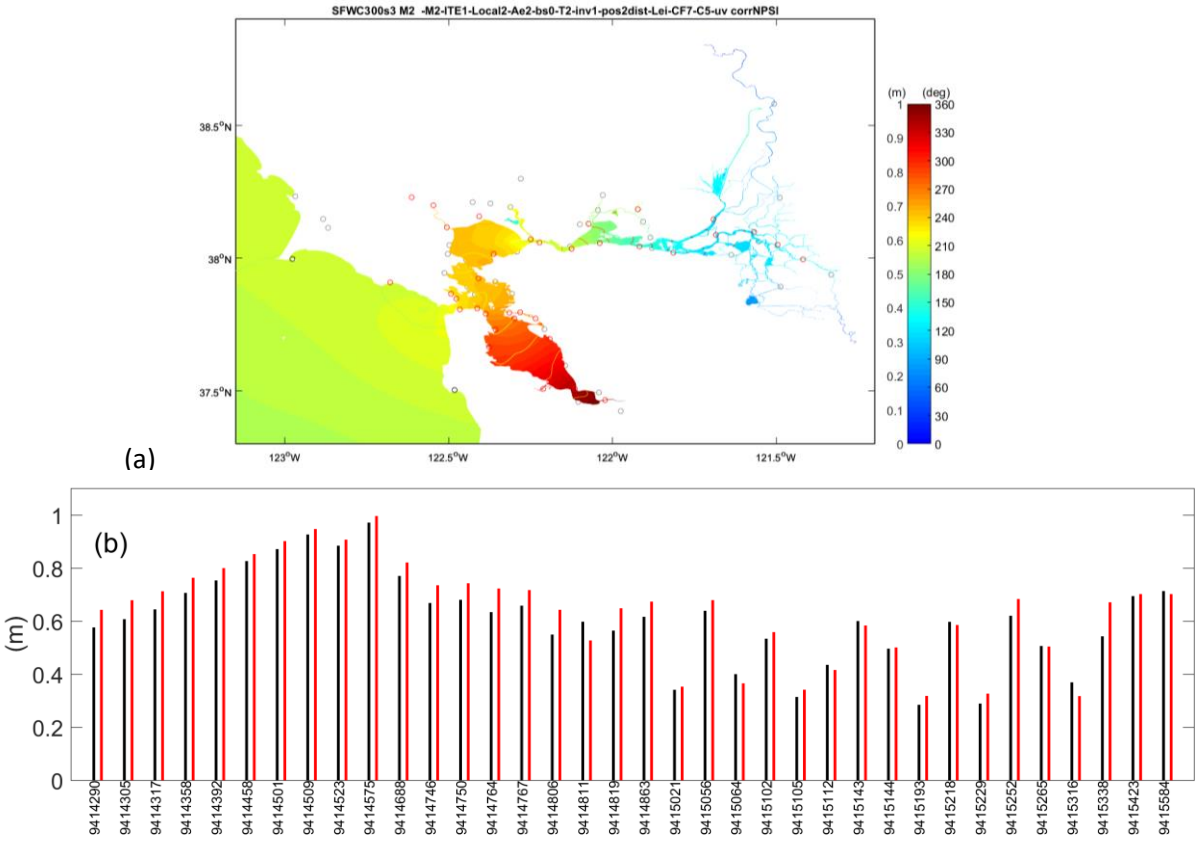

Figure 27 (a) Modeled M_2 amplitude and phase in San Francisco grid. (b) Observed (black) and modeled (red) M2 amplitudes at 36 tide stations (red circles) in the Bay.

4.4.3 Sensitivity to Internal Tides Energy Dissipation

Tests were conducted to evaluate the effect of internal tides energy dissipation to both the dynamic and inverse algorithms for tides assimilation.

Table 11 shows the test results on the global model. The internal tides energy dissipation can significantly reduce the error in the dynamic solution for both deep ocean and open coast tide stations, while it has very small effect on the inverse algorithm.

Figure 28 shows test results on the high-resolution San Francisco model. Changing the dissipation cut-off depth from 10 m to 100m produces better results for the bay and delta stations in shallow water even though the effect is less obvious in the open coast stations.

Table 11 Modeled M_2 amplitude error w/o internal tides dissipation for the dynamic and inverse tides assimilation schemes. Results were from the global tide model.

Internal wave energy dissipation term	Mean |err | (cm) Dynamic *vs.* Inverse	Mean percentage |err| (%) Dynamic *vs.* Inverse	RMSE (cm) Dynamic *vs.* Inverse
151 BPRs in deep ocean			
(a) without	14.3 ***vs.*** 0.6	53.0% ***vs.*** 3%	17.4 ***vs.*** 0.9
(b) with	6.8 ***vs.*** 0.6	27.2% ***vs.*** 2%	10.3 ***vs.*** 0.8
38 open coast tide stations			
(a) without	19.6 ***vs.*** 1.9	33.7 ***vs.***3.0%	20.1 ***vs.***2.5
(b) with	6.6 ***vs.*** 1.9	9.7% ***vs.*** 2.8%	8.4 ***vs.***2.8

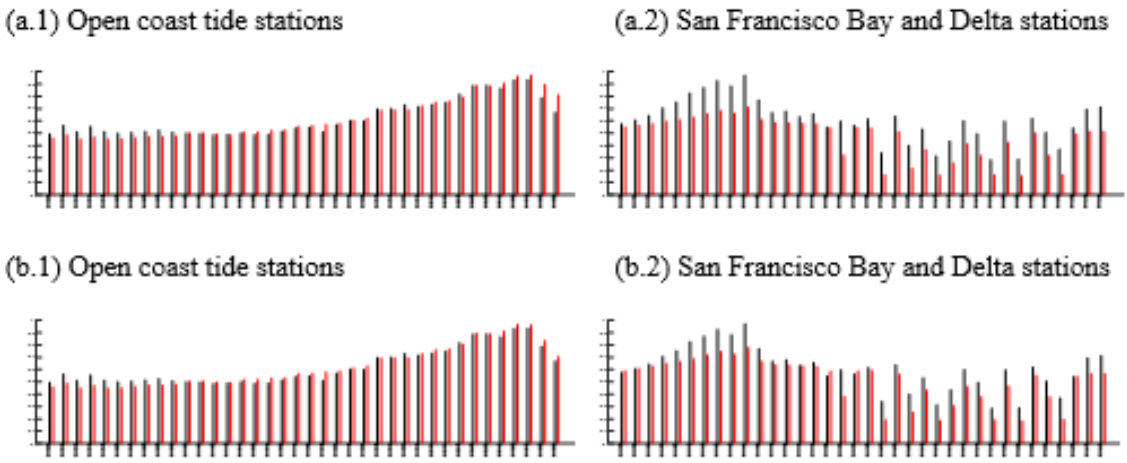

Figure 28 Sensitivity of modeled M_2 amplitude to internal tide dissipation depth up to (a) 10 m and (b) 100m depth. Model-data comparisons at (1) 38 open coast tide stations and (2) 36 San Francisco Bay and Delta stations. Black bars, observations; red bars, model. Station numbers are the same as those in Figure 27.

4.4.4 Sensitivity to Friction Coefficient

Tests were conducted to evaluate the sensitivity of friction coefficient in the tides assimilation scheme. Here we used the high-resolution San Francisco model. Figure 29 displays the mode-data comparison for M_2 amplitude. Doubling the friction coefficient from 0.001 to 0.002 can reduce the M_2 amplitude in the San Francisco Bay and Delta tide stations, while it has little effect on the open coast tide station. This is due to the steep offshore slope for the West Coast, e.g., little continental shelf effect on open coast.

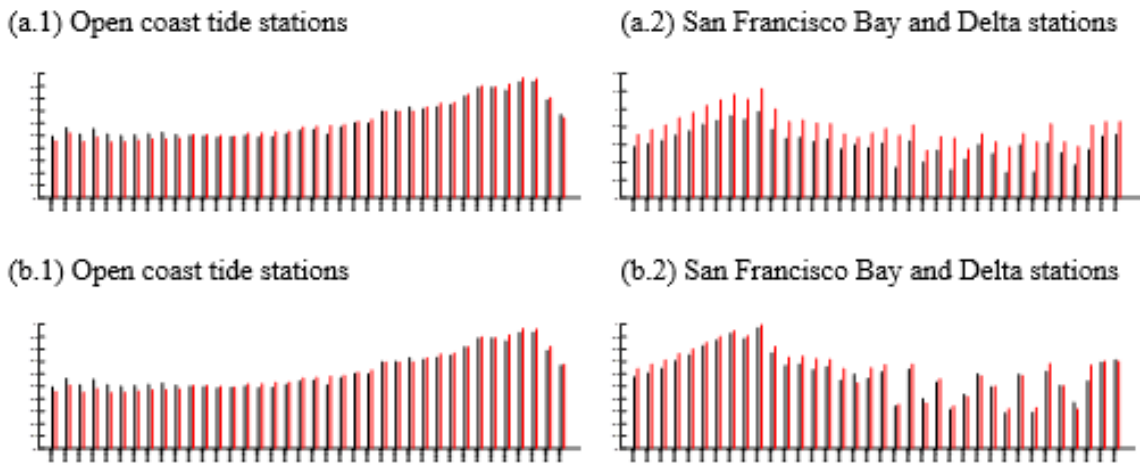

Figure 29 Sensitivity of modeled M_2 amplitude to friction coefficient (a) 0.001 and (b) 0.002. Model-data comparisons at (1) 38 open coast tide stations and (2) 36 San Francisco Bay and Delta stations. Black bars, observations; red bars, model.

4.4.5 Tides Assimilation on the West Coast VDatum Tide Model

After the testing documented in section 4.4.1 to 4.4.4, we then applied the representor tides assimilation to optimize the boundary conditions for the West Coast tide model for VDatum application. In addition, we also tested the future version of the tides assimilation using incremental variational approach, on the model. The incremental variational tides assimilation is currently in the development stage.

Figure 30 compares the modeled amplitudes of eight major tidal constituents without and with the two versions of tides assimilation methods at 149 tide stations with harmonic constants data on U.S. West Coast. Column 1 in Figure 30 displays the original model without tides assimilation; Panels on column 2 are the results from the representor tides assimilation, which uses the six DARTs stations and 17 open coast tide stations to optimize the boundary conditions for ADCIRC model; and Column 3 shows the results from the incremental variational data assimilation, which uses the 149 tide stations to optimize both boundary conditions and tidal potential forcing terms.

The results demonstrate that tides assimilation can reduce model error significantly for 7 tidal constituents. For the four semidiurnal tides, M_2, S_2, N_2 and K_2, the incremental variational approach can further reduce both average error and RMSE to more than half of the errors from the representor approach (Figures 30 a, b, g, and h). Similar results can also be found for Q_1 (Figure 30f). As to K_1 and O_1, even though the mean error for the incremental variational approach increases about 1-2 mm compared to the representor approach, the RMSE decreases by 9.5 and 3.6 mm respectively.

P_1 is the only tested constituent that shows little improvement from tides assimilation. Moreover, the incremental variational approach produces a trend of underestimates with increasing amplitude, resulting in the largest error among the three model results (Figure 30e, column 3). For the harmonic analysis in the ADCIRC input file, the P_1 frequency is set to 0.000072522947993, which is very close to the K_1 frequency of 0.000072921160387. This may result that the P_1 is not well resolved within the 2-month time series.

Figure 31 further compares the modeled tidal datums at 253 tidal from the same three tests shown in Figure 30. The incremental variational approach produces the least model error. Figure 32 displays the subset of 62 stations in area 3, Northern CA, OR, and WA, of which many of them are located on open coast. The original model results show an overestimate trend in MHHW (Figure 32a). The representor approach, which optimized the boundary conditions, has little improvement (Figure 32b). We also did other tests such as increasing friction coefficient, which couldn't resolve the issue. Eventually by using incremental variational data assimilation, which also optimized tidal potential forcing terms, the overestimate issue was resolved, with MHHW average error reducing from 6.8 cm to 3.8 cm over the 62 stations.

(1) No TA (2) Representor (3) Incremental Variational

(a) M2

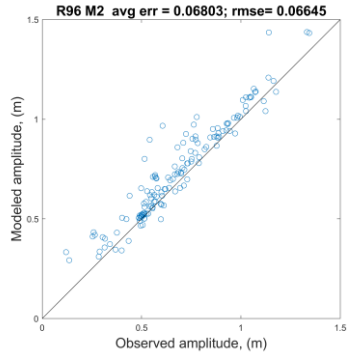

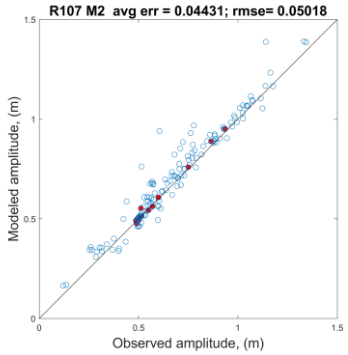

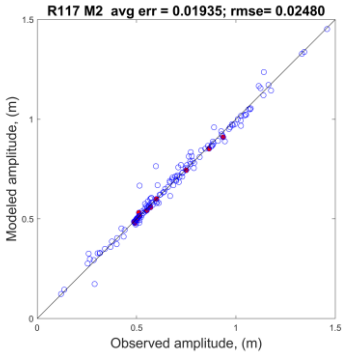

(b) S2

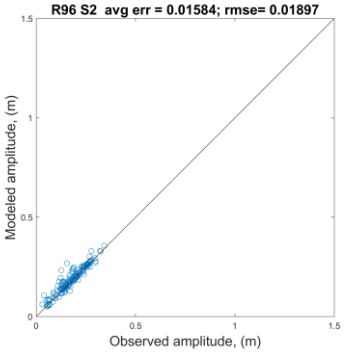

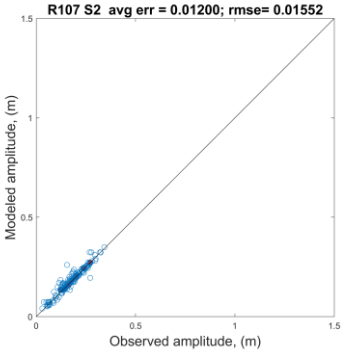

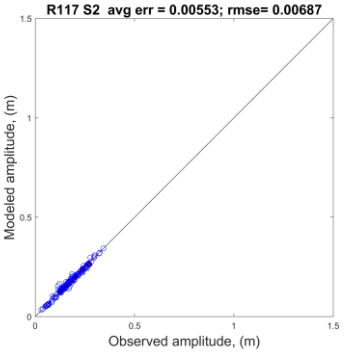

(c) K1

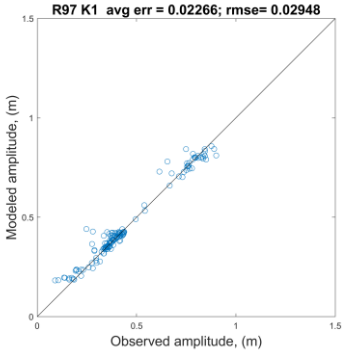

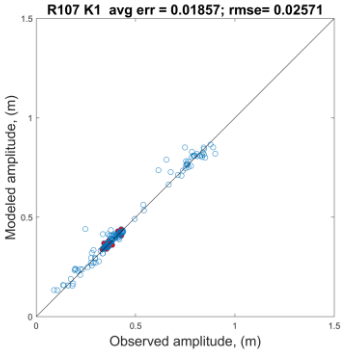

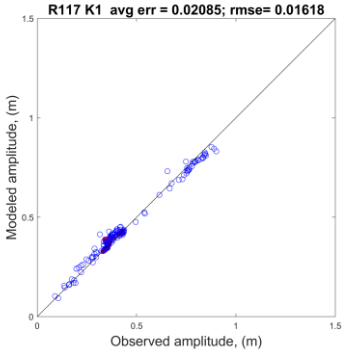

(d) O1

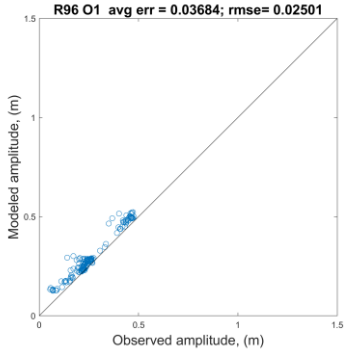

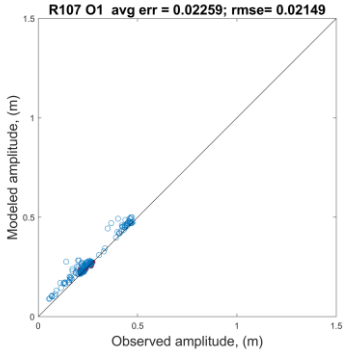

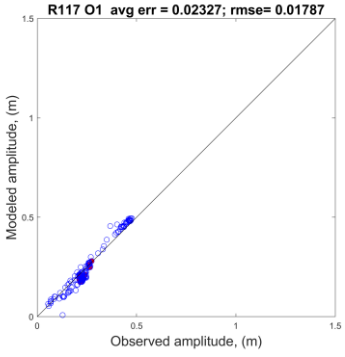

(e) P1

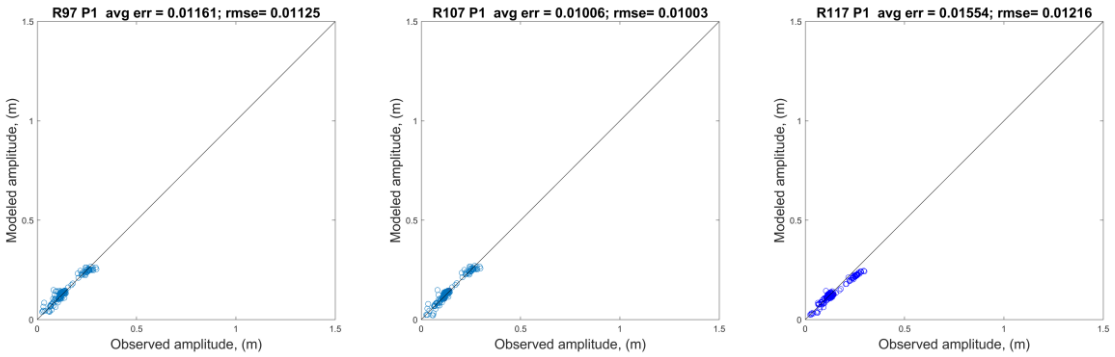

(f) Q1

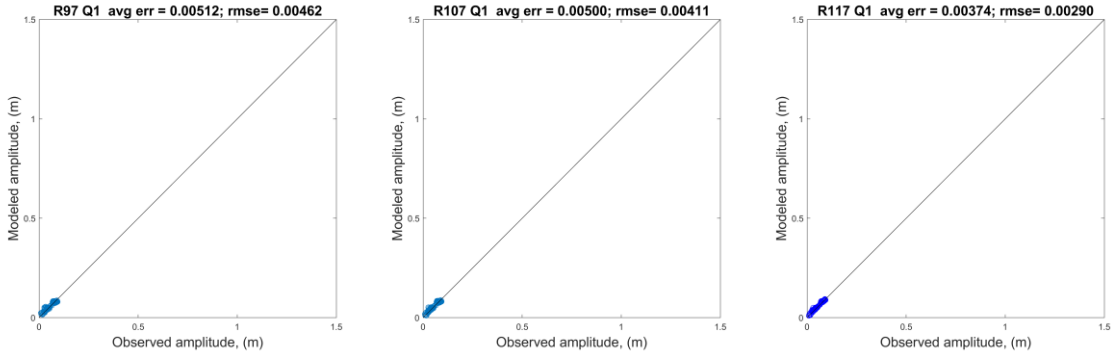

(g) N2

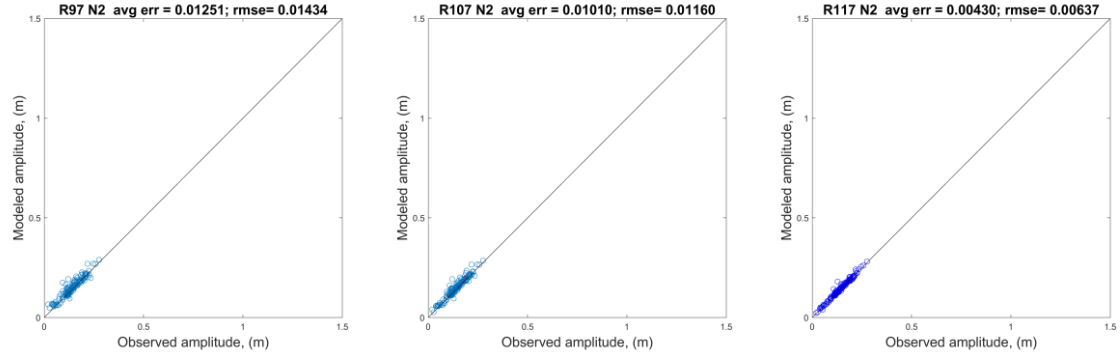

(h) K2

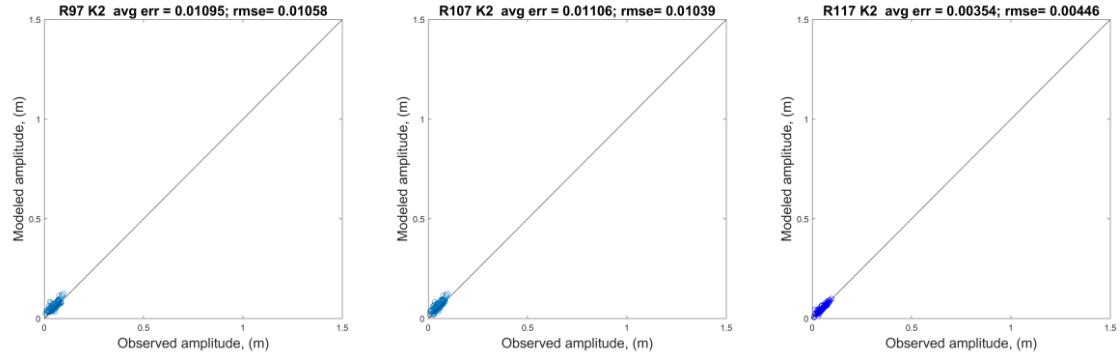

Figure 30 Modeled amplitudes for 8 major tidal constituents at 145 tide stations on the U.S. West Coast. (1) Without tides assimilation, (2) Representor approach to optimize boundary conditions, and (3) Incremental variational approach to optimize both boundary and tidal potential forcing terms.

(a) No TA (b) Representor (c) Incremental Variational

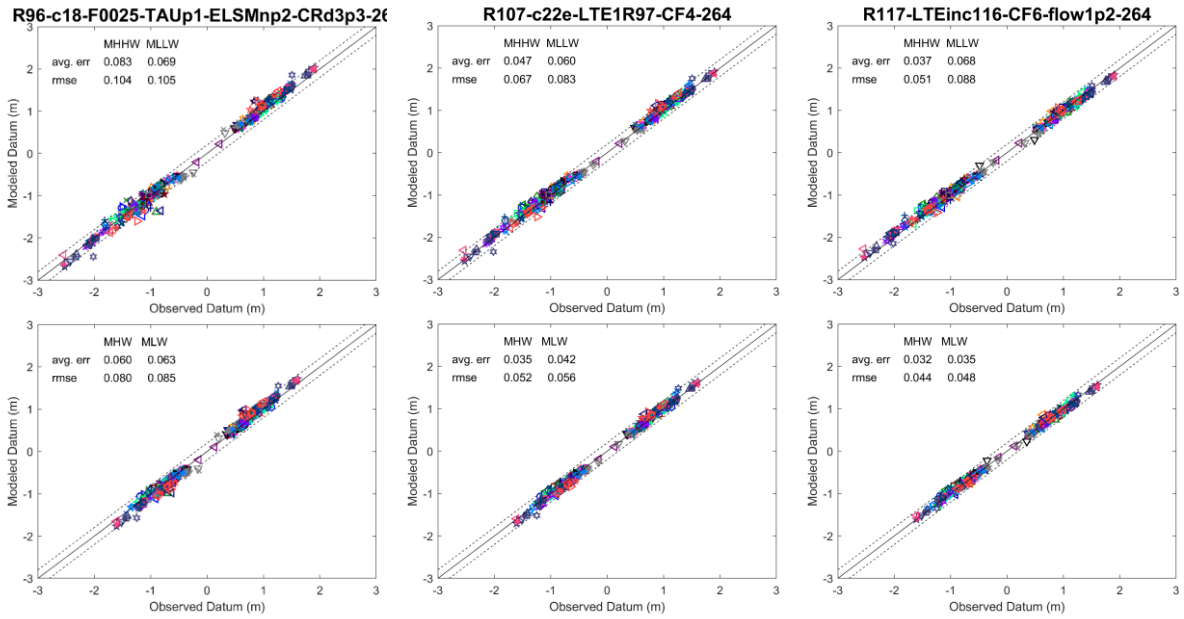

Figure 31 Modeled tidal datums at 253 tide stations. (a) Without tides assimilation and (b) with representor approach and (c) incremental variational approach. See Figure 30 for comparisons of tidal constituents' amplitudes.

(a) No TA (b) Representor (c) Incremental Variational

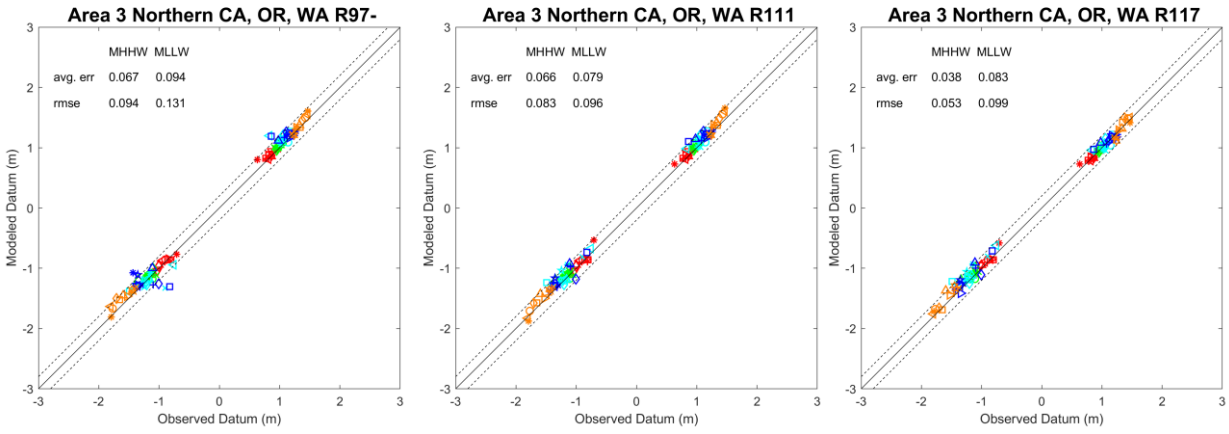

Figure 32 Modeled tidal datums at 62 tide stations at open coast along Northern CA, OR, and WA: (a) without tides assimilation, (b) with representor approach, and (c) incremental variational approach.

5. TOPOGRAPHY OF THE SEA SURFACE

5.1 Generation of Topography of the Sea Surface field

Based on the VDatum transformation roadmap adopted for the U.S. West Coast (shown in Figure 33), the topography of the sea surface (TSS) is defined as the elevation of the xGEOID20 B relative to Local Mean Sea Level (LMSL). xGEOID is a series of experimental geoid models published by the National Geodetic Survey (NGS) using satellite gravity models, terrestrial gravity and airborne gravity (https://beta.ngs.noaa.gov/GEOID/xGEOID/index.shtml). xGEOID is a preliminary product as NGS is progressing towards the final release of a newly updated national geopotential reference frame. Note that xGEOID20B refers to one of xGEOID products that uses source data roughly available until 2020 and, B indicates that this particular product's use of the airborne gravity data that better captures smaller scale signals.

The TSS field for the U.S. West Coast provides the spatial variations between a mean sea-level surface and the geopotential surface realized via xGEOID20B. A positive value specifies that the xGEOID20 B reference value is further from the center of the Earth than the local mean sea-level surface.

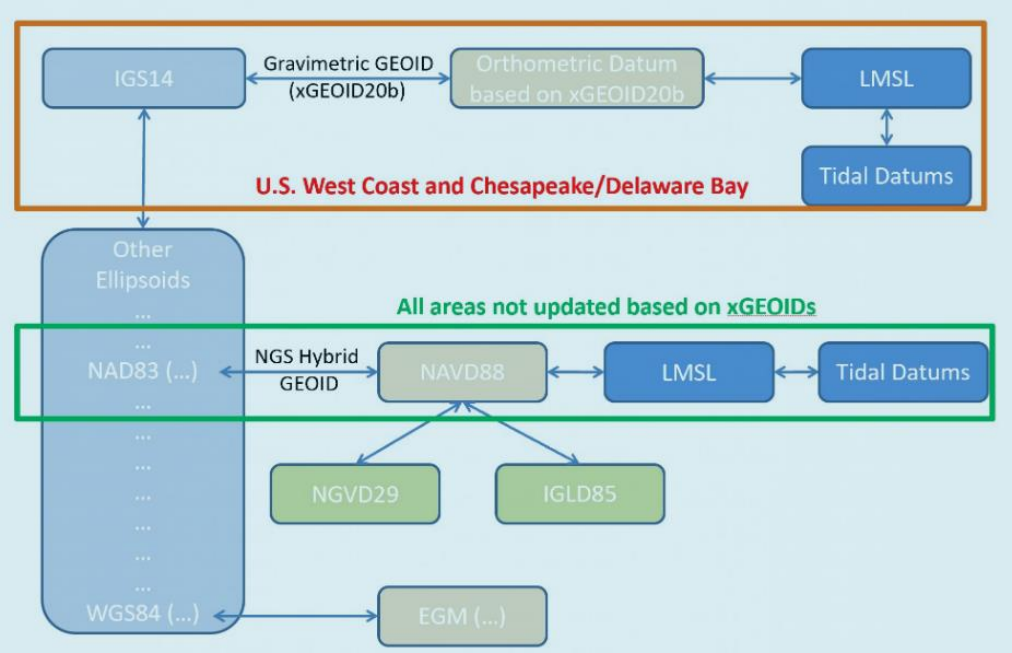

Figure 33 VDatum transformation roadmap adopted for the U.S. West Coast.

For the U.S. West Coast TSS field, both the CO-OPS tide gauge and satellite altimetry datasets are used so that the majority of the development domain is available with long-term observations, as each dataset compensates another in their coverage.

A total of 123 tide stations have observed TSS values in this model domain. All mean sea level data are based on the most (recent?) National Tidal Datum Epoch (1983-2001). The observed TSS and their corresponding standard deviations are listed in Appendix A(?). As all the tide gauges have tidal benchmark(s) that were GNSS campaigned to obtain ellipsoidal heights, all the tide gauge observations are referenced to the local mean sea level with regard to the IGS14 (a published reference frame from International GNSS Service) to which the xGEOID20B is referenced. Figure 34 shows the locations of tide stations with a color code for the observed TSS values and their corresponding standard deviations after all processing is applied. The observed TSS values in this model domain range from -2.291 m to 0.068 m. The observed TSS values in most upstream gauges in the Columbia River are below -0.6 m. The standard deviation of the TSS values range from 0.022 m to 0.044 m, and is less than 0.035 m at most tide stations.

For about the last three decades, high precision satellite altimetry data has been accumulated for many oceanographic studies, among those 6 altimetry satellites and corresponding 8 missions (both repeat and geodetic) are chosen for the U.S. West Coast domain. Datasets are obtained from the Open Altimeter Database (OpenADB) and Radar Altimeter Database System (RADS). Details of these datasets are described in Table 12. Among the 8 missions, merged repeat tracks of Jason 1, 2, and 3 are selected as the reference track to which other missions are referenced. Figure 3 illustrates the merged repeat tracks in the U.S. West Coast area, one from Jason-1, Jason-2 and Jason-3 (or the J123 track), and another from Envisat and Saral/Altika (or the N1SA track). Note that geodetic mission tracks are not drawn in the figure as these tracks cover the domain very densely.

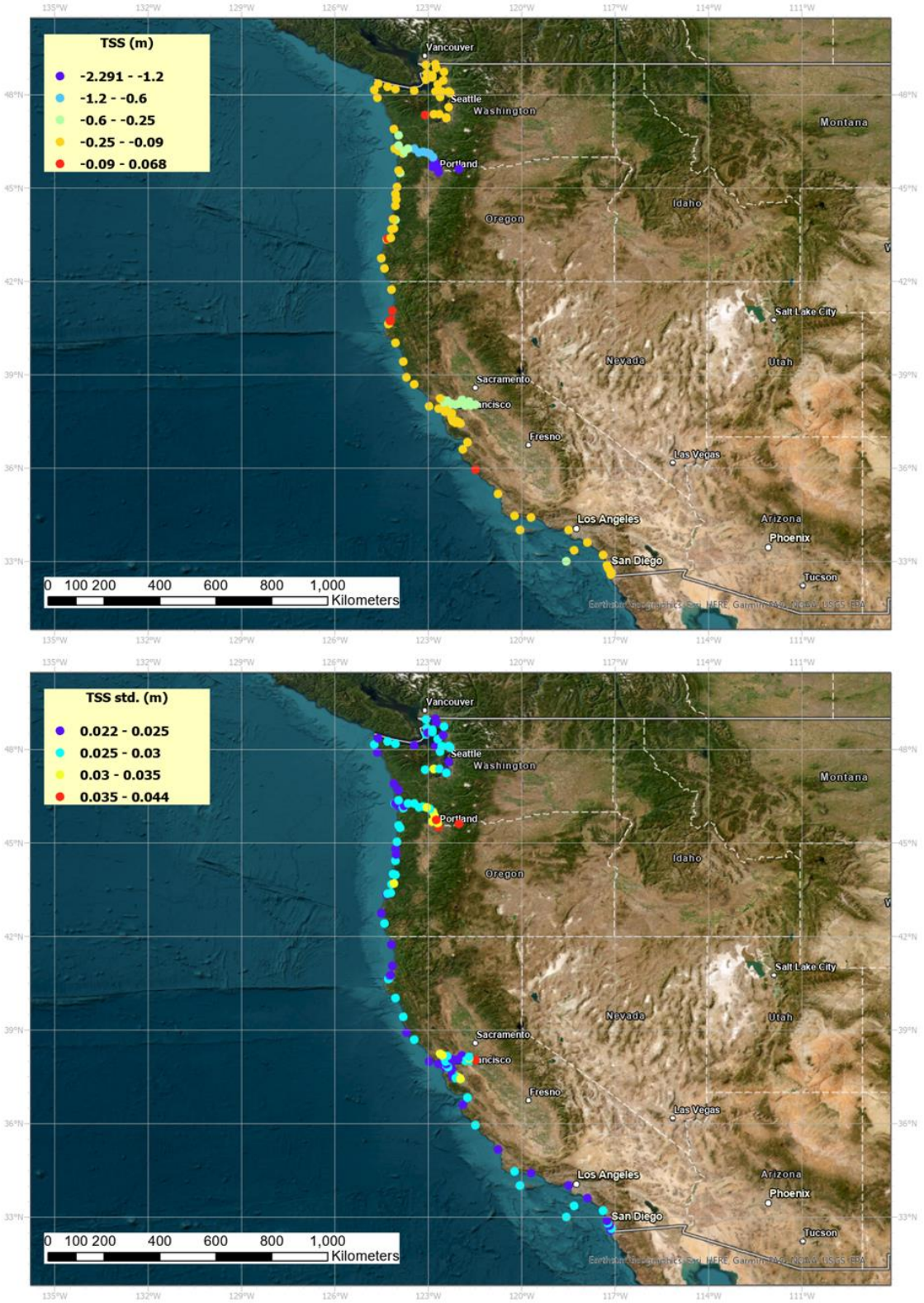

Figure 34 Locations of tide stations with the observed TSS values (top) and their corresponding standard deviations (bottom).

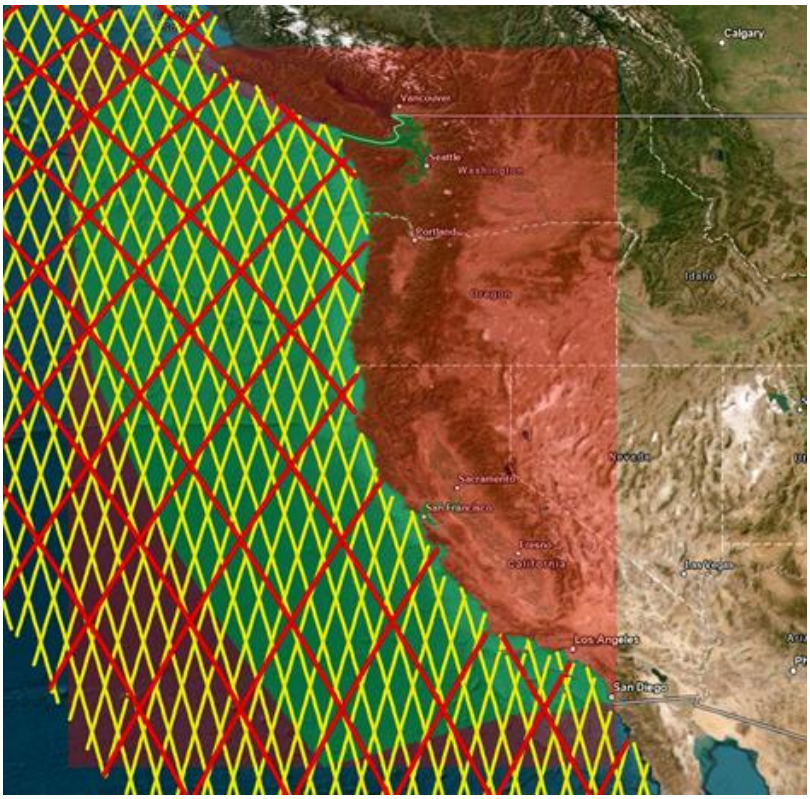

Figure 35 Illustration of merged repeat tracks in the US West Coast area: J123 track (red dots) and N1SA track (yellow dots).

Original sea surface height (SSH) provided in the altimetry dataset is converted to be consistent with TSS values derived from tide gauges by considering i) the reference ellipsoid and ii) permanent tide. In general, altimetric SSH is not referenced to the GRS80 ellipsoid, that IGS14 reference frame uses as its reference ellipsoid. A reference ellipsoid conversion is applied (from TOPEX/Poseidon or T/P reference ellipsoid to GRS80 ellipsoid): for example, an original Jason-1 SSH (i.e., latitude, longitude and SSH referenced to the T/P ellipsoid) is transformed to geocentric coordinates (i.e., Earth centered cartesian coordinate). Then converted back to geographic coordinates referenced to the GRS80 ellipsoid. Here it is assumed that the T/P ellipsoid is defined fairly close to the earth's center similar to the IGS14 reference frame. Secondly, permanent tide conversion (from 'mean tide' to 'tide free') is applied. As the external tidal potential from the sun and moon consists of permanent (i.e., constant) and periodic (i.e., time-varying) components, handling of the permanent component and corresponding solid earth deformation differ by three permanent tide modes, i.e., mean tide, free tide, and zero tide. Typically, as altimetric SSH only corrects for the time-varying periodic parts, SSH is regarded as the 'mean tide' quantity, but xGEOID is defined in the tide free system, which eliminates all the tidal effects. Thus, permanent tide conversion from mean tide to tide free is applied before deriving the TSS.

Table 12 Altimetry datasets used for the TSS field.

Track	Mission	Cycle/Period
J123 repeat track : 2002~2019 (~18 years)	Jason-1 (J1)	001 - 259 (Jan 2002 - Jan 2009)
Same as above	Jason-2 (J2)	001 - 303 (Jul 2008- Oct 2016)
Same as above	Jason-3 (J3)	001 - 117 (Feb 2016- Apr 2019)
N1SA repeat track : 2002-2010, 2013-2016 (~11.5 years)	Envisat (N1)	007 - 093 (Jun 2002 - Oct 2010)
Same as above	SARAL/AltiKa (SA)	001 - 035 (Mar 2013- Jul 2016)
J1GM (~1 year)	Jason-1 (J1GM)	500 - 537 (May 2012- Jun 2013)
SAdp (~3 year)	SARAL/AltiKa drifting phase (SAdp)	100 - 128 (Jul 2016- Apr 2019)
C2 (~10 years)	Cryosat-2 (C2)	003 - 131 (Jul 2010- Jun 2020)

Once the basic conversion is done for all of the altimetry SSH datasets, integration processing of the multi-mission dataset (i.e., 8 missions in the domain) is applied. These steps include: i) determination of horizontal reference location of five repeat missions (i.e., Jason-1, Jason-2, Jason-3, Envisat, and Saral/Altika) using X-Track data (a regional altimetry data product for coastal areas produced by Center of Topography of the Ocean and the Hydrosphere in France), ii) mean SSH estimation along the determined repeat tracks with filtering based on SSH quality statistics, iii) repeat track SSH residual adjustment for cross-over points, iv) geodetic mission SSH track filtering based on SSH quality statistics, v) geodetic mission SSH residual adjustment using the reference tracks, vi) data thinning to merge repeat and geodetic mission SSHs using the stochastic information derived from the cross-over adjustments, and vii) vertical offset adjustment for the bias between altimetric and tide gauge TSS. After these steps, a consistent set of merged data points from altimetry and tide gauge is obtained.

The TSS field was derived by interpolating orthometric-to-MSL relationships which were obtained through the calculation of the xGEOID20B-to-MSL values at derived data points. Breaklines were taken into consideration in the interpolation module when generating the TSS field for representing

the influence of land. A sea surface topography field was then generated using the Surfer© software's minimum curvature algorithm to create a surface that honors the data as closely as possible. The maximum allowed departure value used was 0.001 meters. To control the amount of bowing on the interior and at the edges of the grid, an internal and boundary tension of 0.3 was utilized. Once the gridded TSS field was generated for the entire domain (i.e., all thirteen VDatum sub-regions in the U.S. West Coast), the TSS field is exported to each sub-region based on marine grid extent. Null values were obtained from the tidal datum marine grids and were assigned to the sub-region TSS field as the null value locations represent the presence of land. Grid parameters for the TSS field are listed in Table 13.

Table 13 VDatum TSS grid parameters for the US West Coast domain.

VDatum Region	Latitude-Longitude Window	Zonal Spacing (deg)	Meridional Spacing (deg)	No. of Zonal Nodes	No. of Meridional Nodes
all sub regions	[30.4875 51.5125, -133.0125 -116.4875]	0.001	0.001	21026	16526

5.2 Generation of TSS Spatially Varying Uncertainty Field

The tide gauge observation uncertainty values and estimated uncertainty for altimetry data are used to generate the TSS SVU field. Mean sea level observation uncertainties provided by CO-OPS, geoid uncertainty, and ellipsoid height uncertainty from the GNSS campaign are further considered to obtain the TSS uncertainty at tide gauges. For altimetry datasets, uncertainties are estimated for both repeat and geodetic mission tracks considering the post cross-over adjustment statistic using the J123 track as a reference track. The cross-over adjustment based statistic is a consistent and realistic quantization of uncertainty for multi-mission altimetry dataset by mitigating bias between different altimetry missions. Then geoid uncertainty is further considered to obtain the TSS uncertainty at altimetry data points. Using these two uncertainty sources, SVU field is created by applying i) a rigorous error propagation approach that uses error sensitivity metric and full covariance matrix, and ii) a simple objective analysis that estimates the final TSS uncertainty given tide gauge observation and altimetry data uncertainties.

5.3 Interpolated TSS and TSS SVU Results

The interpolated TSS field and the TSS SVU field are shown in Figure 36. The statistical values of the interpolated TSS field and its SVU field are listed in Table 14. The tide gauge data used to compile the TSS field grid was compared against the TSS grid product, to generalize internal consistency. The delta between TSS value for each tide station and the created TSS field grid is depicted in Table 14. Note that comparisons are made only for tide gauges inside the VDatum TSS model domain. Mean and standard deviation for these delta values are listed in Table 15.

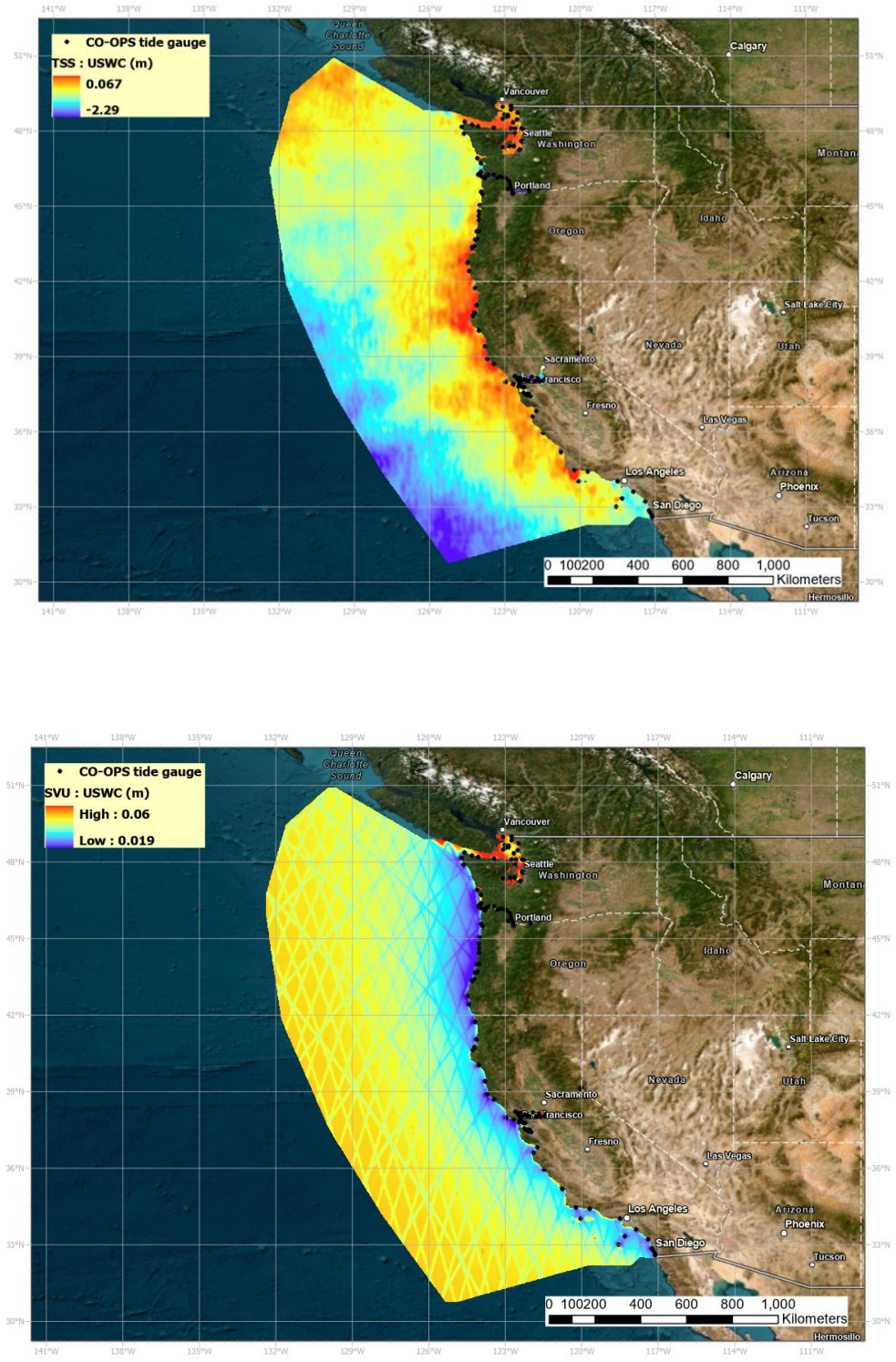

Figure 36 The interpolated TSS field (top) and the TSS SVU field (bottom) for the U.S. West Coast Regional Model).

Table 14 Statistics of the interpolated TSS field and the TSS SVU field (in units of meters).

Region	Field	Minimum	Maximum	Mean	Standard Deviation
all sub regions	TSS	-2.29	0.067	-0.219	0.058
all sub regions	TSS Uncertainty	0.019	0.06	0.029	0.002

Table 15 Mean and stand deviation of delta values tabulated in Table 14 (meters)

Region	Mean Delta Value (m)	Standard Deviation (m)
all sub regions	-0.0001	0.0005

6. SUMMARY AND CONCLUSION

We have developed a regional tide model to replace the several first-generation VDatum coastal tide models on the U.S. West Coast. A tides assimilation method based on the representor approach using finite element method was also developed, to assimilate data from the deep ocean DART stations and open coast tide stations, and therefore to optimize the open boundary conditions for the ADCIRC model. The spatially varying uncertainty method was applied to model results to produce the corrected tidal datums and associated uncertainty. The corrected tidal datums and spatially varying uncertainty were further populated onto 13 structure marine grids for use by the VDatum software. Compared to the single value uncertainty, the upgrade with spatially varying uncertainty provides more accurate representation of the uncertainty for an area. This upgrade also expands VDatum coverage further into rivers as well as offshore West Coast.

For the four tidal datums (MHHW, MHW, MLW and MLLW) at the 253 tide stations on the U.S. West Coast, the average model error is 4.6 cm (5.2%) and RMSE is 6.5 cm. Southern California has the least average model error of 1.1 cm while it is 5.8 cm for the northern part of the open coast. The MLLW has the greatest mean error of 6.0 cm (8.3 cm rmse). The current tidal datums calculation algorithm needs further improvement to better capture the lows for the time series with steep trough, thus to reduce the error of underestimate, especially in MLLW.

In this upgrade, we adapted the latest mesh generation tool, OceanMesh 2D, and the latest available ADCIRC model version 55. The total development time for the West Coast regional model is approximately two years. It considerably reduces the eight years of updating time if the previous coastal modeling approach were used. This shows the power of introducing new technologies in improving our work efficiency.

The report also documents development and testing of the assimilation method. Tests were done on a global model, a high-resolution San Francisco model, and the west coast VDatum model. In addition, we did a preliminary test on the next version of tides assimilation method, based on incremental variation approach, on the west Coast model. By optimizing both open boundary conditions and tidal potential forcing, model accuracy can be further improved.

The study indicates that as we extend VDatum coverage to rivers and intracoastal waterways, high-quality river bathymetry data such as river LiDAR mapping data are needed.

The TSS field and the TSS SVU field were created by the NGS by using observed TSS values (with regard to xGEOID product) and their corresponding uncertainties at 123 tide stations, and ii) ~19 years of multi mission satellite altimetry dataset, and their estimated uncertainties. The TSS field was created by interpolating orthometric-to-MSL relationships in tide gauges and altimetry dataset. The TSS SVU field was generated by applying a rigorous error propagation approach and a simple objective analysis

ACKNOWLEDGEMENTS

We thank CSDL's Dr. Kurt Hess for assistance on tide stations data and discussions, Dr. Zizang Yang for his detailed reviews, comments, and editing of the report, Drs. Mojgan Rostaminia and Saeed Moghimi for reviews, Dr. Yuji Funakoshi for discussion and help; NASA's Dr. Richard Ray for sharing the deep ocean BPR data; Eli Ateljevich from California Department of Water resources, CRITFC's Charles Seaton, and VIMS' Dr. Y. Joseph Zang for sharing Columbia River and San Francisco Bay and Delta mesh, respectively; CSDL's IT group for their support. Liujuan Tang thanks ERT's Chang Zhao and Karen for their support; Pacific Hydrographic Branch and Olivia Hauser for providing office accommodation and support to the project.

REFERENCES

Amante, C.J., M.R. Love, L.A. Taylor, and B.W. Eakins, 2011. Digital Elevation Models of Mobile, Alabama: Procedures, Data Sources and Analysis. U.S. Department of Commerce, National Oceanic and Atmospheric Administration, National Geophysical Data Center, Boulder, Colorado, NOAA Technical Memorandum NESDIS NGDC-44, 43pp.

Bodnar, A. N., 1981. Estimating Accuracies of Tidal Datums from Short Term Observations. National Oceanic and Atmospheric Administration, Center for Operational Oceanographic Products and Services: 32. Silver Spring, Maryland.

Caldwell, R.J., L.A. Taylor, B.W. Eakins, K.S. Carignan, P.R. Grothe, E. Lim, and D.Z. Friday, 2011. Digital Elevation Models of Santa Monica, California: Procedures, Data Sources, and Analysis. NOAA Technical Memorandum NESDIS NGDC-46.

Carignan, K.S., L.A.Taylor, B.W. Eakins, R.R. Warnken, T. Sazonova, and D.C. Schoolcraft, 2008. Digital Elevation Model of Port Orford, Oregon: Procedures, Data Sources and Analysis. NOAA Technical Memorandum NESDIS NGDC-21.

Carignan, K.S., L.A. Taylor, B.W. Eakins, R.R. Warnken, R.J. Caldwell, D.Z. Friday, E. Lim, and P.R. Grothe, 2009a. Digital Elevation Models of Eureka, California: Procedures, Data Sources, and Analysis. NOAA Technical Memorandum NESDIS NGDC-38.

Carignan, K.S., L.A. Taylor, B.W. Eakins, R.R. Warnken, E. Lim, and P.R. Medley, 2009b. Digital Elevation Model of Santa Barbara, California: Procedures, Data Sources, and Analysis. NOAA Technical Memorandum NESDIS NGDC-29.

Carignan, K.S., L.A. Taylor, B.W. Eakins, R.J. Caldwell, D.Z. Friday, P.R. Grothe, and E. Lim, 2011a. Digital Elevation Models of Central California and San Francisco Bay, California: Procedures, Data Sources, and Analysis. NOAA Technical Memorandum NESDIS NGDC-52.

Carignan, K.S., L.A. Taylor, B.W. Eakins, R.J. Caldwell, D.Z. Friday, P.R. Grothe, and E. Lim, 2011b. Digital Elevation Models of Central California and San Francisco Bay: Procedures,

Data Sources and Analysis. NOAA Technical Memorandum NESDIS NGDC-5, NOAA, pp. 49.

Carignan, K.S., L.A. Taylor, B.W. Eakins, D.Z. Friday, P.R. Grothe, and M. Love, 2012. Digital Elevation Models of San Diego, California: Procedures, Data Sources, and Analysis. https://www.ngdc.noaa.gov/mgg/dat/dems/regional_tr/san_diego_13_navd88_2012.pdf

Carignan, K.S., B.W. Eakins, M.R. Love, M.G. Sutherland, and S.J. McLean, 2013. Bathymetric Digital Elevation Model of British Columbia, Canada: Procedures, Data Sources, and Analysis. https://www.ngdc.noaa.gov/mgg/dat/dems/regional_tr/british_columbia_3_msl_2013.pdf

Carignan, K.S., S.J. McLean, B.W. Eakins, L. Beasley, M.R. Love, and M. Sutherland, 2014. Digital Elevation Model of Puget Sound, Washington: Procedures, Data Sources, and Analysis. https://www.ngdc.noaa.gov/mgg/dat/dems/regional_tr/puget_sound_13_navd88_2014.pdf

Carignan, K.S., S.J. McLean, B.W. Eakins, L. Beasley, M.R. Love, and M. Sutherland, 2015a. Digital Elevation Model of the Strait of Juan de Fuca: Procedures, Data Sources, and Analysis. https://www.ngdc.noaa.gov/mgg/dat/dems/regional_tr/strait_of_juan_de_fuca_13_navd88_2015.pdf

Carignan, K.S., S.J. McLean, B.W. Eakins, L. Beasley, M.R. Love, and M. Sutherland, 2015b. Digital Elevation Model of the Central Washington Coast: Procedures, Data Sources, and Analysis. https://www.ngdc.noaa.gov/mgg/dat/dems/regional_tr/central_washington_13_navd88_2015.pdf

Carignan, K.S., S.J. McLean, B.W. Eakins, L. Beasley, M.R. Love1 and M. Sutherland, 2015c. Digital Elevation Model of Orange County, California: Procedures, Data Sources, and Analysis. https://www.ngdc.noaa.gov/mgg/dat/dems/regional_tr/orange_county_13_navd88_2015.pdf

Carignan, K., S.J. McLean, B.W. Eakins, M.R. Love, and M. Sutherland, 2016. Digital Elevation Model of the Central Oregon Coast V2: Procedures, Data Sources and Analysis. https://www.ngdc.noaa.gov/mgg/dat/dems/regional_tr/central_oregon_13_navd88_2015.pdf

CO-OPS, 2003. Computational Techniques for Tidal Datum Handbook; NOAA Special Publication NOS-OPS 2: Silver Spring, Maryland, p. 98.

DeWitt, N.C., C.A. Stalk, C.G. Smith , S.D. Locker, J. Fredericks , T.A. McCloskey, and C. Wheaton, 2015. Single beam bathymetry data collected in 2015 from Grand Bay, Mississippi/Alabama. https://doi.org/10.5066/F7NP22M2

Dhingra, E. A., K. W. Hess, and S. A. White, 2008. VDatum for the Northeast Gulf of Mexico from Mobile Bay, Alabama, to Cap San Blas, Florida: Tidal Datum Modeling and Population of the marine Grids., NOAA Technical Memorandum NOS CS 14, 64 pp. National Oceanic and Atmospheric Administration, National Ocean Service, Office of Coast Survey, Coast Survey Development Laboratory, Silver Spring, Maryland.

Egbert, G. D., A. F. Bennett, and M. G. G. Foreman (1994), TOPEX/Poseidon tides estimated using a global inverse model. J. Geophys. Res, 99, 24821–24852.

Egbert, Gary D., and Svetlana Y. Erofeeva, 2002. Efficient inverse modeling of barotropic ocean tides. Journal of Atmospheric and Oceanic Technology 19.2 (2002): 183-204.

Friday, D.Z., L.A. Taylor, B.W. Eakins, R.R. Warnken, K.S. Carignan, R.J. Caldwell, E. Lim, and P.R. Grothe, 2010. Digital Elevation Model of Arena Cove, California: Procedures, Data Sources, and Analysis. NOAA Technical Memorandum NESDIS NGDC-39.

Friday, D.Z., L.A. Taylor, B.W. Eakins, K.S. Carignan, P.R. Grothe, E. Lim, and M.R. Love , 2011. Digital Elevation Model of Port San Luis, California: Procedures, Data Sources, and Analysis. https://www.ngdc.noaa.gov/mgg/dat/dems/regional_tr/port_san_luis_13_navd88_2011.pdf

Gill, S. K. and J. R. Schultz, 2001. Tidal Datums and Their Applications. NOAA Special Publication NOS CO-OPS 1, 111p. + appendix. Silver Spring, Maryland.

Grothe, P.R., L.A. Taylor, B.W. Eakins, K.S. Carignan, R.J. Caldwell, E. Lim, and D.Z. Friday, 2010. Digital Elevation Models of Crescent City, California: Procedures, Data Sources, and Analysis. NOAA Technical Memorandum NESDIS NGDC-51.

Grothe, P.G., L.A. Taylor, B.W. Eakins, K.S. Carignan, D.Z. Friday, and M. Love, 2012. Digital Elevation Models of Monterey, California: Procedures, Data Sources, and Analysis. https://www.ngdc.noaa.gov/mgg/dat/dems/regional_tr/monterey_13_navd88_2012.pdf

Hess, K. W., R.A. Schmalz, C. Zervas, and W.C. Collier, 1999. Tidal constituent and residual interpolation (TCARI): A new method for the tidal correction of bathymetric data: 99.

Hess, K. W., 2002. Spatial interpolation of tidal data in irregularly-shaped coastal regions by numerical solution of laplace's equation. Estuarine, Coastal and Shelf Science 54: 175-192.

Hess, W.K. and S.K. Grill, 2003. Puget Sound Tidal Datum by Spatial Interpolation. In Proceedings of the American Meteorological Society Fifth Conference on Coastal Atmospheric and Oceanic Prediction and Processes, Seattle, WA.

Hess, K. W. and S. A. White, 2004. VDatum for Puget Sound: Generation of the Grid and Population with Tidal Datums and Sea Surface Topography. NOAA Technical Memorandum NOS CS 4, 27 pp. National Oceanic and Atmospheric Administration, National Ocean Service, Office of Coast Survey, Coast Survey Development Laboratory, Silver Spring, Maryland.

Hess, K. W. S., E. Anne; A.M. Wong, S.A. White, and S.K. Gill, 2005. VDatum for central coastal North Carolina : tidal datums, marine grids, and sea surface topography. NOAA technical report NOS CS 21. National Oceanic and Atmospheric Administration, National Ocean Service, Office of Coast Survey, Coast Survey Development Laboratory, Silver Spring, Maryland.

Hess, K. W., 2012. REVISED VDATUM FOR THE NORTHEAST GULF OF MEXICO. Unpublished document, 7 pp.

Karna, Tuomas & Baptista, Antonio. (2016). Evaluation of a long-term hindcast simulation for the Columbia River estuary. Ocean Modelling. 99. 1-14. 10.1016/j.ocemod.2015.12.007.

Lim, E., L.A. Taylor, B.W. Eakins, K.S. Carignan, R.J. Caldwell, P.R. Grothe, and D.Z. Friday, 2012. Digital Elevation Models of Port Townsend, Washington: Procedures, Data Sources, and Analysis. NOAA Technical Memorandum NESDIS NGDC-60.

Love M.R., D.Z. Friday, P.R. Grothe, K.S. Carignan, B.W. Eakins, and L.A.Taylor, 2012. Digital Elevation Models of Fort Bragg, California: Procedures, Data Sources, and Analysis. https://www.ngdc.noaa.gov/mgg/dat/dems/regional_tr/fort_bragg_13_navd88_2012.pdf

Luettich, R.A., J.J. Westerink, and N.W. Scheffner, 1992. ADCIRC: An Advanced Three-Dimensional Circulation Model of Shelves, Coasts, and Estuaries, Report 1: theory and methodology of ADCIRC-2DDI and ADCIRC-3DL. U.S. Department of the Army, Technical Report DRP-92-6.

Luettich, R. A. J., Westerink, and J.J, Ed. (1995). Continental shelf scale convergence studies with a barotropic tidal model. Quantitative Skill Assessment for Coastal Ocean Models, American Geophysical Union press.

Luettich, R.A. and J.J. Westerink, 2004. Formulation and Numerical Implementation of the 2D/3D ADCIRC Finite Element Model version 44. http://www.unc.edu/ims/adcirc/publications/2004/2004_Luettich.pdf.

Mukai A.Y., J.J. Westerink, R.A. Luettich Jr., and D. Mark, 2002. East coast 2001, a tidal constituent database for the western North Atlantic, Gulf of Mexico and Caribbean Sea, US Army Engineer Research and Development Center, Coastal and Hydraulics Laboratory, Technical Report, ERDC/CHL TR-02-24, September 2002, 201p.

Myers, E.P.; A. Wong, K. Hess, S. White, E. Spargo, J. Feyen, Z. Yang, P. Richardson, C. Auer, J. Sellars, et al. Development of a national VDatum, and its application to sea level rise in North Carolina. In Proceedings of the U. S. Hydrographic Conference, San Diego, CA, USA, 29–31 March 2005.

NOS, 2010. Standard Procedures to Develop and Support NOAA's Vertical Datum Transformation Tool, VDATUM, version 2010.08.03, 120p.

Pringle, W. J., Wirasaet, D., Roberts, K. J., and Westerink, J. J., 2021. Global storm tide modeling with ADCIRC v55: unstructured mesh design and performance, Geosci. Model Dev., 14, 1125–1145, https://doi.org/10.5194/gmd-14-1125-2021.

Ray, R. D. (2013), Precise comparisons of bottom-pressure and altimetric ocean tides, J. Geophys. Res. Oceans, 118, 4570–4584, doi: 10.1002/jgrc.20336.

Roberts, K. J. and Pringle, W. J., 2018: OceanMesh2D: User guide – Precise distance-based two-dimensional automated mesh generation toolbox intended for coastal ocean/shallow water, ResearchGate, Computational Hydraulics Laboratory, University of Notre Dame, Notre Dame, https://doi.org/10.13140/RG.2.2.21840.61446/2, 2018.

Roberts, K. J., Pringle, W. J., and Westerink, J. J. 2019. OceanMesh2D 1.0: MATLAB-based software for two-dimensional unstructured mesh generation in coastal ocean modeling, Geosci. Model Dev., 12, 1847–1868, https://doi.org/10.5194/gmd-12-1847-2019.

Sandwell, D. T., R. D. Müller, W. H. F. Smith, E. Garcia, R. Francis (2014), New global marine gravity model from CryoSat-2 and Jason-1 reveals buried tectonic structure, Science, Vol. 346, no. 6205, pp. 65-67, doi: 10.1126/science.1258213.

Shi, L., and E.P. Myers, 2016. Statistical Interpolation of Tidal Datums and Computation of Its Associated Spatially Varying Uncertainty. J. Mar. Sci. Eng. 4(4): 64.

Shi, Lei, L. Tang, and E. Myers, 2020. Variational Data Assimilation of Tides. Journal of Marine Science and Engineering 8, no. 1: 54. https://doi.org/10.3390/jmse8010054

Spargo, E., J.J. Westerink, R.A. Luettich, and D. Mark, 2004. Developing a Tidal Constituent Database for the Eastern North Pacific Ocean, Estuarine and Coastal Modeling VIII, M. Spaulding et al. [eds], ASCE, p.217-235.

Spargo, E. A. and J.W. Woolard, 2005. VDatum for the Calcasieu River from Lake Charles to the Gulf of Mexico, Louisiana: tidal datum modeling and population of the grid. NOAA Technical Report NOSCS 19, 25p. National Oceanic and Atmospheric Administration, National Ocean Service, Office of Coast Survey, Coast Survey Development Laboratory, Silver Spring, Maryland.

Sutherland, M.G., L.A. Taylor, M.R. Love, B.W. Eakins, and K.S. Carignan, 2013. Digital Elevation Models of Garibaldi, Oregon: Data Sources, Processing and Evaluation. https://www.ngdc.noaa.gov/mgg/dat/dems/regional_tr/garibaldi_13_navd88_2013.pdf

Szpilka, C, K. Dresback., R. Kolar, J. Feyen, and J. Wang, 2016: Improvements for the Western North Atlantic, Caribbean and Gulf of Mexico ADCIRC Tidal Database (EC2015). J. Mar. Sci. Eng., 4(4), 72; doi:10.3390/jmse4040072.

Tang, L., E. Myers, L. Shi, K. Hess, A. Carisio, M. Michalski, S. White, and C. Hoang, 2018. Tidal Datums with Spatially Varying Uncertainty in North-East Gulf of Mexico for VDatum Application. J. Mar. Sci. Eng. 2018, 6(4), 114; doi:10.3390/jmse6040114

Tang, L., L. Shi, E. Myers, L. Huang, M. Michalski and S. White, 2019. Assimilating DART Data into an Upgrade of VDatum for the US West Coast, *OCEANS 2019 MTS/IEEE SEATTLE*, Seattle, WA, USA, 2019, pp. 1-4, doi: 10.23919/OCEANS40490.2019.8962832.

Taylor, L.A., B.W. Eakins, K.S. Carignan, R.R. Warneken, T. Sazonova, D.C. Schoollcraft, and G.F. Sharman, 2008a. Digital Elevation Model of Panama City, Florida, 2008. Procedures, Data Sources and Analysis. NOAA Technical Memorandum NESDIS NGDC-8, 27pp. National Oceanic and Atmospheric Administration, National Geophysical Data Center, Boulder, Colorado,

Taylor, L.A., B.W. Eakins, K.S. Carignan, R.R. Warneken, T. Sazonova, and D.C. Schoollcraft, 2008: Digital Elevation Model of Biloxi, Mississippi, 2008b: Procedures, Data Sources and

Analysis. NOAA Technical Memorandum NESDIS NGDC-9, 32pp. National Oceanic and Atmospheric Administration, National Geophysical Data Center, Boulder, Colorado.

Pringle, W. J., Wirasaet, D., Roberts, K. J., and Westerink, J. J.: Global storm tide modeling with ADCIRC v55: unstructured mesh design and performance, Geosci. Model Dev., 14, 1125–1145, https://doi.org/10.5194/gmd-14-1125-2021, 2021.

Wessel, P., and W. H. F. Smith, 1996. A Global Self-consistent, Hierarchical, High-resolution Shoreline Database, J. Geophys. Res., 101, 8741-8743, 1996.

Xu, J., E. Myers, S. White (2010). VDatum for the Coastal Waters of North/Central California, Oregon and Western Washington: Tidal Datums and Sea Surface Topography. NOAA Technical Memorandum NOS CS 22.

Xu, J., E.P. Myers, I. Jeong, and S.A. White, 2013. VDatum for the coastal waters of Texas and western Louisiana : tidal DAtums and topography of the sea surface. NOAA Technical Memorandum NOS CS 29, 48 pp. National Oceanic and Atmospheric Administration, National Ocean Service, Office of Coast Survey, Coast Survey Development Laboratory, Silver Spring, Maryland.

Yang, E. P. Myers, E.A. Dhingra, A. M. Wong, and S. A. White, 2009. VDatum for the coastal waters of southern california tidal datums and sea surface topography. NOAA Technical Memorandum NOS CS 17, 59 pp. National Oceanic and Atmospheric Administration, National Ocean Service, Office of Coast Survey, Coast Survey Development Laboratory, Silver Spring, Maryland.

Yang, E. P. Myers, A. M. Wong, and S. A. White, 2010. VDatum for Eastern Louisiana and Mississippi Coastal Waters: Tidal Datums, Marine Grids, and Sea Surface Topography. NOAA Technical Memorandum NOS CS 19, 56 pp. National Oceanic and Atmospheric Administration, National Ocean Service, Office of Coast Survey, Coast Survey Development Laboratory, Silver Spring, Maryland.

Yang, Z.Y., E. P. Myers, I. Jeong, and S. A. White, 2012. VDatum for the Coastal Waters from the Florida Shelf to the South Atlantic Bight: Tidal Datums, Marine Grids, and Sea Surface Topography. NOAA Technical Memorandum NOS CS 27, 97 pp. National Oceanic and Atmospheric Administration, National Ocean Service, Office of Coast Survey, Coast Survey Development Laboratory, Silver Spring, Maryland.

APPENDIX A TIDE STATION DATA AND MODEL RESULTS

TABLE A.1 TIDE STATION DATA AND MODEL RESULTS

No.	Station ID	Location Name	Longitude Latitude	Obs rms	MHHW	Tidal MHW	Datums MLW	MLLW	Source ID
1	9410079	AVALON, SANTA CATALINA ISLAND	-118.325000 33.345000	0.01	0.80 0.79 -0.01 -1%	0.57 0.56 -0.01 -2%	-0.56 -0.56 0.00 -0%	-0.83 -0.81 0.02 -2%	obs model diff error
2	9410120	IMPERIAL BEACH, PACIFIC OCEAN	-117.135000 32.578300	0.01	0.80 0.80 -0.00 -0%	0.57 0.57 -0.00 -0%	-0.57 -0.57 -0.00 0%	-0.84 -0.81 0.03 -3%	obs model diff error
3	9410135	SOUTH SAN DIEGO BAY	-117.107778 32.629139	0.01	0.88 0.89 0.02 2%	0.65 0.67 0.02 3%	-0.64 -0.66 -0.01 2%	-0.93 -0.91 0.02 -2%	obs model diff error
4	9410155	BALLAST POINT	-117.233000 32.686700	0.01	0.82 0.82 0.00 1%	0.60 0.60 0.00 0%	-0.59 -0.58 0.01 -2%	-0.86 -0.82 0.03 -4%	obs model diff error
5	9410170	SAN DIEGO, SAN DIEGO BAY	-117.173583 32.714190	0.00	0.85 0.86 0.01 1%	0.62 0.63 0.01 1%	0.61 0.62 0.01 2%	-0.90 -0.89 0.01 -1%	obs model diff error
6	9410179	OCEAN BEACH, POINT LOMA	-117.255000 32.748300	0.01	0.80 0.80 0.00 0%	0.57 0.57 -0.00 -0%	0.56 0.57 0.01 1%	-0.83 -0.81 0.01 -1%	obs model diff error
7	9410196	MISSION BAY	-117.223778 32.793722	0.01	0.80 0.81 0.01 1%	0.58 0.59 0.00 1%	0.58 0.60 0.02 3%	-0.86 -0.86 -0.00 0%	obs model diff error
8	9410230	LA JOLLA, PACIFIC OCEAN	-117.257139 32.866889	0.00	0.79 0.80 0.01 1%	0.57 0.57 0.00 0%	0.56 0.57 0.01 2%	-0.83 -0.82 0.01 -1%	obs model diff error
9	9410396	OCEANSIDE HARBOR	-117.395000 33.210000	0.01	0.80 0.80 0.00 0%	0.57 0.57 -0.00 -0%	0.56 0.57 0.01 2%	-0.83 -0.83 0.00 -0%	obs model diff error
10	9410580	NEWPORT BEACH, NEWPORT BAY ENTRANCE	-117.883000 33.603300	0.00	0.80 0.81 0.00 0%	0.58 0.58 -0.00 -0%	0.57 0.57 0.01 1%	-0.84 -0.83 0.01 -1%	obs model diff error
11	9410650	CABRILLO BEACH	-118.273000 33.706700	0.01	0.81 0.81 0.00 0%	0.59 0.58 -0.01 -1%	0.57 0.58 0.00 0%	-0.86 -0.84 0.02 -2%	obs model diff erro
12	9410660	LOS ANGELES, OUTER HARBOR	-118.272861 33.719944	0.00	0.81 0.81 -0.00 -0%	0.59 0.58 -0.01 -2%	0.57 0.58 0.00 0%	-0.86 -0.84 0.02 -2%	obs model diff error
13	9410680	LONG BEACH, TERMINAL ISLAND	-118.227000 33.751700	0.00	0.81 0.81 -0.00 -0%	0.59 0.58 -0.01 -2%	0.58 0.58 0.00 -0%	-0.87 -0.84 0.02 -2%	obs model diff error

14	9410738	KING HARBOR, SANTA MONICA BAY	-118.398000 33.846700	0.01	0.79 0.80 0.01 2%	0.56 0.57 0.01 1%	0.55 0.57 0.02 4%	-0.83 -0.83 0.00 -0%	obs model diff error
15	9410840	SANTA MONICA, PACIFIC OCEAN	-118.500000 34.008300	0.00	0.80 0.80 -0.00 -0%	0.58 0.57 -0.01 -2%	0.57 0.57 0.00 0%	-0.85 -0.83 0.02 -2%	obs model diff error
16	9410962	BECHERS BAY, SANTA ROSA ISLAND	-120.047000 34.008300	0.02	0.75 0.77 0.01 2%	0.53 0.53 0.00 0%	0.52 0.53 0.01 3%	-0.81 -0.80 0.02 -2%	obs model diff error
17	9410971	PRISONERS HARBOR, SANTA CRUZ IS.	-119.683000 34.020000	0.01	0.78 0.78 -0.00 -0%	0.55 0.54 -0.00 -1%	0.53 0.54 0.01 1%	-0.82 -0.80 0.02 -2%	obs model diff error
18	9411270	RINCON ISLAND, PACIFIC OCEAN	-119.443000 34.348300	0.00	0.80 0.81 0.01 1%	0.57 0.57 -0.00 -1%	-0.6 0.57 0.01 1%	-0.86 -0.84 0.02 -2%	obs model diff error
19	9411340	SANTA BARBARA, PACIFIC OCEAN	-119.692806 34.403111	0.00	0.79 0.80 0.01 1%	0.56 0.56 -0.00 -0%	0.55 0.56 0.01 1%	-0.85 -0.83 0.02 -2%	obs model diff error
20	9411399	GAVIOTA STATE PARK, PACIFIC OCEAN	-120.228306 34.469389	0.01	0.77 0.78 0.01 1%	0.55 0.54 -0.01 -1%	-0.54 -0.54 0.00 -0%	-0.84 -0.82 0.02 -3%	obs model diff error
21	9411406	OIL PLATFORM HARVEST (TOPEX PROJECT)	-120.681944 34.469167	0.01	0.77 0.76 -0.00 -1%	0.54 0.53 -0.02 -3%	-0.53 -0.52 0.01 -1%	-0.83 -0.80 0.03 -4%	obs model diff error
22	9412110	PORT SAN LUIS, SAN LUIS OBISPO BAY	-120.754194 35.168806	0.00	0.77 0.78 0.01 1%	0.56 0.54 -0.01 -2%	-0.54 -0.54 0.00 -0%	-0.85 -0.82 0.03 -4%	obs model diff error
23	9412553	SAN SIMEON	121.188000 35.641700	0.02	0.76 0.77 0.01 2%	0.54 0.54 0.00 -1%	0.52 0.53 0.01 2%	-0.84 -0.82 0.02 -3%	obs model diff error
24	9412802	Mansfield Cone, Pacific Ocean	121.481944 35.949528	0.02	0.76 0.77 0.01 1%	0.55 0.54 0.01 -2%	0.52 0.53 0.01 1%	-0.83 -0.81 0.02 -3%	obs model diff error
25	9413450	MONTEREY, MONTEREY HARBOR	-121.888054 36.605000	0.00	0.76 0.77 0.01 1%	0.55 0.54 -0.01 -1%	0.53 0.53 -0.00 1%	-0.86 -0.82 0.04 -4%	obs model diff error
26	9413616	MOSS LANDING,OCEAN PIER	-121.790000 36.801700	0.01	0.76 0.77 0.01 2%	0.54 0.54 -0.00 -0%	-0.52 -0.53 -0.02 3%	-0.83 -0.82 0.01 -1%	obs model diff error
27	9413623	ELKHORN SLOUGH, ENTRANCE BRIDGE	-121.785000 36.810000	0.01	0.77 0.77 0.00 0%	0.56 0.55 -0.02 -3%	-0.51 -0.53 -0.02 4%	-0.84 -0.83 0.01 -1%	obs model diff error
28	9413631	ELKHORN SLOUGH AT ELKHORN	-121.747000 36.818300	0.01	0.77 0.78 0.01 1%	0.56 0.55 -0.00 -1%	-0.55 -0.55 0.01 -1%	-0.86 -0.84 0.02 -3%	obs model diff error

29	9413643	TIDAL CREEK, ELKHORN SLOUGH	-121.745000 36.833330	0.01	0.76 0.78 0.02 3%	0.54 0.55 0.01 2%	-0.55 -0.55 -0.00 0%	-0.87 -0.85 0.03 -3%	obs model diff error
30	9413651	KIRBY PARK, ELKHORN SLOUGH	-121.745278 36.841330	0.01	0.78 0.78 0.00 1%	0.56 0.55 -0.01 -1%	-0.57 -0.55 0.02 -3%	-0.90 -0.85 0.05 -6%	obs model diff error
31	9413663	ELKHORN SLOUGH RAILROAD BRIDGE	-121.755000 36.856670	0.01	0.79 0.78 -0.00 -0%	0.57 0.56 -0.01 -2%	-0.57 -0.56 0.01 -2%	-0.89 -0.86 0.04 -4%	obs model diff error
32	9414131	PILLAR POINT, HALF MOON BAY	-122.482167 37.502500	0.02	0.80 0.82 0.02 3%	0.60 0.59 -0.01 -2%	-0.57 -0.57 -0.00 0%	-0.91 -0.88 0.03 -3%	obs model diff error
33	9414290	SAN FRANCISCO, SAN FRANCISCO BAY	-122.465889 37.806306	0.00	0.83 0.88 0.05 6%	0.64 0.65 0.01 1%	-0.60 -0.62 -0.02 3%	-0.95 -0.94 0.01 -1%	obs model diff error
34	9414317	PIER 22 1/2, SAN FRANCISCO	-122.387000 37.790000	0.01	0.91 0.99 0.08 9%	0.72 0.76 0.03 5%	-0.65 -0.70 -0.05 7%	-0.99 -1.02 -0.02 2%	obs model diff error
35	9414358	HUNTERS POINT, S.F. BAY	-122.357000 37.730000	0.01	0.99 1.07 0.08 8%	0.80 0.83 0.03 4%	-0.74 -0.78 -0.05 6%	-1.08 -1.11 -0.02 2%	obs model diff error
36	9414392	OYSTER POINT MARINA, SAN FRANCISCO BAY	-122.377000 37.665000	0.01	1.04 1.11 0.07 7%	0.84 0.87 0.03 3%	-0.80 -0.85 -0.05 7%	-1.15 -1.19 -0.04 3%	obs model diff error
37	9414458	SAN MATEO BRIDGE, WEST SIDE	-122.253000 37.580000	0.01	1.10 1.18 0.08 7%	0.91 0.94 0.03 4%	-0.89 -0.95 -0.05 6%	-1.25 -1.29 -0.04 3%	obs model diff error
38	9414509	DUMBARTON BRIDGE, SAN FRANCISCO BAY	-122.115000 37.506700	0.02	1.20 1.26 0.07 6%	1.01 1.02 0.01 1%	-1.04 -1.07 -0.02 2%	-1.43 -1.41 0.01 -1%	obs model diff error
39	9414519	MOWRY SLOUGH, SAN FRANCISCO BAY	-122.042000 37.493300	0.02	1.21 1.28 0.07 5%	1.02 1.04 0.01 1%	-1.07 -1.12 -0.05 5%	-1.42 -1.46 -0.04 3%	obs model diff error
40	9414523	REDWOOD CITY, WHARF 5, S. F. BAY	-122.211528 37.506778	0.00	1.16 1.23 0.07 6%	0.97 0.99 0.02 2%	-0.98 -1.02 -0.04 4%	-1.34 -1.36 -0.02 1%	obs model diff error
41	9414525	PALO ALTO YACHT HARBOR, S. F. BAY	-122.105000 37.458300	0.01	1.17 1.27 0.10 8%	0.98 1.03 0.04 5%	-0.92 -1.05 -0.13 14%	-1.15 -1.32 -0.17 15%	obs model diff error
42	9414551	GOLD STREET BRIDGE, ALVISO SLOUGH	-121.975000 37.423300	0.03	1.31 1.30 -0.02 -1%	1.14 1.05 -0.09 -8%	-1.19 -1.07 0.11 -10%	-1.52 -1.31 0.21 -14%	obs model diff error
43	9414575	COYOTE CREEK, ALVISO SLOUGH	-122.023000 37.465000	0.02	1.24 1.28 0.04 3%	1.06 1.04 -0.02 -2%	-1.12 -1.04 0.09 -8%	-1.50 -1.28 0.22 -15%	obs model diff error

44	9414632	ALAMEDA CREEK, SAN FRANCISCO BAY	-122.145000 37.595000	NaN	NaN 0.00 NaN NaN%	NaN 0.00 NaN NaN%	NaN 0.00 NaN NaN%	NaN 0.00 NaN NaN%	obs model diff error
45	9414688	SAN LEANDRO MARINA, SAN FRANCISCO BAY	-122.192000 37.695000	0.01	1.07 1.15 0.08 8%	0.88 0.91 0.04 4%	-0.84 -0.89 -0.05 6%	-1.19 -1.22 -0.03 2%	obs model diff error
46	9414711	OAKLAND AIRPORT, SAN FRANCISCO BAY	-122.208000 37.731700	0.01	0.97 1.06 0.09 9%	0.78 0.82 0.04 5%	-0.75 -0.78 -0.04 5%	-1.09 -1.10 -0.01 1%	obs model diff error
47	9414746	OAKLAND/ALAMEDA PARK ST. BRIDGE	-122.235000 37.771700	0.01	0.96 1.05 0.09 10%	0.77 0.81 0.04 6%	-0.69 -0.73 -0.04 6%	-1.03 -1.05 -0.02 2%	obs model diff error
48	9414750	ALAMEDA, SAN FRANCISCO BAY	-122.300000 37.771700	0.00	0.96 1.04 0.08 8%	0.77 0.80 0.03 4%	-0.71 -0.75 -0.04 6%	-1.05 -1.07 -0.02 2%	obs model diff error
49	9414764	OAKLAND INNER HARBOR, SAN FRANCISCO BAY	-122.282000 37.795000	0.01	0.93 1.01 0.08 8%	0.74 0.77 0.03 4%	-0.68 -0.73 -0.05 8%	-1.01 -1.05 -0.03 3%	obs model diff error
50	9414767	ALAMEDA NAS, NAVY FUEL PIER	-122.315000 37.793300	0.01	0.92 1.00 0.07 8%	0.73 0.76 0.03 3%	-0.68 -0.72 -0.04 6%	-1.03 -1.04 -0.01 1%	obs model diff error
51	9414777	OAKLAND MIDDLE HARBOR, PIER 40	-122.338000 37.805000	0.01	0.90 0.98 0.09 10%	0.72 0.75 0.03 5%	-0.66 -0.71 -0.05 8%	-1.00 -1.03 -0.04 4%	obs model diff error
52	9414782	YERBA BUENA ISLAND, SAN FRANCISCO BAY	-122.360000 37.810000	0.01	0.89 0.97 0.08 9%	0.70 0.73 0.03 4%	-0.67 -0.70 -0.03 5%	-1.01 -1.02 -0.02 2%	obs model diff error
53	9414806	SAUSALITO, SAN FRANCISCO BAY	-122.477000 37.846700	0.01	0.80 0.86 0.06 7%	0.62 0.63 0.02 2%	-0.59 -0.62 -0.04 6%	-0.93 -0.94 -0.00 0%	obs model diff error
54	9414811	BRADMOOR ISLAND, NURSE SLOUGH	-121.923000 38.183300	0.01	0.79 0.77 -0.02 -2%	0.63 0.57 -0.06 -9%	-0.65 -0.58 0.08 -12%	-0.88 -0.74 0.14 -16%	obs model diff error
55	9414816	BERKELEY,S.F.BAY	-122.307000 37.865000	0.01	0.86 0.94 0.08 10%	0.67 0.71 0.04 6%	-0.65 -0.70 -0.04 7%	-1.00 -1.02 -0.02 2%	obs model diff error
56	9414818	ANGEL ISLAND, EAST GARRISON, S.F. BAY	-122.420000 37.863300	0.01	0.83 0.89 0.07 8%	0.64 0.66 0.02 3%	-0.63 -0.66 -0.04 6%	-0.97 -0.98 -0.01 1%	obs model diff error
57	9414819	SAUSALITO, COE DOCK, S.F. BAY	-122.493000 37.865000	0.01	0.80 0.88 0.07 9%	0.62 0.65 0.03 4%	-0.60 -0.64 -0.04 7%	-0.94 -0.95 -0.01 1%	obs model diff error
58	9414835	BORDEN HIGHWAY BRIDGE, MIDDLE RIVER	-121.488000 37.891700	0.02	0.49 0.54 0.05 10%	0.37 0.36 -0.01 -3%	-0.39 -0.38 0.01 -3%	-0.53 -0.47 0.06 -11%	obs model diff error

59	9414837	POINT CHAUNCEY, RICHARDSON BAY	-122.443000 37.891700	0.01	0.82 0.89 0.07 9%	0.64 0.67 0.03 4%	-0.60 -0.65 -0.05 8%	-0.93 -0.96 -0.02 2%	obs model diff error
60	9414849	RICHMOND INNER HARBOR, SAN FRANCISCO BAY	-122.358000 37.910000	0.01	0.85 0.92 0.07 8%	0.66 0.70 0.04 6%	-0.65 -0.62 0.03 -5%	-0.99 -0.83 0.16 -16%	obs model diff error
61	9414863	RICHMOND, CHEVRON OIL PIER	-122.409583 37.923000	0.00	0.85 0.91 0.06 6%	0.67 0.68 0.01 2%	-0.65 -0.67 -0.02 3%	-0.99 -0.98 0.01 -1%	obs model diff error
62	9414867	BORDEN HIGHWAY BRIDGE, SAN JOAQUIN RIVER	-121.333000 37.936700	0.02	0.58 0.67 0.09 16%	0.45 0.47 0.03 6%	-0.45 -0.49 -0.03 7%	-0.60 -0.61 -0.01 2%	obs model diff error
63	9414873	POINT SAN QUENTIN, SAN FRANCISCO BAY	-122.475000 37.945000	0.01	0.82 0.90 0.07 9%	0.64 0.67 0.03 4%	-0.61 -0.66 -0.04 7%	-0.94 -0.95 -0.02 2%	obs model diff error
64	9414874	CORTE MADERA CREEK	-122.513000 37.943300	0.01	0.82 0.89 0.07 9%	0.64 0.66 0.03 4%	-0.62 -0.63 -0.02 3%	-0.95 -0.90 0.05 -5%	obs model diff error
65	9414958	BOLINAS, BOLINAS LAGOON	-122.678612 37.907780	0.01	0.63 0.73 0.10 15%	0.45 0.48 0.03 7%	-0.47 -0.40 0.06 -14%	-0.71 -0.53 0.18 -25%	obs model diff error
66	9415009	POINT SAN PEDRO, SAN FRANCISCO BAY	-122.447000 37.993300	0.01	0.85 0.91 0.06 7%	0.67 0.69 0.02 3%	-0.61 -0.67 -0.05 8%	-0.94 -0.96 -0.02 2%	obs model diff error
67	9415020	POINT REYES, DRAKES BAY	-122.976669 37.996113	0.00	0.81 0.81 -0.00 -0%	0.61 0.59 -0.02 -4%	-0.59 -0.57 0.01 -2%	-0.95 -0.87 0.07 -8%	obs model diff error
68	9415021	BLACKSLOUGH LANDING, SAN JOAQUIN RIVER	-121.419044 37.994694	0.03	0.55 0.66 0.11 20%	0.41 0.46 0.05 13%	-0.42 -0.47 -0.05 11%	-0.56 -0.59 -0.03 6%	obs model diff error
69	9415052	GALLINAS, GALLINAS CREEK	-122.503000 38.015000	0.02	0.85 0.91 0.06 7%	0.66 0.68 0.02 2%	-0.65 -0.68 -0.04 6%	-0.95 -0.96 -0.01 1%	obs model diff error
70	9415053	DUTCH SLOUGH	-121.638000 38.011700	0.02	0.51 0.57 0.05 11%	0.37 0.38 0.01 2%	-0.38 -0.39 -0.01 3%	-0.54 -0.52 0.02 -4%	obs model diff error
71	9415056	PINOLE POINT, SAN PABLO BAY	-122.363000 38.015000	0.01	0.89 0.93 0.04 4%	0.71 0.70 -0.01 -1%	-0.68 -0.70 -0.01 2%	-1.01 -0.97 0.04 -4%	obs model diff error
72	9415064	ANTIOCH, SAN JOAQUIN RIVER	-121.815000 38.020000	0.01	0.56 0.59 0.03 5%	0.42 0.39 -0.03 -7%	-0.44 -0.43 0.01 -3%	-0.62 -0.58 0.04 -7%	obs model diff error
73	9415074	HERCULES WHARF	-122.292000 38.023300	0.02	0.87 0.91 0.03 4%	0.69 0.68 -0.01 -2%	-0.69 -0.69 -0.00 0%	-0.98 -0.94 0.04 -4%	obs model diff error

74	9415096	PITTSBURG, NEW YORK SLOUGH, SUISUN BAY	-121.880000 38.036700	0.02	0.63 0.63 -0.00 -1%	0.48 0.42 -0.05 -11%	-0.48 -0.45 0.03 -6%	-0.68 -0.60 0.07 -11%	obs model diff error
75	9415102	MARTINEZ-AMORCO PIER, CARQUINEZ STRAIT	-122.125194 38.034639	0.01	0.76 0.78 0.02 2%	0.60 0.57 -0.03 -5%	-0.60 -0.57 0.03 -5%	-0.87 -0.76 0.11 -12%	obs model diff error
76	9415105	WARDS ISLAND, SAN JOAQUIN RIVER	-121.496856 38.050025	0.03	0.51 0.62 0.11 21%	0.38 0.43 0.05 14%	-0.38 -0.44 -0.06 15%	-0.52 -0.56 -0.04 8%	obs model diff error
77	9415111	BENICIA, CARQUINEZ STRAIT	-122.130000 38.043300	0.01	0.76 0.77 0.01 2%	0.60 0.57 -0.03 -5%	-0.60 -0.57 0.04 -6%	-0.87 -0.76 0.11 -13%	obs model diff error
78	9415112	MALLARD ISLAND, SUISUN BAY	-121.918000 38.043300	0.01	0.64 0.63 -0.00 -1%	0.49 0.44 -0.05 -10%	-0.50 -0.46 0.04 -7%	-0.71 -0.62 0.09 -13%	obs model diff error
79	9415124	HAMILTON AFB OUTSIDE GAUGE	-122.498000 38.048300	0.02	0.86 0.91 0.05 6%	0.68 0.68 0.00 0%	-0.65 -0.68 -0.03 4%	-0.99 -0.95 0.04 -4%	obs model diff error
80	9415126	HAMILTON AIR FORCE BASE INSIDE GAUGE	-122.498000 38.048300	0.01	NaN 0.91 NaN NaN%	NaN 0.68 NaN NaN%	NaN -0.68 NaN NaN%	NaN -0.95 NaN NaN%	obs model diff error
81	9415143	CROCKETT, CARQUINEZ STRAIT	-122.223000 38.058300	0.01	0.83 0.83 -0.00 -1%	0.66 0.61 -0.05 -7%	-0.68 -0.63 0.05 -7%	-0.98 -0.86 0.12 -12%	obs model diff error
82	9415144	PORT CHICAGO, SUISUN BAY	-122.039500 38.056000	0.00	0.72 0.72 0.01 1%	0.56 0.52 -0.04 -7%	-0.56 -0.52 0.03 -6%	-0.78 -0.68 0.10 -13%	obs model diff error
83	9415149	PRISONERS POINT, SAN JOAQUIN RIVER	-121.555000 38.061700	0.02	0.56 0.60 0.04 8%	0.42 0.41 -0.01 -3%	-0.40 -0.42 -0.01 3%	-0.56 -0.54 0.02 -4%	obs model diff error
84	9415193	THREE MILE SLOUGH,SAN JOAQUIN R.	-121.685000 38.086700	0.02	0.51 0.56 0.05 10%	0.36 0.37 0.01 2%	-0.38 -0.39 -0.01 4%	-0.54 -0.52 0.02 -3%	obs model diff error
85	9415205	MONTEZUMA SLOUGH, SUISUN BAY	-121.885000 38.076700	0.02	0.62 0.63 0.01 2%	0.48 0.43 -0.04 -9%	-0.50 -0.47 0.04 -7%	-0.70 -0.61 0.09 -12%	obs model diff error
86	9415218	MARE IS.NAVAL SHIPYARD,CARQUINEZ STRAIT	-122.250000 38.070000	0.01	0.82 0.85 0.03 3%	0.65 0.63 -0.02 -3%	-0.64 -0.63 0.02 -3%	-0.94 -0.86 0.08 -9%	obs model diff error
87	9415228	INVERNESS, TOMALES BAY	-122.868000 38.113300	0.01	0.83 0.88 0.05 6%	0.61 0.66 0.06 9%	-0.58 -0.59 -0.01 3%	-0.89 -0.86 0.04 -4%	obs model diff error
88	9415229	KORTHS HBR, SAN JOAQUIN RIVER	-121.568383 38.097611	0.03	0.49 0.59 0.10 21%	0.35 0.40 0.05 14%	-0.35 -0.41 -0.06 16%	-0.49 -0.53 -0.04 9%	obs model diff error

89	9415252	PETALUMA RIVER ENTRANCE	-122.505667 38.115306	0.01	0.85 0.93 0.08 10%	0.68 0.70 0.02 2%	-0.70 -0.71 -0.01 2%	-0.98 -0.98 0.00 -0%	obs model diff error
90	9415265	SUISUN SLOUGH ENTRANCE	-122.074110 38.121530	0.01	0.72 0.74 0.02 2%	0.57 0.54 -0.03 -6%	-0.57 -0.53 0.04 -7%	-0.80 -0.69 0.11 -13%	obs model diff error
91	9415266	PIERCE HARBOR,GOODYEAR SLOUGH	-122.100000 38.126700	0.01	0.71 0.74 0.03 4%	0.57 0.54 -0.03 -5%	-0.57 -0.54 0.03 -5%	-0.79 -0.70 0.09 -11%	obs model diff error
92	9415307	MEINS LANDING, MONTEZUMA SLOUGH	-121.907000 38.136700	0.01	0.72 0.75 0.02 3%	0.57 0.55 -0.03 -5%	-0.60 -0.56 0.03 -5%	-0.82 -0.73 0.09 -11%	obs model diff error
93	9415316	RIO VISTA, SACRAMENTO RIVER	-121.692000 38.145000	0.02	0.59 0.59 -0.00 -0%	0.45 0.40 -0.05 -12%	-0.47 -0.43 0.04 -9%	-0.65 -0.57 0.08 -12%	obs model diff error
94	9415320	REYNOLDS, TOMALES BAY	-122.883000 38.146700	0.02	0.81 0.88 0.06 8%	0.59 0.65 0.06 11%	-0.55 -0.59 -0.04 7%	-0.84 -0.85 -0.01 1%	obs model diff error
95	9415338	SONOMA CK.ENTR.,SAN PABLO BAY	-122.407000 38.156700	0.01	0.83 0.91 0.08 10%	0.65 0.68 0.03 5%	-0.62 -0.70 -0.07 12%	-0.83 -0.94 -0.12 14%	obs model diff error
96	9415379	JOICE ISLAND, SUISUN SLOUGH	-122.045000 38.180000	0.01	0.76 0.76 0.00 1%	0.60 0.56 -0.05 -7%	-0.61 -0.56 0.05 -8%	-0.83 -0.72 0.11 -13%	obs model diff error
97	9415415	EDGERLEY ISLAND, NAPA RIVER	-122.312000 38.191700	0.02	0.88 0.93 0.05 6%	0.70 0.70 0.00 0%	-0.72 -0.68 0.04 -6%	-0.98 -0.87 0.11 -11%	obs model diff error
98	9415423	LAKEVILLE, PETALUMA RIVER	-122.547000 38.198300	0.02	0.89 0.98 0.09 10%	0.74 0.77 0.02 3%	-0.78 -0.75 0.03 -4%	-1.05 -1.01 0.04 -4%	obs model diff error
99	9415438	SKAGGS ISLAND, HUDEMAN SLOUGH	-122.373000 38.205000	0.02	0.87 0.91 0.04 5%	0.70 0.68 -0.02 -3%	-0.72 -0.68 0.04 -5%	-0.97 -0.88 0.09 -9%	obs model diff error
100	9415447	SONOMA CREEK, WINGO	-122.427000 38.210000	0.02	0.86 0.92 0.06 8%	0.68 0.69 0.01 1%	-0.69 -0.71 -0.03 4%	-0.93 -0.95 -0.01 2%	obs model diff error
101	9415477	SAND POINT, TOMALES BAY	-122.968000 38.231700	0.01	0.77 0.83 0.06 7%	0.55 0.60 0.05 9%	-0.50 -0.56 -0.06 12%	-0.80 -0.86 -0.06 7%	obs model diff error
102	9415478	NEW HOPE BRIDGE, MOKELUMNE RIVER	-121.490000 38.226700	0.02	0.50 0.66 0.16 32%	0.37 0.47 0.10 27%	-0.38 -0.49 -0.11 28%	-0.49 -0.60 -0.11 22%	obs model diff error
103	9415498	SUISUN CITY, SUISUN SLOUGH	-122.030000 38.236700	0.01	0.78 0.78 -0.00 -0%	0.63 0.58 -0.05 -8%	-0.64 -0.58 0.06 -10%	-0.87 -0.75 0.12 -13%	obs model diff error

104	9415584	PETALUMA RIVER, UPPER DRAWBRIDGE	-122.613000 38.228300	0.03	0.89 1.02 0.13 14%	0.75 0.81 0.06 8%	-0.84 -0.77 0.06 -8%	-1.14 -1.02 0.11 -10%	obs model diff error
105	9415623	NAPA, NAPA RIVER	-122.280000 38.298300	0.02	0.93 0.97 0.05 5%	0.78 0.75 -0.04 -4%	-0.85 -0.73 0.12 -14%	-1.17 -0.94 0.23 -20%	obs model diff error
106	9416174	SACRAMENTO, SACRAMENTO RIVER	-121.507000 38.580000	0.01	0.22 0.25 0.03 12%	0.13 0.12 -0.01 -6%	-0.15 -0.15 -0.00 3%	-0.19 -0.17 0.01 -6%	obs model diff error
107	9416409	Green Cove, Pacific Ocean	-123.449389 38.704333	0.01	0.78 0.82 0.04 5%	0.58 0.60 0.02 3%	-0.53 -0.58 -0.06 11%	-0.81 -0.89 -0.08 10%	obs model diff error
108	9416841	ARENA COVE, PACIFIC OCEAN	-123.711083 38.914556	0.00	0.83 0.83 -0.00 -0%	0.63 0.61 -0.02 -3%	-0.61 -0.59 0.01 -2%	-0.96 -0.91 0.05 -5%	obs model diff error
109	9417426	NOYO HARBOR	-123.805111 39.425778	0.01	0.86 0.86 -0.00 -0%	0.66 0.64 -0.02 -3%	-0.63 -0.62 0.01 -1%	-1.00 -0.94 0.06 -6%	obs model diff error
110	9418024	SHELTER COVE	-124.057999 40.025002	0.02	0.86 0.87 0.01 1%	0.66 0.65 -0.01 -2%	-0.64 -0.64 0.00 -0%	-1.01 -0.96 0.04 -4%	obs model diff error
111	9418637	COCKROBIN ISLAND BRIDGE, EEL RIVER	-124.282222 40.637222	0.01	0.87 0.94 0.08 9%	0.66 0.72 0.06 10%	-0.68 -0.71 -0.02 4%	-1.03 -1.05 -0.02 2%	obs model diff error
112	9418686	HOOKTON SLOUGH,HUMBOLDT BAY	-124.222000 40.686700	0.01	0.97 0.99 0.03 3%	0.75 0.77 0.02 3%	-0.77 -0.75 0.02 -2%	-1.15 -1.10 0.05 -4%	obs model diff error
113	9418723	FIELDS LANDING, HUMBOLDT BAY	-124.222000 40.723300	0.01	0.97 0.99 0.02 2%	0.75 0.77 0.01 2%	-0.75 -0.75 0.00 -0%	-1.13 -1.09 0.04 -3%	obs model diff error
114	9418739	RED BLUFF, HUMBOLDT BAY	-124.212000 40.740000	0.02	0.94 0.98 0.04 4%	0.73 0.76 0.03 4%	-0.74 -0.74 -0.00 0%	-1.11 -1.08 0.03 -3%	obs model diff error
115	9418767	NORTH SPIT, HUMBOLDT BAY	-124.217200 40.766300	0.00	0.96 0.99 0.03 3%	0.74 0.77 0.03 4%	-0.75 -0.73 0.01 -2%	-1.13 -1.07 0.06 -5%	obs model diff error
116	9418778	BUCKSPORT, HUMBOLDT BAY	-124.197000 40.778300	0.01	0.98 1.02 0.04 4%	0.76 0.80 0.04 6%	-0.76 -0.74 0.02 -2%	-1.15 -1.08 0.06 -5%	obs model diff error
117	9418799	FRESHWATER SLOUGH, HUMBOLDT BAY	-124.120000 40.798300	0.01	1.05 1.09 0.04 4%	0.83 0.86 0.03 4%	-0.78 -0.82 -0.04 5%	-1.11 -1.18 -0.07 6%	obs model diff error
118	9418801	EUREKA, HUMBOLDT BAY	-124.167000 40.806700	0.01	0.98 1.08 0.10 10%	0.78 0.85 0.08 10%	-0.80 -0.80 0.00 -0%	-1.19 -1.15 0.05 -4%	obs model diff error

119	9418802	EUREKA SLOUGH, HUMBOLDT BAY	-124.142000 40.806700	0.02	1.04 1.09 0.05 4%	0.82 0.86 0.05 6%	-0.82 -0.82 0.00 -0%	-1.21 -1.17 0.04 -3%	obs model diff error
120	9418817	SAMOA, HUMBOLDT BAY	-124.174453 40.821621	0.01	1.03 1.09 0.06 6%	0.81 0.86 0.05 6%	-0.82 -0.80 0.02 -2%	-1.22 -1.15 0.06 -5%	obs model diff error
121	9418865	MAD RIVER SLOUGH, ARCATA BAY	-124.148000 40.865000	0.02	1.03 1.09 0.06 6%	0.81 0.87 0.06 7%	-0.89 -0.83 0.06 -7%	-1.29 -1.18 0.11 -9%	obs model diff error
122	9418983	UPPER MAD RIVER SLOUGH	-124.135000 40.898300	0.02	1.04 1.09 0.06 5%	0.82 0.87 0.05 6%	-0.94 -0.83 0.11 -12%	-1.34 -1.19 0.15 -11%	obs model diff error
123	9419059	TRINIDAD HARBOR	-124.147000 41.056700	0.01	0.95 0.96 0.01 1%	0.74 0.74 -0.01 -1%	-0.73 -0.69 0.04 -5%	-1.10 -1.00 0.10 -9%	obs model diff error
124	9419750	CRESCENT CITY, PACIFIC OCEAN	-124.183000 41.745000	0.00	0.96 0.99 0.03 3%	0.77 0.77 -0.00 -0%	-0.75 -0.75 0.00 -0%	-1.13 -1.10 0.03 -3%	obs model diff error
125	9419945	PYRAMID POINT, SMITH RIVER	-124.200917 41.945250	0.01	0.91 1.01 0.10 11%	0.73 0.78 0.06 8%	-0.70 -0.77 -0.07 9%	-1.04 -1.12 -0.08 7%	obs model diff error
126	9431011	Gold Beach, Rogue River	-124.418722 42.421639	0.01	0.99 1.03 0.04 4%	0.79 0.80 0.01 1%	-0.78 -0.78 -0.01 1%	-1.19 -1.14 0.06 -5%	obs model diff error
127	9431647	PORT ORFORD, PACIFIC OCEAN	-124.498278 42.738970	0.00	1.02 1.03 0.01 1%	0.80 0.81 0.00 0%	-0.78 -0.79 -0.01 1%	-1.20 -1.14 0.06 -5%	obs model diff error
128	9432373	BANDON, COQUILLE RIVER	-124.411935 43.120400	0.03	1.02 1.02 -0.00 -0%	0.80 0.78 -0.02 -2%	-0.78 -0.71 0.07 -9%	-1.14 -0.94 0.20 -18%	obs model diff error
129	9432436	COQUILLE RIVER	-124.181806 43.157917	0.03	0.83 0.99 0.15 19%	0.61 0.70 0.08 13%	-0.60 -0.55 0.05 -8%	-0.76 -0.67 0.09 -11%	obs model diff error
130	9432771	CAPE ARAGO LIGHTHOUSE	-124.367000 43.341700	0.01	1.14 1.09 -0.05 -4%	0.93 0.86 -0.07 -8%	-0.84 -0.84 -0.00 0%	-1.18 -1.20 -0.01 1%	obs model diff error
131	9432780	CHARLESTON, COOS BAY	-124.322000 43.345000	0.00	1.08 1.13 0.05 4%	0.88 0.90 0.02 2%	-0.86 -0.85 0.00 -0%	-1.24 -1.20 0.04 -3%	obs model diff error
132	9432796	ISTHMUS SLOUGH, COOS BAY	-124.192000 43.351700	0.02	1.17 1.28 0.11 9%	0.97 1.06 0.09 9%	-1.08 -0.94 0.14 -13%	-1.49 -1.24 0.26 -17%	obs model diff error
133	9432879	SITKA DOCK, COOS BAY	-124.297000 43.376700	0.01	1.08 1.17 0.09 8%	0.88 0.93 0.06 7%	-0.88 -0.87 0.01 -2%	-1.27 -1.22 0.05 -4%	obs model diff error

134	9432895	NORTH BEND, COOS BAY	-124.218000 43.410000	0.01	1.14 1.27 0.12 11%	0.95 1.04 0.09 10%	-1.02 -0.96 0.06 -6%	-1.42 -1.29 0.14 -10%	obs model diff error
135	9433445	Half Moon Bay, Umpqua River	-124.192000 43.675000	0.01	1.02 1.13 0.12 12%	0.82 0.91 0.09 11%	-0.79 -0.85 -0.05 7%	-1.16 -1.19 -0.03 2%	obs model diff error
136	9433501	REEDSPORT	-124.095000 43.705000	0.03	1.06 1.22 0.16 15%	0.86 0.99 0.13 16%	-0.86 -0.94 -0.08 9%	-1.20 -1.27 -0.07 6%	obs model diff error
137	9434098	FLORENCE USCG PIER, SUISLAW RIVER	-124.123000 44.002111	0.02	1.04 1.13 0.09 9%	0.84 0.90 0.05 6%	-0.84 -0.86 -0.02 3%	-1.22 -1.20 0.02 -1%	obs model diff error
138	9434938	DRIFT CREEK, ALSEA RIVER	-123.990000 44.413300	0.02	1.06 1.01 -0.06 -5%	0.85 0.78 -0.07 -9%	-0.70 -0.65 0.05 -7%	-0.90 -0.81 0.09 -10%	obs model diff error
139	9434939	WALDPORT, ALSEA BAY	-124.058083 44.434361	0.01	1.07 1.12 0.05 5%	0.85 0.88 0.03 4%	-0.86 -0.79 0.08 -9%	-1.25 -1.04 0.21 -17%	obs model diff error
140	9435308	WEISER POINT, YAQUINA RIVER	-124.012695 44.594772	0.03	1.20 1.23 0.04 3%	1.00 1.01 0.01 1%	-0.98 -0.95 0.02 -2%	-1.38 -1.30 0.08 -6%	obs model diff error
141	9435362	TOLEDO	-123.938160 44.616917	0.03	1.26 1.29 0.03 3%	1.05 1.07 0.01 1%	-1.04 -1.02 0.02 -2%	-1.43 -1.38 0.06 -4%	obs model diff error
142	9435380	SOUTH BEACH, YAQUINA RIVER	-124.043000 44.625000	0.00	1.19 1.21 0.03 2%	0.97 0.98 0.01 1%	-0.94 -0.93 0.00 -0%	-1.36 -1.30 0.06 -4%	obs model diff error
143	9435385	YAQUINA USCG STA, NEWPORT	-124.055000 44.626700	0.01	1.14 1.21 0.06 5%	0.96 0.97 0.01 1%	-0.93 -0.93 0.00 -0%	-1.36 -1.29 0.06 -5%	obs model diff error
144	9435827	DEPOE BAY	-124.058000 44.810000	0.01	1.17 1.17 0.00 0%	0.95 0.93 -0.02 -2%	-0.93 -0.92 0.01 -1%	-1.35 -1.28 0.06 -5%	obs model diff error
145	9435992	CHINOOK BEND, SILETZ RIVER	-123.963611 44.880000	0.02	0.86 1.11 0.24 28%	0.65 0.86 0.21 33%	-0.63 -0.61 0.02 -3%	-0.82 -0.73 0.09 -11%	obs model diff error
146	9436381	CASCADE HEAD, SALMON RIVER	-124.007306 45.047944	0.02	1.08 1.12 0.05 4%	0.87 0.89 0.02 3%	-0.80 -0.77 0.03 -3%	-1.10 -0.98 0.12 -11%	obs model diff error
147	9436641	NESTUCCA BAY, LITTLE NESTUCCA RIVER	-123.937778 45.161111	0.02	NaN 1.25 NaN NaN%	NaN 1.22 NaN NaN%	NaN 0.04 NaN NaN%	NaN 0.03 NaN NaN%	obs model diff error
148	9437262	NETARTS, NETARTS BAY	-123.945000 45.430000	0.03	0.98 1.15 0.17 17%	0.75 0.91 0.16 21%	-0.79 -0.71 0.07 -9%	-1.11 -0.92 0.19 -17%	obs model diff error

149	9437381	DICK POINT, TILLAMOOK BAY	-123.902000 45.481700	0.02	1.11 1.27 0.16 14%	0.90 1.04 0.14 16%	-0.79 -0.90 -0.11 14%	-1.01 -1.18 -0.18 17%	obs model diff error
150	9437540	Garibaldi, Tillamook Bay	-123.918944 45.554530	0.01	1.17 1.24 0.08 7%	0.95 1.01 0.06 7%	-0.95 -0.93 0.02 -3%	-1.37 -1.28 0.09 -7%	obs model diff error
151	9437585	NORTH JETTY, TILLAMOOK BAY	-123.964996 45.570000	0.01	1.15 1.20 0.05 4%	0.94 0.97 0.03 3%	-0.89 -0.92 -0.02 3%	-1.30 -1.28 0.02 -1%	obs model diff error
152	9437954	NORTH FORK, NEHALEM RIVER	-123.876417 45.733778	0.03	1.25 1.23 -0.01 -1%	1.03 1.01 -0.02 -2%	-1.00 -0.92 0.08 -8%	-1.35 -1.16 0.19 -14%	obs model diff error
153	9438125	MULTNOMAH CHANNEL, COLUMBIA RIVER	-122.827000 45.811700	0.03	0.53 0.57 0.04 8%	0.37 0.43 0.06 16%	-0.36 -0.42 -0.06 16%	-0.43 -0.47 -0.04 10%	obs model diff error
154	9438478	SEASIDE (12TH AVE. BRIDGE)	-123.922000 46.000000	0.02	NaN 1.21 NaN NaN%	NaN 0.98 NaN NaN%	NaN -0.96 NaN NaN%	NaN -1.34 NaN NaN%	obs model diff error
155	9438772	Cathcart Landing, Youngs River	-123.804333 46.124250	0.01	1.27 1.30 0.03 2%	1.06 1.08 0.02 2%	-1.07 -1.07 0.00 -0%	-1.42 -1.41 0.01 -1%	obs model diff error
156	9439008	FORT STEVENS	-123.950000 46.206700	0.01	1.24 1.25 0.01 1%	1.02 1.03 0.01 1%	-0.99 -1.00 -0.01 1%	-1.39 -1.36 0.03 -2%	obs model diff error
157	9439011	HAMMOND, COLUMBIA RIVER	-123.945000 46.201700	0.01	1.21 1.24 0.03 2%	1.00 1.02 0.02 2%	-0.95 -1.00 -0.05 5%	-1.33 -1.35 -0.02 1%	obs model diff error
158	9439026	ASTORIA, YOUNGS BAY	-123.842030 46.169907	0.01	1.26 1.28 0.02 2%	1.04 1.06 0.01 1%	-1.04 -1.05 -0.00 0%	-1.43 -1.39 0.04 -3%	obs model diff error
159	9439040	ASTORIA, TONGUE POINT, COLUMBIA RIVER	-123.768306 46.207310	0.00	1.25 1.27 0.02 2%	1.04 1.06 0.01 1%	-1.02 -1.06 -0.04 4%	-1.37 -1.39 -0.02 1%	obs model diff error
160	9439069	KNAPPA	-123.589840 46.188900	0.01	1.21 1.27 0.06 5%	1.01 1.05 0.05 5%	-1.03 -1.09 -0.07 6%	-1.33 -1.38 -0.05 4%	obs model diff error
161	9439099	WAUNA, COLUMBIA RIVER	-123.408342 46.161959	0.01	1.09 1.13 0.04 4%	0.91 0.93 0.02 2%	-0.83 -0.84 -0.01 1%	-1.04 -1.00 0.04 -3%	obs model diff error
162	9439135	BEAVER	-123.180206 46.182217	0.02	0.94 1.01 0.07 7%	0.77 0.82 0.06 8%	-0.66 -0.70 -0.04 7%	-0.79 -0.82 -0.03 4%	obs model diff error
163	9439189	ROCKY POINT, MULTNOMAH CHANNEL	-122.868000 45.696700	0.02	0.58 0.57 -0.01 -2%	0.41 0.44 0.03 9%	-0.36 -0.42 -0.05 15%	-0.43 -0.47 -0.03 8%	obs model diff error

164	9439201	ST. HELENS, COLUMBIA RIVER	-122.795666 45.863538	0.02	0.53 0.58 0.04 8%	0.39 0.43 0.05 12%	-0.38 -0.43 -0.04 12%	-0.45 -0.49 -0.04 8%	obs model diff error
165	9439221	PORTLAND, MORRISON STREET BRIDGE	-122.673000 45.510000	0.03	0.64 0.59 -0.04 -7%	0.48 0.47 -0.02 -4%	-0.39 -0.44 -0.06 15%	-0.46 -0.49 -0.03 7%	obs model diff error
166	9440047	WASHOUGAL, COLUMBIA RIVER	-122.381960 45.577469	0.03	0.32 0.29 -0.02 -8%	0.20 0.18 -0.02 -10%	-0.16 -0.22 -0.06 37%	-0.25 -0.25 -0.00 1%	obs model diff error
167	9440079	BEACON ROCK STATE PARK, COLUMBIA RIVER	-122.019717 45.620231	0.04	0.29 0.30 0.01 2%	0.17 0.18 0.01 3%	-0.14 -0.20 -0.06 43%	-0.24 -0.23 0.01 -5%	obs model diff error
168	9440083	VANCOUVER, COLUMBIA RIVER	-122.697053 45.631514	0.02	0.56 0.54 -0.02 -3%	0.40 0.43 0.03 7%	-0.34 -0.41 -0.07 20%	-0.41 -0.46 -0.05 13%	obs model diff error
169	9440171	KNAPP(THORNES)LNDG, WILLOW BAR	-122.757741 45.741548	0.03	0.54 0.54 -0.00 -1%	0.38 0.41 0.03 9%	-0.33 -0.40 -0.06 19%	-0.42 -0.45 -0.03 8%	obs model diff error
170	9440357	TEMCO KALAMA TERMINAL, COLUMBIA RIVER	-122.837099 45.986443	0.03	0.60 0.63 0.03 5%	0.46 0.48 0.02 4%	-0.42 -0.47 -0.06 13%	-0.51 -0.55 -0.04 8%	obs model diff error
171	9440422	LONGVIEW, COLUMBIA RIVER	-122.954766 46.105169	0.01	0.76 0.75 -0.01 -1%	0.62 0.60 -0.01 -2%	-0.52 -0.55 -0.03 5%	-0.63 -0.64 -0.02 2%	obs model diff error
172	9440482	CAPE HORN, COLUMBIA RIVER	-123.289930 46.150260	0.02	1.03 1.06 0.03 3%	0.85 0.86 0.01 2%	-0.73 -0.73 0.00 -1%	-0.91 -0.86 0.06 -6%	obs model diff error
173	9440483	BARLOW POINT, COLUMBIA RIVER	-123.040601 46.152105	0.02	0.85 0.86 0.02 2%	0.69 0.70 0.01 1%	-0.57 -0.61 -0.04 7%	-0.69 -0.71 -0.02 3%	obs model diff error
174	9440569	SKAMOKAWA, COLUMBIA RIVER	-123.452506 46.266043	0.01	1.15 1.20 0.05 5%	0.95 0.99 0.04 4%	-0.90 -0.96 -0.06 6%	-1.14 -1.17 -0.03 3%	obs model diff error
175	9440571	ALTOONA, COLUMBIA RIVER	-123.653000 46.265000	0.01	1.19 1.25 0.06 5%	0.99 1.04 0.05 5%	-0.98 -1.06 -0.08 8%	-1.28 -1.35 -0.07 5%	obs model diff error
176	9440572	JETTY A, COLUMBIA RIVER	-124.037000 46.268300	0.02	1.19 1.20 0.01 1%	0.96 0.98 0.01 2%	-0.96 -0.94 0.02 -3%	-1.40 -1.30 0.10 -7%	obs model diff error
177	9440574	NORTH JETTY	-124.070880 46.271570	0.01	1.12 1.17 0.05 5%	0.91 0.95 0.04 4%	-0.87 -0.93 -0.06 7%	-1.25 -1.30 -0.05 4%	obs model diff error
178	9440575	KNAPPTON	-123.827000 46.268300	0.01	1.25 1.25 0.00 0%	1.04 1.04 0.00 0%	-1.03 -1.05 -0.02 2%	-1.40 -1.40 0.00 -0%	obs model diff error

179	9440581	CAPE DISAPPOINTMENT	-124.046278 46.281028	0.02	1.13 1.21 0.07 7%	0.93 0.98 0.06 6%	-0.86 -0.96 -0.10 12%	-1.23 -1.33 -0.10 8%	obs model diff error
180	9440650	GREENHEAD SLOUGH, WILLAPA BAY	-123.950302 46.372200	0.02	1.47 1.65 0.19 13%	1.24 1.43 0.19 15%	-1.43 -1.48 -0.05 3%	-1.79 -1.88 -0.08 5%	obs model diff error
181	9440691	NASELLE RIVER SWING BRIDGE	-123.903000 46.430000	0.02	1.46 1.60 0.14 10%	1.23 1.37 0.14 11%	-1.35 -1.42 -0.07 5%	-1.81 -1.83 -0.02 1%	obs model diff error
182	9440747	NAHCOTTA, WILLAPA BAY	-124.023000 46.501700	0.02	1.43 1.56 0.13 9%	1.20 1.32 0.12 10%	-1.33 -1.32 0.01 -1%	-1.77 -1.71 0.06 -3%	obs model diff error
183	9440846	BAY CENTER, PALIX RIVER, WILLAPA BAY	-123.945402 46.623312	0.01	1.28 1.38 0.10 8%	1.05 1.13 0.08 7%	-1.10 -1.13 -0.03 2%	-1.53 -1.50 0.03 -2%	obs model diff error
184	9440875	SOUTH BEND	-123.798000 46.663300	0.01	1.34 1.37 0.03 2%	1.12 1.12 -0.00 -0%	-1.21 -1.19 0.02 -2%	-1.65 -1.57 0.08 -5%	obs model diff error
185	9440910	TOKE POINT, WILLAPA BAY	-123.966917 46.707470	0.00	1.26 1.35 0.09 7%	1.03 1.10 0.06 6%	-1.04 -1.08 -0.04 4%	-1.46 -1.45 0.01 -1%	obs model diff error
186	9441102	Westport, Grays Harbor	-124.105083 46.904310	0.01	1.30 1.37 0.07 5%	1.08 1.14 0.06 6%	-1.06 -1.04 0.02 -2%	-1.48 -1.39 0.10 -7%	obs model diff error
187	9441156	POINT BROWN	-124.128000 46.950000	0.02	1.33 1.41 0.08 6%	1.10 1.18 0.08 7%	-1.14 -1.08 0.06 -6%	-1.60 -1.43 0.17 -10%	obs model diff error
188	9441187	ABERDEEN, GRAYS HARBOR	-123.853000 46.968300	0.01	1.37 1.49 0.12 8%	1.16 1.26 0.10 9%	-1.26 -1.23 0.03 -2%	-1.71 -1.58 0.13 -7%	obs model diff error
189	9441644	TAHOLAH, QUINAULT RIVER	-124.284750 47.348167	0.02	NaN 1.23 NaN NaN%	NaN 1.00 NaN NaN%	NaN -0.98 NaN NaN%	NaN -1.35 NaN NaN%	obs model diff error
190	9442396	LA PUSH, QUILLAYUTE RIVER	-124.637000 47.913300	0.01	1.20 1.23 0.03 3%	0.99 1.00 0.02 2%	-0.96 -0.97 -0.01 1%	-1.38 -1.31 0.07 -5%	obs model diff error
191	9442705	TSKAWAHYAH ISLAND, CAPE ALAVA, PACIFIC OCEAN	-124.736900 48.171101	0.01	1.23 1.23 -0.01 -1%	1.01 1.00 -0.00 -0%	-0.98 -0.99 -0.01 1%	-1.42 -1.37 0.05 -4%	obs model diff error
192	9442861	MAKAH BAY	-124.672000 48.296700	0.01	1.24 1.20 -0.04 -3%	1.01 0.98 -0.03 -3%	-0.99 -0.95 0.04 -4%	-1.45 -1.35 0.10 -7%	obs model diff error
193	9443090	NEAH BAY, STRAIT OF JUAN DE FUCA	-124.601944 48.370278	0.00	1.11 1.08 -0.03 -3%	0.85 0.82 -0.03 -4%	-0.83 -0.80 0.03 -4%	-1.32 -1.23 0.08 -6%	obs model diff error

194	9443361	SEKIU, CLALLAM BAY	-124.297000 48.263300	0.01	1.02 0.95 -0.06 -6%	0.76 0.73 -0.04 -5%	-0.72 -0.70 0.03 -4%	-1.27 -1.15 0.12 -9%	obs model diff error
195	9443551	JIM CREEK, STRAIT OF JUAN DE FUCA	-124.062500 48.187199	0.02	0.95 0.89 -0.06 -6%	0.74 0.71 -0.03 -4%	-0.75 -0.70 0.05 -6%	-1.24 -1.13 0.10 -8%	obs model diff error
196	9443826	CRESCENT BAY	-123.725000 48.161700	0.03	0.87 0.80 -0.06 -7%	0.69 0.66 -0.03 -4%	-0.63 -0.70 -0.07 12%	-1.28 -1.14 0.15 -12%	obs model diff error
197	9444090	PORT ANGELES, STRAIT OF JUAN DE FUCA	-123.441139 48.124722	0.00	0.86 0.81 -0.05 -6%	0.69 0.68 -0.02 -2%	-0.71 -0.69 0.02 -3%	-1.29 -1.20 0.10 -7%	obs model diff error
198	9444122	EDIZ HOOK, PORT ANGELES	-123.414314 48.138355	0.02	0.85 0.81 -0.04 -5%	0.64 0.68 0.03 5%	-0.60 -0.69 -0.09 15%	-1.28 -1.20 0.08 -7%	obs model diff error
199	9444900	PORT TOWNSEND, ADMIRALTY INLET	-122.759500 48.112900	0.00	1.07 1.10 0.03 3%	0.87 0.88 0.01 2%	-0.76 -0.77 -0.01 1%	-1.52 -1.44 0.08 -5%	obs model diff error
200	9445016	FOULWEATHER BLUFF, TWIN SPITS	-122.617000 47.926700	0.02	1.26 1.28 0.02 1%	1.01 1.02 0.02 2%	-0.96 -1.00 -0.04 4%	-1.79 -1.75 0.04 -2%	obs model diff error
201	9445088	LOFALL	-122.657000 47.815000	0.02	1.35 1.35 0.00 0%	1.08 1.09 0.01 1%	-1.04 -1.09 -0.05 5%	-1.91 -1.87 0.05 -2%	obs model diff error
202	9445133	BANGOR	-122.726946 47.748799	0.01	1.40 1.40 0.00 0%	1.13 1.13 0.00 0%	-1.10 -1.17 -0.06 6%	-1.98 -1.96 0.02 -1%	obs model diff error
203	9445246	WHITNEY POINT	-122.849387 47.761878	0.02	1.46 1.46 -0.00 -0%	1.16 1.18 0.01 1%	-1.15 -1.24 -0.09 8%	-2.07 -2.05 0.02 -1%	obs model diff error
204	9445272	QUILCENE, DABOB BAY, HOOD CANAL	-122.858000 47.800000	0.02	1.41 1.46 0.04 3%	1.16 1.18 0.02 2%	-1.16 -1.24 -0.09 7%	-2.05 -2.05 0.00 -0%	obs model diff error
205	9445296	SEABECK, HOOD CANAL	-122.828000 47.641700	0.02	1.45 1.45 0.00 0%	1.16 1.17 0.01 1%	-1.15 -1.23 -0.09 7%	-2.06 -2.04 0.02 -1%	obs model diff error
206	9445441	LYNCH COVE DOCK	-122.900000 47.418300	0.02	1.53 1.53 -0.00 -0%	1.22 1.24 0.02 2%	-1.23 -1.34 -0.11 9%	-2.16 -2.17 -0.01 0%	obs model diff error
207	9445478	UNION, HOOD CANAL	-123.098000 47.358300	0.02	1.49 1.50 0.01 1%	1.19 1.22 0.03 2%	-1.21 -1.30 -0.10 8%	-2.12 -2.13 -0.01 0%	obs model diff error
208	9445526	HANSVILLE	-122.545000 47.918300	0.01	1.33 1.33 -0.00 -0%	1.08 1.08 0.00 0%	-1.00 -1.02 -0.02 2%	-1.85 -1.77 0.07 -4%	obs model diff error

209	9445719	POULSBO	-122.638000 47.725000	0.01	1.49 1.50 0.00 0%	1.23 1.23 0.01 1%	-1.21 -1.28 -0.07 6%	-2.08 -2.09 -0.01 0%	obs model diff error
210	9445832	BROWNSVILLE	-122.615000 47.651700	0.01	1.50 1.49 -0.01 -1%	1.23 1.23 -0.00 -0%	-1.22 -1.26 -0.05 4%	-2.11 -2.06 0.05 -2%	obs model diff error
211	9445958	BREMERTON	-122.623000 47.561700	0.01	1.50 1.50 0.00 0%	1.23 1.24 0.01 0%	-1.21 -1.26 -0.04 4%	-2.08 -2.05 0.03 -2%	obs model diff error
212	9446281	ALLYN	-122.823000 47.383300	0.02	1.84 1.85 0.01 0%	1.56 1.58 0.02 1%	-1.56 -1.64 -0.08 5%	-2.49 -2.49 0.00 -0%	obs model diff error
213	9446291	WAUNA, CARR INLET, PUGET SOUND	-122.634003 47.378300	0.01	1.79 1.76 -0.03 -2%	1.50 1.49 -0.02 -1%	-1.43 -1.52 -0.09 6%	-2.33 -2.35 -0.02 1%	obs model diff error
214	9446451	GREEN POINT	-122.682000 47.301700	0.02	1.75 1.75 0.00 0%	1.47 1.48 0.01 1%	-1.45 -1.51 -0.06 4%	-2.35 -2.34 0.01 -1%	obs model diff error
215	9446484	TACOMA, COMMENCEMENT BAY	-122.413333 47.266670	0.00	1.50 1.51 0.00 0%	1.24 1.25 0.01 1%	-1.22 -1.26 -0.04 3%	-2.08 -2.04 0.04 -2%	obs model diff error
216	9446491	ARLETTA	-122.652000 47.280000	0.02	1.74 1.74 -0.00 -0%	1.46 1.47 0.01 0%	-1.42 -1.47 -0.05 4%	-2.32 -2.29 0.02 -1%	obs model diff error
217	9446545	TACOMA	-122.432000 47.255000	0.02	1.51 1.51 -0.00 -0%	1.24 1.25 0.01 0%	-1.22 -1.26 -0.03 3%	-2.10 -2.04 0.05 -3%	obs model diff error
218	9446583	BALLOW	-122.861619 47.246097	0.02	1.82 1.83 0.01 1%	1.53 1.56 0.03 2%	-1.52 -1.61 -0.09 6%	-2.43 -2.45 -0.02 1%	obs model diff error
219	9446705	YOMAN POINT, ANDERSON ISLAND	-122.675000 47.180000	0.01	1.76 1.75 -0.00 -0%	1.48 1.48 0.01 1%	-1.45 -1.51 -0.06 4%	-2.35 -2.34 0.01 -1%	obs model diff error
220	9446742	BARRON POINT, LITTLE SKOOKUM INLET ENT	-123.000560 47.155887	0.02	1.90 1.91 0.01 1%	1.60 1.64 0.04 2%	-1.61 -1.71 -0.10 6%	-2.53 -2.57 -0.04 2%	obs model diff error
221	9446804	SANDY POINT ANDERSON ISLAND, PUGET SOUND	-122.674668 47.153093	0.01	1.51 1.75 0.25 16%	1.26 1.48 0.22 18%	-1.25 -1.52 -0.27 22%	-2.02 -2.34 -0.33 16%	obs model diff error
222	9446807	BUDD INLET, SOUTH OF GULL HARBOR	-122.900083 47.099898	0.02	1.88 1.87 -0.01 -1%	1.59 1.60 0.01 0%	-1.60 -1.66 -0.06 4%	-2.54 -2.51 0.03 -1%	obs model diff error
223	9446969	OLYMPIA, BUD INLET, PUGET SOUND	-122.903076 47.060870	0.02	1.89 1.88 -0.01 -1%	1.58 1.60 0.02 1%	-1.61 -1.60 0.02 -1%	-2.55 -2.31 0.24 -9%	obs model diff error

224	9447110	LOCKHEED SHIPYARD	-122.362000 47.585000	0.01	1.44 1.44 -0.01 -0%	1.18 1.18 -0.00 -0%	-1.16 -1.19 -0.03 2%	-2.03 -1.96 0.07 -3%	obs model diff error
225	9447130	SEATTLE, PUGET SOUND	-122.339306 47.602640	0.00	1.44 1.44 -0.00 -0%	1.17 1.18 0.00 0%	-1.16 -1.19 -0.03 2%	-2.02 -1.96 0.06 -3%	obs model diff error
226	9447427	EDMONDS	-122.384732 47.813867	0.01	1.37 1.37 -0.00 -0%	1.11 1.11 0.00 0%	-1.10 -1.12 -0.02 2%	-1.96 -1.88 0.08 -4%	obs model diff error
227	9447659	EVERETT	-122.223000 47.980000	0.02	1.40 1.39 -0.01 -1%	1.14 1.14 -0.00 -0%	-1.12 -1.14 -0.02 2%	-1.98 -1.91 0.07 -3%	obs model diff error
228	9447717	PRIEST POINT	-122.227194 48.034944	0.01	1.40 1.40 0.00 0%	1.14 1.15 0.01 1%	-1.12 -1.17 -0.05 4%	-1.94 -1.95 -0.01 0%	obs model diff error
229	9447729	EBEY SLOUGH, QWULOOLT, POSSESSION SOUND	-122.168000 48.040000	NaN	NaN 1.40 NaN NaN%	NaN 1.14 NaN NaN%	NaN -1.15 NaN NaN%	NaN -1.89 NaN NaN%	obs model diff error
230	9447773	TULALIP, TULALIP BAY	-122.287879 48.063301	0.01	1.40 1.40 0.01 0%	1.14 1.15 0.00 0%	-1.13 -1.15 -0.02 2%	-1.97 -1.92 0.05 -3%	obs model diff error
231	9447814	GLENDALE, POSSESSION SOUND	-122.357000 47.940000	0.02	1.39 1.38 -0.01 -0%	1.13 1.13 -0.01 -0%	-1.12 -1.13 -0.01 1%	-1.98 -1.90 0.08 -4%	obs model diff error
232	9447854	BUSH POINT WHIDBEY ISLAND	-122.607000 48.033300	0.02	1.14 1.21 0.07 6%	0.90 0.97 0.07 8%	-0.89 -0.88 0.01 -1%	-1.71 -1.59 0.12 -7%	obs model diff error
233	9447855	HOLLY HARBOR FARMS	-122.535000 48.026700	0.02	1.46 1.44 -0.03 -2%	1.19 1.17 -0.02 -1%	-1.18 -1.18 -0.00 0%	-2.02 -1.95 0.08 -4%	obs model diff error
234	9447856	SANDY POINT, SARATOGA PASSAGE	-122.377000 48.035000	0.02	1.43 1.41 -0.02 -2%	1.16 1.15 -0.01 -1%	-1.14 -1.15 -0.01 1%	-2.00 -1.92 0.09 -4%	obs model diff error
235	9447883	GREENBANK, PUGET SOUND	-122.570000 48.105000	0.01	1.45 1.43 -0.01 -1%	1.18 1.17 -0.01 -1%	-1.17 -1.17 -0.01 1%	-2.02 -1.94 0.07 -4%	obs model diff error
236	9447952	CRESCENT HARBOR, WHIDBEY ISLAND	-122.617000 48.286700	0.02	1.48 1.46 -0.02 -1%	1.21 1.19 -0.02 -1%	-1.22 -1.19 0.03 -2%	-2.07 -1.96 0.11 -5%	obs model diff error
237	9447973	NAS WHIDBEY ISLAND, STRAIT OF JAUN DE FUCA	-122.687614 48.344373	0.02	0.91 0.97 0.06 7%	0.72 0.77 0.05 7%	-0.69 -0.71 -0.03 4%	-1.35 -1.32 0.03 -2%	obs model diff error
238	9448009	SPEE-BI-DAH	-122.324201 48.087527	0.01	1.42 1.41 -0.01 -1%	1.16 1.15 -0.01 -1%	-1.15 -1.15 -0.01 1%	-2.00 -1.92 0.08 -4%	obs model diff error

239	9448043	TULARE BEACH, PORT SUSAN	-122.347785 48.106459	0.01	1.41 1.41 -0.00 -0%	1.15 1.15 0.00 0%	-1.13 -1.16 -0.02 2%	-1.97 -1.92 0.04 -2%	obs model diff error
240	9448558	LA CONNER, SWINOMISH SLOUGH	-122.497000 48.391700	0.02	1.34 1.30 -0.04 -3%	1.06 1.02 -0.04 -3%	-1.00 -0.90 0.10 -10%	-1.82 -1.53 0.29 -16%	obs model diff error
241	9448576	SNEEOOSH POINT, SKAGIT BAY	-122.548000 48.400000	0.02	1.42 1.44 0.02 1%	1.16 1.13 -0.04 -3%	-1.16 -1.03 0.13 -11%	-1.95 -1.76 0.18 -9%	obs model diff error
242	9448614	BOWMAN BAY, FIDALGO ISLAND	-122.652000 48.415001	0.01	0.94 0.99 0.05 6%	0.74 0.79 0.05 6%	-0.66 -0.73 -0.07 11%	-1.41 -1.35 0.06 -4%	obs model diff error
243	9448657	TURNER BAY, SIMILK BAY	-122.555000 48.445000	0.02	1.34 1.32 -0.02 -2%	1.08 1.04 -0.04 -4%	-1.05 -0.92 0.13 -12%	-1.81 -1.60 0.21 -12%	obs model diff error
244	9448682	SWINOMISH, PUGET SOUND	-122.513902 48.458349	0.01	1.12 1.19 0.07 6%	0.88 0.95 0.07 8%	-0.78 -0.83 -0.06 8%	-1.54 -1.48 0.06 -4%	obs model diff error
245	9449161	VILLAGE POINT, LUMMI ISLAND	-122.708000 48.716700	0.01	1.11 1.24 0.12 11%	0.87 0.98 0.11 13%	-0.75 -0.87 -0.13 17%	-1.52 -1.58 -0.06 4%	obs model diff error
246	9449211	BELLINGHAM	-122.495000 48.745000	0.01	1.08 1.21 0.12 11%	0.87 0.96 0.09 11%	-0.79 -0.86 -0.07 9%	-1.51 -1.55 -0.04 3%	obs model diff error
247	9449292	SANDY POINT, LUMMI BAY	-122.708000 48.790000	0.01	1.16 1.28 0.12 10%	0.92 1.02 0.10 11%	-0.80 -0.91 -0.11 14%	-1.59 -1.64 -0.05 3%	obs model diff error
248	9449424	CHERRY POINT, STRAIT OF GEORGIA	-122.758000 48.863300	0.00	1.18 1.30 0.13 11%	0.92 1.04 0.11 12%	-0.81 -0.94 -0.12 15%	-1.61 -1.67 -0.06 4%	obs model diff error
249	9449639	POINT ROBERTS, PUGET SOUND	-123.083000 48.974998	0.01	1.26 1.41 0.14 11%	1.00 1.12 0.12 12%	-0.89 -1.01 -0.12 13%	-1.72 -1.78 -0.06 4%	obs model diff error
250	9449679	BLAINE, DRAYTON HARBOR	-122.765000 48.991700	0.01	1.23 1.34 0.11 9%	0.97 1.04 0.07 7%	-0.86 -0.97 -0.11 13%	-1.67 -1.73 -0.06 3%	obs model diff error
251	9449746	WALDRON ISLAND, PUGET SOUND	-123.037598 48.686798	0.02	0.90 1.17 0.27 30%	0.72 0.93 0.21 29%	-0.64 -0.84 -0.20 30%	-1.24 -1.52 -0.28 22%	obs model diff error
252	9449771	ROSARIO, ORCAS ISLAND	-122.870003 48.646702	0.02	0.99 1.08 0.09 9%	0.79 0.86 0.07 9%	-0.71 -0.78 -0.07 10%	-1.42 -1.42 -0.01 1%	obs model diff error
253	9449828	HANBURY POINT, SAN JUAN ISLAND	-123.171837 48.581673	0.01	0.96 1.00 0.05 5%	0.76 0.80 0.04 6%	-0.66 -0.72 -0.06 9%	-1.37 -1.33 0.03 -2%	obs model diff error

254	9449856	KANAKA BAY, SAN JUAN ISLAND, KANAKA BAY	-123.084238 48.484657	0.02	0.89 0.90 0.00 0%	0.72 0.73 0.01 2%	-0.66 -0.69 -0.03 4%	-1.34 -1.24 0.10 -7%	obs model diff error
255	9449880	FRIDAY HARBOR, SAN JUAN CHANNEL	-123.012253 48.545053	0.00	0.98 1.09 0.11 11%	0.78 0.86 0.08 10%	-0.69 -0.75 -0.06 9%	-1.39 -1.40 -0.02 1%	obs model diff error
256	9449911	UPRIGHT HEAD, PUGET SOUND	-122.885002 48.571701	0.02	0.98 1.07 0.09 9%	0.78 0.85 0.07 9%	-0.71 -0.78 -0.07 10%	-1.41 -1.42 -0.01 1%	obs model diff error
257	9449932	ARMITAGE ISLAND	-122.797000 48.535000	0.01	0.97 1.06 0.09 10%	0.78 0.85 0.07 9%	-0.71 -0.79 -0.07 10%	-1.42 -1.42 -0.00 0%	obs model diff error
258	9449982	RICHARDSON, LOPEZ ISLAND	-122.900000 48.446700	0.01	0.87 0.92 0.05 6%	0.71 0.75 0.04 6%	-0.68 -0.69 -0.02 3%	-1.31 -1.26 0.05 -4%	obs model diff error
259	9449988	TELEGRAPH BAY, PUGET SOUND	-122.805000 48.443298	0.02	0.76 0.99 0.23 30%	0.61 0.79 0.18 29%	-0.56 -0.71 -0.15 26%	-1.13 -1.30 -0.17 15%	obs model diff error
260	46404		-128.778000 45.859000		1.05 1.06 0.01 1%	0.83 0.84 0.02 2%	-0.80 -0.83 -0.03 3%	-1.23 -1.17 0.06 -5%	obs model diff error
261	46407		-128.900000 42.604000		0.91 0.89 -0.01 -1%	0.70 0.69 -0.00 -0%	-0.67 -0.68 -0.00 0%	-1.06 -0.99 0.06 -6%	obs model diff error
262	46411		-127.013000 39.331000		0.75 0.76 0.01 2%	0.58 0.56 -0.02 -3%	-0.57 -0.55 0.02 -3%	-0.87 -0.85 0.02 -3%	obs model diff error
263	46419		-129.617000 48.762000		1.16 1.18 0.03 2%	0.97 0.96 -0.01 -1%	-0.95 -0.94 0.01 -1%	-1.31 -1.30 0.01 -1%	obs model diff error
264	46412		-120.699000 32.247000		0.68 0.69 0.02 2%	0.48 0.48 0.00 0%	-0.47 -0.48 -0.01 1%	-0.71 -0.71 0.00 -0%	obs model diff error

APPENDIX B TIDE STATION DATA FOR TSS CREATION AND UNCERTAINTY

Table B.1 Tide station data utilized for TSS creation and deltas computed against the TSS grid.

ID	Longitude (deg)	Latitude (deg)	xGEOID20B to MSL (m)	TSS Derived Value (m)	Delta (m)
9410032	-118.55700	33.00500	-0.308	-0.308	0.000
9410079	-118.32500	33.34500	-0.248	-0.248	0.000
9410120	-117.13500	32.57830	-0.184	-0.185	0.001
9410135	-117.10778	32.62914	-0.201	-0.201	0.000
9410170	-117.17358	32.71419	-0.194	-0.194	0.000
9410196	-117.22378	32.79372	-0.181	-0.181	0.000
9410230	-117.25714	32.86689	-0.226	-0.226	0.000
9410396	-117.39500	33.21000	-0.244	-0.244	0.000
9410580	-117.88300	33.60330	-0.211	-0.211	0.000
9410840	-118.50000	34.00830	-0.195	-0.195	0.000
9410962	-120.04700	34.00830	-0.181	-0.181	0.000
9411340	-119.69281	34.40311	-0.195	-0.195	0.000
9411399	-120.22831	34.46939	-0.112	-0.110	-0.002
9412110	-120.75419	35.16881	-0.165	-0.165	0.000
9412802	-121.48194	35.94953	-0.074	-0.075	0.001
9413450	-121.88805	36.60500	-0.115	-0.115	0.000
9413631	-121.74700	36.81830	-0.144	-0.144	0.000
9414290	-122.46589	37.80631	-0.147	-0.147	0.000
9414458	-122.25300	37.58000	-0.185	-0.185	0.000
9414509	-122.11500	37.50670	-0.219	-0.219	0.000
9414519	-122.04200	37.49330	-0.198	-0.198	0.000
9414523	-122.21153	37.50678	-0.200	-0.200	0.000
9414525	-122.10500	37.45830	-0.215	-0.215	0.000
9414551	-121.97500	37.42330	-0.119	-0.120	0.001
9414746	-122.23500	37.77170	-0.227	-0.227	0.000
9414750	-122.30000	37.77170	-0.202	-0.202	0.000
9414764	-122.28200	37.79500	-0.223	-0.223	0.000
9414782	-122.36000	37.81000	-0.186	-0.186	0.000
9414811	-121.92300	38.18330	-0.361	-0.361	0.000
9414837	-122.44300	37.89170	-0.190	-0.190	0.000
9414863	-122.40958	37.92300	-0.193	-0.193	0.000
9414958	-122.67861	37.90778	-0.228	-0.226	-0.002
9415009	-122.44700	37.99330	-0.189	-0.189	0.000
9415020	-122.97667	37.99611	-0.151	-0.151	0.000
9415053	-121.63800	38.01170	-0.315	-0.315	0.000
9415056	-122.36300	38.01500	-0.205	-0.205	0.000
9415064	-121.81500	38.02000	-0.471	-0.470	-0.001

ID	Longitude (deg)	Latitude (deg)	xGEOID20B to MSL (m)	TSS Derived Value (m)	Delta (m)
9415102	-122.12519	38.03464	-0.257	-0.257	0.000
9415105	-121.49686	38.05003	-0.373	-0.372	-0.001
9415144	-122.03950	38.05600	-0.344	-0.344	0.000
9415193	-121.68500	38.08670	-0.402	-0.401	-0.001
9415218	-122.25000	38.07000	-0.255	-0.255	0.000
9415252	-122.50567	38.11531	-0.254	-0.254	0.000
9415316	-121.69200	38.14500	-0.334	-0.334	0.000
9415338	-122.40700	38.15670	-0.302	-0.301	-0.001
9415423	-122.54700	38.19830	-0.252	-0.252	0.000
9415584	-122.61300	38.22830	-0.232	-0.232	0.000
9416409	-123.44939	38.70433	-0.137	-0.136	-0.001
9416841	-123.71108	38.91456	-0.092	-0.092	0.000
9418024	-124.05800	40.02500	-0.129	-0.129	0.000
9418637	-124.28222	40.63722	-0.108	-0.108	0.000
9418723	-124.22200	40.72330	0.026	0.027	-0.001
9418739	-124.21200	40.74000	0.068	0.067	0.001
9418767	-124.21720	40.76630	0.025	0.025	0.000
9419059	-124.14700	41.05670	-0.056	-0.056	0.000
9419750	-124.18300	41.74500	-0.152	-0.152	0.000
9431011	-124.41872	42.42164	-0.174	-0.173	-0.001
9431647	-124.49828	42.73897	-0.092	-0.092	0.000
9432780	-124.32200	43.34500	-0.097	-0.097	0.000
9432879	-124.29700	43.37670	-0.025	-0.026	0.001
9432895	-124.21800	43.41000	-0.102	-0.102	0.000
9433445	-124.19200	43.67500	-0.153	-0.153	0.000
9433501	-124.09500	43.70500	-0.219	-0.219	0.000
9434098	-124.12300	44.00211	-0.165	-0.165	0.000
9434939	-124.05808	44.43436	-0.207	-0.207	0.000
9435380	-124.04300	44.62500	-0.111	-0.111	0.000
9435827	-124.05800	44.81000	-0.162	-0.162	0.000
9436381	-124.00731	45.04794	-0.200	-0.200	0.000
9437381	-123.90200	45.48170	-0.257	-0.257	0.000
9437585	-123.96500	45.57000	-0.113	-0.114	0.001
9438772	-123.80433	46.12425	-0.333	-0.332	-0.001
9439011	-123.94500	46.20170	-0.228	-0.228	0.000
9439026	-123.84200	46.17170	-0.248	-0.249	0.001
9439040	-123.76831	46.20731	-0.353	-0.354	0.001
9439135	-123.18000	46.18170	-0.851	-0.851	0.000
9439189	-122.86800	45.69670	-1.359	-1.359	0.000
9439201	-122.79620	45.86330	-1.262	-1.262	0.000
9439221	-122.67300	45.51000	-1.493	-1.493	0.000
9440079	-122.02030	45.62030	-2.291	-2.290	-0.001
9440083	-122.69700	45.63169	-1.444	-1.445	0.001

ID	Longitude (deg)	Latitude (deg)	xGEOID20B to MSL (m)	TSS Derived Value (m)	Delta (m)
9440171	-122.75500	45.74170	-1.410	-1.410	0.000
9440357	-122.83670	45.98670	-1.134	-1.134	0.000
9440422	-122.95419	46.10614	-1.016	-1.016	0.000
9440482	-123.29000	46.15170	-0.808	-0.808	0.000
9440483	-123.03920	46.15220	-0.924	-0.924	0.000
9440569	-123.45200	46.26670	-0.622	-0.622	0.000
9440571	-123.65300	46.26500	-0.446	-0.446	0.000
9440574	-124.07200	46.27330	-0.232	-0.231	-0.001
9440581	-124.04628	46.28103	-0.224	-0.224	0.000
9440650	-123.95030	46.37220	-0.333	-0.333	0.000
9440910	-123.96692	46.70747	-0.250	-0.250	0.000
9441102	-124.10508	46.90431	-0.147	-0.147	0.000
9442396	-124.63700	47.91330	-0.167	-0.167	0.000
9442705	-124.73690	48.17110	-0.206	-0.206	0.000
9443090	-124.60194	48.37028	-0.137	-0.137	0.000
9443361	-124.29700	48.26330	-0.133	-0.133	0.000
9443551	-124.06250	48.18720	-0.126	-0.126	0.000
9444090	-123.44114	48.12472	-0.123	-0.123	0.000
9444900	-122.75950	48.11290	-0.099	-0.099	0.000
9445016	-122.61700	47.92670	-0.105	-0.105	0.000
9445478	-123.09800	47.35830	-0.088	-0.088	0.000
9446281	-122.82300	47.38330	-0.186	-0.186	0.000
9446291	-122.63400	47.37830	-0.119	-0.119	0.000
9446484	-122.41333	47.26667	-0.161	-0.160	-0.001
9446545	-122.43200	47.25500	-0.111	-0.111	0.000
9447130	-122.33931	47.60264	-0.120	-0.120	0.000
9447773	-122.28800	48.06500	-0.163	-0.163	0.000
9447883	-122.57000	48.10500	-0.139	-0.139	0.000
9447973	-122.68580	48.34280	-0.105	-0.105	0.000
9448009	-122.32233	48.08825	-0.224	-0.222	-0.002
9448043	-122.34728	48.10681	-0.168	-0.169	0.001
9448682	-122.51300	48.45830	-0.206	-0.205	-0.001
9449211	-122.49500	48.74500	-0.136	-0.136	0.000
9449424	-122.75800	48.86330	-0.170	-0.170	0.000
9449639	-123.08300	48.97500	-0.212	-0.212	0.000
9449746	-123.03760	48.68680	-0.188	-0.187	-0.001
9449771	-122.87000	48.64670	-0.123	-0.123	0.000
9449856	-123.08300	48.48500	-0.113	-0.113	0.000
9449880	-123.01289	48.54531	-0.155	-0.155	0.000
9449911	-122.88500	48.57170	-0.152	-0.152	0.000

Table B.2 Tide station data utilized for TSS creation and their corresponding uncertainty in terms of standard deviations.

ID	Longitude (deg)	Latitude (deg)	TSS (xGEOID20B to MSL) (m)	Uncertainty (m)
9410032	-118.55700	33.00500	-0.308	0.029
9410079	-118.32500	33.34500	-0.248	0.026
9410120	-117.13500	32.57830	-0.184	0.024
9410135	-117.10778	32.62914	-0.201	0.025
9410170	-117.17358	32.71419	-0.194	0.022
9410196	-117.22378	32.79372	-0.181	0.025
9410230	-117.25714	32.86689	-0.226	0.022
9410396	-117.39500	33.21000	-0.244	0.026
9410580	-117.88300	33.60330	-0.211	0.022
9410840	-118.50000	34.00830	-0.195	0.022
9410962	-120.04700	34.00830	-0.181	0.028
9411340	-119.69281	34.40311	-0.195	0.022
9411399	-120.22831	34.46939	-0.112	0.027
9412110	-120.75419	35.16881	-0.165	0.022
9412802	-121.48194	35.94953	-0.074	0.029
9413450	-121.88805	36.60500	-0.115	0.022
9413631	-121.74700	36.81830	-0.144	0.026
9414290	-122.46589	37.80631	-0.147	0.022
9414458	-122.25300	37.58000	-0.185	0.023
9414509	-122.11500	37.50670	-0.219	0.028
9414519	-122.04200	37.49330	-0.198	0.031
9414523	-122.21153	37.50678	-0.200	0.022
9414525	-122.10500	37.45830	-0.215	0.027
9414551	-121.97500	37.42330	-0.119	0.034
9414746	-122.23500	37.77170	-0.227	0.025
9414750	-122.30000	37.77170	-0.202	0.022
9414764	-122.28200	37.79500	-0.223	0.025
9414782	-122.36000	37.81000	-0.186	0.025
9414811	-121.92300	38.18330	-0.361	0.024
9414837	-122.44300	37.89170	-0.190	0.025
9414863	-122.40958	37.92300	-0.193	0.022
9414958	-122.67861	37.90778	-0.228	0.023
9415009	-122.44700	37.99330	-0.189	0.026
9415020	-122.97667	37.99611	-0.151	0.022
9415053	-121.63800	38.01170	-0.315	0.030
9415056	-122.36300	38.01500	-0.205	0.027
9415064	-121.81500	38.02000	-0.471	0.026
9415102	-122.12519	38.03464	-0.257	0.023
9415105	-121.49686	38.05003	-0.373	0.035
9415144	-122.03950	38.05600	-0.344	0.022

ID	Longitude (deg)	Latitude (deg)	TSS (xGEOID20B to MSL) (m)	Uncertainty (m)
9415193	-121.68500	38.08670	-0.402	0.033
9415218	-122.25000	38.07000	-0.255	0.023
9415252	-122.50567	38.11531	-0.254	0.026
9415316	-121.69200	38.14500	-0.334	0.028
9415338	-122.40700	38.15670	-0.302	0.027
9415423	-122.54700	38.19830	-0.252	0.033
9415584	-122.61300	38.22830	-0.232	0.034
9416409	-123.44939	38.70433	-0.137	0.026
9416841	-123.71108	38.91456	-0.092	0.022
9417426	-123.80511	39.42578	-0.101	0.027
9418024	-124.05800	40.02500	-0.129	0.029
9418637	-124.28222	40.63722	-0.108	0.026
9418723	-124.22200	40.72330	0.026	0.025
9418739	-124.21200	40.74000	0.068	0.029
9418767	-124.21720	40.76630	0.025	0.022
9419059	-124.14700	41.05670	-0.056	0.024
9419750	-124.18300	41.74500	-0.152	0.022
9431011	-124.41872	42.42164	-0.174	0.026
9431647	-124.49828	42.73897	-0.092	0.022
9432780	-124.32200	43.34500	-0.097	0.022
9432879	-124.29700	43.37670	-0.025	0.025
9432895	-124.21800	43.41000	-0.102	0.027
9433445	-124.19200	43.67500	-0.153	0.027
9433501	-124.09500	43.70500	-0.219	0.034
9434068	-124.04500	43.98500	-0.311	0.028
9434098	-124.12300	44.00211	-0.165	0.027
9434939	-124.05808	44.43436	-0.207	0.026
9435380	-124.04300	44.62500	-0.111	0.022
9435827	-124.05800	44.81000	-0.162	0.023
9436381	-124.00731	45.04794	-0.200	0.027
9437381	-123.90200	45.48170	-0.257	0.027
9437585	-123.96500	45.57000	-0.113	0.026
9438772	-123.80433	46.12425	-0.333	0.025
9439011	-123.94500	46.20170	-0.228	0.024
9439026	-123.84200	46.17170	-0.248	0.026
9439040	-123.76831	46.20731	-0.353	0.022
9439135	-123.18000	46.18170	-0.851	0.030
9439189	-122.86800	45.69670	-1.359	0.031
9439201	-122.79620	45.86330	-1.262	0.031
9439221	-122.67300	45.51000	-1.493	0.038
9440079	-122.02030	45.62030	-2.291	0.044
9440083	-122.69700	45.63169	-1.444	0.031

ID	Longitude (deg)	Latitude (deg)	TSS (xGEOID20B to MSL) (m)	Uncertainty (m)
9440171	-122.75500	45.74170	-1.410	0.037
9440357	-122.83670	45.98670	-1.134	0.034
9440422	-122.95419	46.10614	-1.016	0.025
9440482	-123.29000	46.15170	-0.808	0.029
9440483	-123.03920	46.15220	-0.924	0.031
9440569	-123.45200	46.26670	-0.622	0.026
9440571	-123.65300	46.26500	-0.446	0.026
9440574	-124.07200	46.27330	-0.232	0.027
9440581	-124.04628	46.28103	-0.224	0.024
9440650	-123.95030	46.37220	-0.333	0.028
9440910	-123.96692	46.70747	-0.250	0.022
9441102	-124.10508	46.90431	-0.147	0.023
9442396	-124.63700	47.91330	-0.167	0.023
9442705	-124.73690	48.17110	-0.206	0.027
9443090	-124.60194	48.37028	-0.137	0.022
9443361	-124.29700	48.26330	-0.133	0.026
9443551	-124.06250	48.18720	-0.126	0.028
9444090	-123.44114	48.12472	-0.123	0.022
9444900	-122.75950	48.11290	-0.099	0.022
9445016	-122.61700	47.92670	-0.105	0.029
9445478	-123.09800	47.35830	-0.088	0.027
9446281	-122.82300	47.38330	-0.186	0.031
9446291	-122.63400	47.37830	-0.119	0.027
9446484	-122.41333	47.26667	-0.161	0.023
9446545	-122.43200	47.25500	-0.111	0.028
9447130	-122.33931	47.60264	-0.120	0.022
9447773	-122.28800	48.06500	-0.163	0.027
9447883	-122.57000	48.10500	-0.139	0.027
9447973	-122.68580	48.34280	-0.105	0.029
9448009	-122.32233	48.08825	-0.224	0.027
9448043	-122.34728	48.10681	-0.168	0.027
9448682	-122.51300	48.45830	-0.206	0.024
9449211	-122.49500	48.74500	-0.136	0.026
9449424	-122.75800	48.86330	-0.170	0.022
9449639	-123.08300	48.97500	-0.212	0.026
9449679	-122.76500	48.99170	-0.096	0.025
9449746	-123.03760	48.68680	-0.188	0.029
9449771	-122.87000	48.64670	-0.123	0.029
9449856	-123.08300	48.48500	-0.113	0.028
9449880	-123.01289	48.54531	-0.155	0.022
9449911	-122.88500	48.57170	-0.152	0.028